Proceedings of the
Annual Stability Conference
Structural Stability Research Council
Atlanta, Georgia, April 21-24, 2020

Flexural-torsional failure and DSM design of CFS lipped channel and rack-section columns at elevated temperatures

Antonio Albuquerque Bicelli[1], Alexandre Landesmann[1], Dinar Camotim[2], Pedro Borges Dinis[2]

Abstract

Recently, Dinis *et al.* (2019a,b) reported in-depth numerical investigations showing that the current Direct Strength Method (DSM) global design curve underestimates the flexural-torsional (FT) failure loads of fixed-ended cold-formed steel columns with slenderness higher than 1.5. This finding was based on the analysis of columns (i) exhibiting various cross-section shapes and geometries, and (ii) covering wide slenderness ranges. Moreover, these authors used the failure load data gathered to develop and assess the merits of a novel DSM column design curve set, aimed at improving considerably the failure load prediction for the aforementioned columns. This work extends the scope of the previous studies to cover fixed-ended cold-formed steel lipped channel and rack-section columns under elevated temperatures (up to 800 ºC). The results presented and discussed consist of column FT post-buckling equilibrium paths and failure loads, obtained through geometrically and materially non-linear ANSYS shell finite element analyses – to cover a wide FT slenderness range, several room-temperature yield stresses are considered. The model prescribed in Part 1-2 of Eurocode 3 (EC3:1-2), for cold-formed steel, is adopted to describe the temperature-dependence of the steel material properties. Finally, the numerical failure loads obtained in this work, together with the numerical and experimental ones collected from the literature, are used to propose a modification of the DSM-based FT strength curve set developed by Dinis *et al.* (2019b), making it capable of handling FT failures under elevated temperatures. Since the merit assessment of the new strength curve set shows a visible improvement of the FT failure load prediction quality, it may be argued that it constitutes a good starting point for the search for an efficient DSM-based design approach for columns failing in FT modes at elevated temperatures.

1 Introduction

Cold-formed steel (CFS) structures offer very flexible design solutions, due to their exceptional fabrication adaptability, high structural efficiency (strength-to-weight ratio) and continuously lower production and erection costs. However, since many CFS members display very slender thin-walled open cross-sections, which makes them highly prone to several instability phenomena, namely local, distortional or global buckling, the current design specifications contain provisions dealing with the corresponding failures. In particular, the Direct Strength Method (DSM – *e.g.*, Camotim *et al.* 2016 or Schafer 2019), which is prescribed by the current North-American (AISI 2016), Australian/New Zealand (AS/NZS 2018) and

[1] Civil Engineering Program, COPPE/UFRJ, Federal University of Rio de Janeiro, Brazil. <antonio.bicelli; alandes@coc.ufrj.br>
[2] CERIS, Instituto Superior Técnico, Universidade de Lisboa, Portugal. <dcamotim@civil.ist.utl.pt; dinis@civil.ist.utl.pt>

Brazilian (ABNT 2010) specifications for CFS structures. It is nowadays widely accepted as the most rational approach to the design such members and its universal popularity stems also from the fact that its application requires only the knowledge of the member yield and buckling stresses. In the context of this investigation, the relevant codified nominal strength is the global one (f_{nG}), given by

$$f_{nG} = \begin{cases} f_y \left(0.658^{\lambda_G^2} \right) & if \quad \lambda_G \leq 1.5 \\ f_y \left(\dfrac{0.877}{\lambda_G^2} \right) & if \quad \lambda_G > 1.5 \end{cases} \qquad \text{with} \qquad \lambda_{\mathrm{G}} = \sqrt{\frac{\sigma_y}{f_{cr\mathrm{G}}}} \quad , \qquad (1)$$

where (i) f_{crG} and λ_G are the column global critical buckling stress and slenderness, and (ii) σ_y is the material (steel) yield stress. This design curve, combining an exponential expression (Ziemian 2010) with the (lowered) Euler curve, was first included in the CFS design manual in 1996 (AISI 1996), due to the work of Peköz & Sümer (1992), who showed that the above design curve, already codified in the context of hot-rolled steel members used in buildings (AISC 1986), provided better quality estimates than that adopted at that time by the CFS community (AISI 1986). These authors based their findings on 214 test results concerning concentrically loaded CFS columns with various cross-sections (lipped channels, hat-sections, box-sections and I-sections formed by back-to-back plain channels), all exhibiting low-to-moderate global slenderness values ($\lambda_G \leq 1.75$).

Recently, Dinis *et al.* (2019a,b) reported numerical investigations intended to assess the accuracy of the current DSM column global strength curve (Eq. (1)) in predicting the failure loads of fixed-ended CFS columns collapsing in major-axis flexural-torsional (FT) modes. These authors gathered a total of 1710 FT failure loads, concerning columns having (i) six cross-section shapes (plain, return lip, web-stiffened and web/flange-stiffened lipped channels, hat-sections and rack-sections), combined with various cross-section dimensions and lengths, (ii) critical-mode (FT) initial geometrical imperfections with L/1000 amplitude (L is the column length), and (iii) 5 (room temperature) yield stresses, making it possible to cover wide slenderness ranges. Based on these numerical FT failure load data, Dinis *et al.* (2019a) readily concluded that the current DSM column global design curve only provides adequate FT failure load estimates for fixed-ended columns with low-to-moderate slenderness ($\lambda_G \leq 1.5$) – it considerably underestimates the FT failure loads of the most slender columns ($\lambda_G > 1.5$). In fact, this underestimation was already perceptible for (i) the five lipped channel and hat-section column specimens with $\lambda_G > 1.6$ considered by Peköz & Sümer (1992) and (ii) the three lipped channel columns with $\lambda_G > 1.7$ tested, at room temperature, by Bandula Heva & Mahendran (2012) – these eight experimental FT failure loads are all visibly underestimated by the current DSM global design curve.

Following an in-depth investigation on the mechanics of FT buckling and failure in CFS columns, Dinis *et al.* (2019b) proposed a new DSM-based design approach (f_{nFT}) involving a set of strength curves dependent on a geometric parameter β_{FT}, given by

$$\beta_{FT} = \frac{I_I + I_w / A}{I_{II}} \qquad (2)$$

and relating the cross-section major (I_I) and minor (I_{II}) moments of inertia, warping constant (I_w) and area (A). For λ_G ($\equiv \lambda_{FT}$)>1.5, the strength curve becomes β_{FT}-dependent and is defined by a general "Euler-type" expression similar to that appearing in the current curve (see Eq. (1)) – this strength curve set is defined by the expressions

$$f_{nFT} = \begin{cases} f_y\left(0.658^{\lambda_{FT}^2}\right) & if \quad \lambda_{FT} \le 1.5 \\ f_y\left(\dfrac{a}{\lambda_{FT}^b}\right) & if \quad \lambda_{FT} > 1.5 \end{cases} \qquad \text{with} \quad \lambda_{FT} = \sqrt{\frac{\sigma_y}{f_{crFT}}} \quad , \quad (3)$$

where the β_{FT}-dependence is felt through parameters a and b, which are functions of β given by

$$a = 0.39 \times 1.5^b \quad , \quad (4)$$

$$b = \begin{cases} 0.06\beta_{FT} + 0.71 & if \quad \beta_{FT} < 21.5 \\ 2 & if \quad \beta_{FT} \ge 21.5 \end{cases} \quad . \quad (5)$$

Note that (i) in order to make a clear distinction between the current DSM global design curve (Eq. (1)) and the DSM-based strength curve set proposed by Dinis *et al.* (2019b), concerning exclusively columns failing in FT modes (Eq. (3)), λ_G is replaced by λ_{FT} in the latter, (ii) the exponential expression (also displayed in Eq. (1)) is kept in the low-to-moderate slenderness range ($\lambda_{FT} \le 1.5$), (iii) the a and b expressions (Eqs. (4)-(5)) were obtained by means of "trial-and-error curve-fitting procedures" (Dinis *et al.* 2019a,b) and, finally, (v) Eq. (1) is recovered for high β_{FT} values, beyond which the role played by torsion becomes negligible (*i.e.*, a=0.877 and b=2). It is still worth noting that the warping constant I_w can nowadays be easily calculated numerically, by means of freely available softwares like CUFSM (Li *et al.* 2014) or GBTUL (Bebiano *et al.* 2018).

Dinis *et al.* (2019b) also showed that the above β_{FT}-dependent DSM strength curve set predict very well all the available FT failure loads concerning columns with moderate or high slenderness (λ_{FT}>1.5), namely (i) the 1710 numerical ones obtained by these same authors (Dinis *et al.* 2018, 2019a,b) and (ii) the 3 experimental ones reported by Bandula Heva & Mahendran (2012). However, it remains to be assessed whether this strength curve set can also be adopted (with more or less relevant modifications) to estimate the failure loads of columns subjected to members elevated temperatures, namely those caused by fire conditions – recall that such conditions may alter substantially the steel constitutive law, namely its Young's modulus, yield strength and amount of non-linearity. In addition, Bandula Heva & Mahendran (2012)[3] reported that the numerical failure loads of CFS lipped channel columns subjected to uniform elevated temperatures, ranging between 400ºC and 500ºC, and exhibiting low-to-moderate slenderness values ($\lambda_G \le 1.5$) are clearly overestimated by the current DSM column design curve, already taking into account the appropriate reduction of the steel mechanical properties – recall that the strength curve set proposed by Dinis *et al.* (2019b) only differ from the current design curve for λ_G>1.5.

Therefore, the aim of this work is to present and discuss the results of an extensive numerical investigation on how accurately the available DSM design curves are capable of predicting the failure loads of CFS fixed-ended columns failing in FT modes at elevated temperatures. As done previously by Dinis *et al.* (2018, 2019a,b), all the numerical FT failure loads reported in this work (i) concern columns containing critical-mode (FT) initial imperfections with L/1000 amplitude and (ii) are obtained by means of non-linear elastic-plastic shell finite element analyses (SFEA), adopting a model often employed by the authors

[3] More details on this extensive experimental and numerical investigation on the FT behavior and DSM design of CFS lipped channel columns under room and elevated temperatures (the latter due to fire conditions) can be found in Bandula Heva (2009).

in the past. The columns analyzed (i) exhibit lipped channel and rack cross-section shapes, (ii) display a wide variety of cross-section dimensions, lengths and room temperature yield stresses (values selected to cover wide critical slenderness ranges), and (iii) are subjected to several uniform elevated temperatures, reaching up to 800 ºC. It is worth noting that some results concerning columns at room temperature have already been reported by Dinis *et al.* (2018, 2019a,b) – they are presented here for comparison proposes.

The paper begins with the column geometry selection (Section 2), carried out by means of sequences of "trial-and-error" buckling analyses and aimed at identifying lipped channel and rack-section column cross-section dimensions and lengths associated with "pure" FT buckling and failure modes. In other words, the selected columns exhibit FT critical buckling loads that are significantly lower than their local and distortional counterparts, both at room and elevated temperature. Next, in Section 3, the ANSYS (SAS 2009) shell finite element model employed to perform the geometrically and materially non-linear analyses is briefly described and validated, by reproducing simulations reported by Bandula Heva (2009). Then, Section 4 addresses the influence of the temperature on the column elastic-plastic post-buckling behavior, failure load and associated DSM estimation – in order to cover a wide FT slenderness range, several room-temperature yield stresses are considered. The model prescribed in parte 1-2 of Eurocode 3 (EC3:1-2 – CEN 2005) is employed to describe the temperature dependence of the CFS material properties[4]. Finally, the numerical failure load data obtained in this work, together with other experimental and numerical values reported in the literature, are used in Section 5 to assess the merits of DSM-based FT strength curves either proposed in the past (Dinis *et al.* 2019b) or modified by the authors in this work. Since it is shown that such modifications improve visibly the failure load prediction quality, it may be argued that the modified strength curves constitute a good starting point for the search for an efficient DSM-based design approach for columns failing in FT modes at elevated temperatures.

2 Column Geometry Selection – Buckling Behavior

The first task in this work consists of carefully selecting the cross-section dimensions and lengths of the CFS lipped channel (C) and rack-section (R) fixed-ended columns to be analyzed at room and elevated temperatures. As done in previous works, the selection procedure involves sequences of "trial-and-error" buckling analyses, performed in code GBTUL (Bebiano *et al.* 2018), based on Generalized Beam Theory (GBT), which makes it possible to obtain buckling loads/stresses associated with "pure" FT modes.

The output of the above effort are the 72 C and R columns whose cross-section dimensions (b_w, b_f, b_s, b_l, t – see the schematic representations included in Figs. 1(a)-(b)) and lengths are given in Table 1. This table also provides the column areas (A), major (I_I) and minor (I_{II}) moments of inertia, warping constants (I_w) and β_{FT} parameter values – the values of these geometrical properties were calculated on the basis of the cross-section mid-line dimensions.

The illustrative signature curves depicted in Figs. 1(a)-(b) concern the C_1 and R_1 column cross-section dimensions and provide the variation of $P_{cr.T}$ (elastic critical buckling load at temperature T) with the columns length L (logarithmic scale) for three different temperatures: 20/100 ºC (*i.e.*, room temperature), 400 ºC and 600 ºC. The EC3-1.2 (2005) constitutive model, presented in Section 3.1, is adopted and all buckling loads were calculated for E_{20}=210 *GPa* (steel Young's modulus at room temperature) and ν=0.3 (Poisson's ratio, deemed independent from the temperature). Moreover, the 6 column lengths considered

[4] Although AISI (2016) provides detailed specifications for the structural analysis and design of steel members under fire conditions (see Appendix 4), including values to account for the deterioration in strength and stiffness of structural steel at elevated temperatures (see Table A-4.2.1), there is no information about the stress-strain-temperature curve (model) for cold-formed steel under these (elevated temperatures) conditions. Thus, the EC3:1-2 relationship for CFS is adopted in this work.

Table 1: Cross-section geometry, cross-sectional geometrical properties and lengths of the selected lipped channel (C) and rack-section (R) columns failing in FT modes (b_w, b_f, b_s, b_l, t, A, L, I_I, I_{II}, I_w, values in *mm*, *mm*^{2}, *mm*^{4}, *mm*^{6})

Column	b_w	b_f	b_s	b_l	t	A	I_I (×10^4)	I_{II} (×10^4)	I_W (×10^6)	β_{FT}	L_1	L_2	L_3	L_4	L_5	L_6
C_1	60	50	11	-	1.2	224.64	14.67	9.35	79.54	5.36	1700	2380	3060	3500	4400	5100
C_2	100	60	10	-	2	464	78.55	21.38	405.01	7.76	2380	2700	3060	3500	4400	5100
C_3	140	70	10	-	3	864	274.02	50.09	1751.7	9.52	3000	3500	4000	4500	5000	5500
C_4	150	100	10	-	4	1416	543.62	164.38	6431.4	6.07	4000	4500	5000	5500	6000	6500
C_5	80	45	11	-	1.6	296.96	31.59	8.26	110.66	8.34	2500	2500	3000	3500	4000	4500
R_1	80	50	15	20	1	245	24.9	13.13	299.67	11.21	3500	4200	4900	5600	6300	7000
R_2	150	110	23	20	2.4	1065.6	411.86	213.38	13489	7.86	5500	6300	7000	7800	8600	9500
R_3	67	35	10	20	0.8	154.4	10.9	4.87	66.04	11.02	3000	3500	4000	4500	5000	5500
R_4	120	60	20	30	1.5	498.75	110.85	42.65	1962	11.82	5500	6000	6500	7000	7500	8000
R_5	110	100	20	15	2	740	157.45	117.27	4395.2	6.41	6000	6500	7000	7500	8000	8500

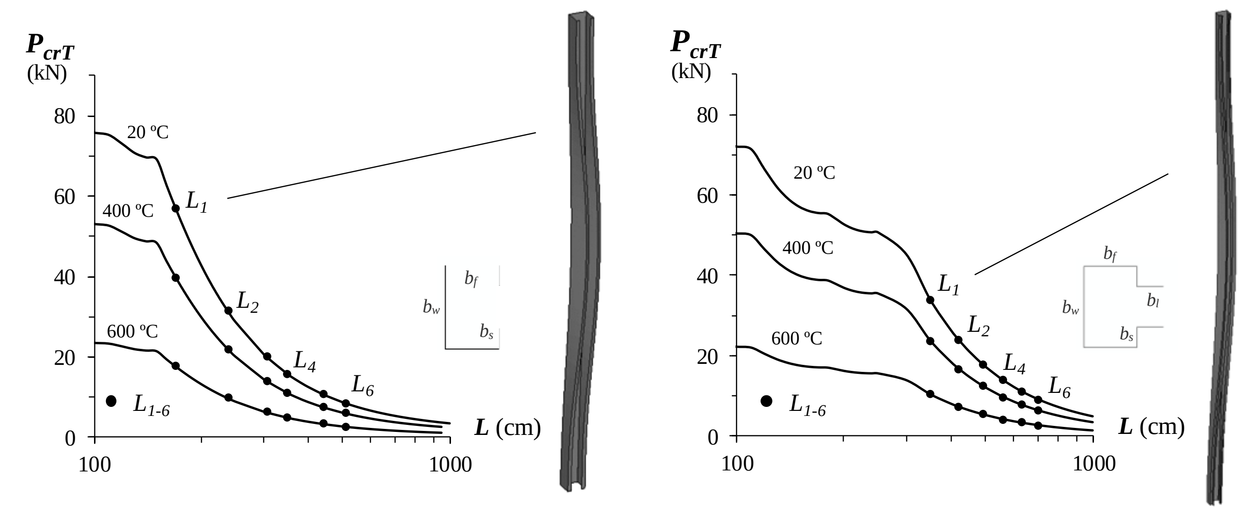

(a) (b)

Figure 1. Variation of $P_{cr.T}$ with L for T= 20/100, 400, 600 ºC: (a) C_1 and (b) R_1 columns (EC3-1.2 constitutive model)

(L_1-L_6) are indicated on the various signature curves and figures showing the critical (FT) buckling modes of the C_1 and R_1 columns with length L_1 (see Table 1) are also provided. It is worth noting that a signature curve associated with an elevated temperature (400 ºC or 600 ºC) is obtained, from its room-temperature counterpart, through a "vertical translation" whose magnitude depending only on the Young's modulus erosion cause by the temperature rise[5] – therefore, the flexural-torsional buckling loads $P_{crFT.T}$ correspond to the same length (L_{1-6}) for each temperature value.

3 Numerical Model

The column flexural-torsional post-buckling equilibrium paths and failure loads ultimate were determined by means of ANSYS (2009) geometrically and materially non-linear, employing models similar to those used in recent studies involving CFS columns subjected to elevated temperatures (*e.g.*, Landesmann *et al.* 2019). The columns were discretized into SHELL181 elements (ANSYS nomenclature – 4-node shear

[5] Naturally, the Young's modulus reduction factor k_e, whose variation with the temperature T is illustrated in Fig. 2(a), makes it possible to quantify the decrease in the critical buckling load P_{crT} corresponding to a given column length.

deformable thin-shell elements with six degrees of freedom per node and full integration). The analyses were performed by means of an incremental-iterative technique combining Newton-Raphson's method with an arc-length control strategy. They simulate the response of columns subjected to an uniform temperature distribution (*i.e.*, they are deemed engulfed in flames, thus sharing the surrounding air temperature – Landesmann & Camotim 2011) and subsequently axially compressed up to failure – steady state analyses providing failure loads. Convergence studies (Dinis *et al.* 2019a,b) showed that $5mm \times 5mm$ finite element meshes provide accurate results, while involving a reasonable computational effort.

The column fixed-ended support conditions are modeled by attaching the column end cross-sections to rigid plates with all the rotations and the bending translations restrained – the axial translations are free, thus enabling the load application. The axial compression is applied by means of point loads acting on the rigid end plate points corresponding to the cross-section centroid. The above loads are always increased in small increments, by means of the ANSYS automatic load stepping procedure. All the columns analyzed contain critical-mode (FT) initial geometrical imperfections with amplitude $L/1000$, a value often adopted in numerical simulations. The critical buckling mode shapes were determined by means of preliminary ANSYS buckling analyses, performed with the shell finite element mesh employed to carry out the subsequent post-buckling analyses – this procedure makes it very easy to "transform" the buckling analysis output into a non-linear analysis input. It is still worth noting that strain-hardening, residual stress and rounded corner strength effects were disregarded in this work, since their combined influence on the column failure load has been shown to be negligible by several authors (*e.g.*, Ellobody & Young 2005).

3.1 Steel Material Behavior

The multi-linear stress-strain curve available in ANSYS is adopted to model the steel material behavior corresponding to several yield stresses. The cold-formed steel constitutive law at elevated temperature adopted in this work is defined by the analytical expressions prescribed in EC3:1-2 CEN 2005). Fig. 2(a) makes it possible to compare the temperature dependence of the reduction factors applicable to the CFS Young's modulus ($k_e=E_T/E_{20}$), nominal yield stress ($k_y=\sigma_{yT}/\sigma_{y20}$) and proportionality limit stress ($k_p=\sigma_{pT}/\sigma_{p20}$), which are tabulated in EC3:1-2[6]. As for Fig. 2(b), it illustrates the qualitative

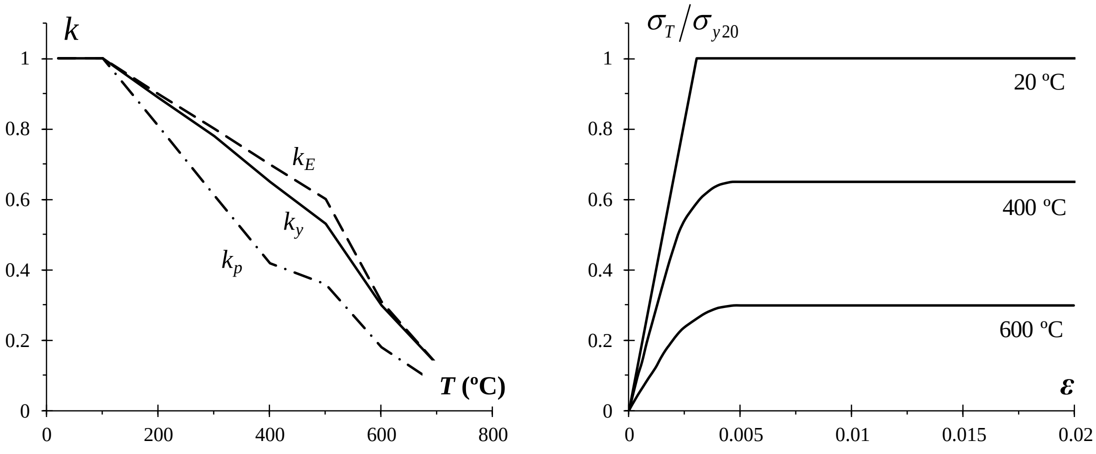

(a) (b)

Figure 2. (a) Variation of the reduction factors k_e, k_y, k_p with the temperature for $T \leq 800\,°C$ and (b) cold-formed steel stress-strain curves σ_T/σ_{y20} *vs.* ε ($\varepsilon \leq 2\%$) for T=20/100-400-600 ºC – as prescribed by the EC3:1-2 model

[6] For T=20/100-200-300-400-500-600-700-800 ºC, EC3:1-2 prescribes k_p=1.0-0.807-0.613-0.42-0.36-0.18-0.075-0.05, k_y=1.0-0.89-0.78-0.65-0.53-0.3-0.13-0.07 and k_E=1.0-0.9-0.8-0.7-0.6-0.31-0.13-0.09.

differences between the stress-strain curves prescribed by EC3:1-2 for T=20/100 ºC (room temperature), T=400 ºC and T=600 ºC – σ_T/σ_{y20} *vs.* ε, where the applied stress at a given temperature (σ_T) is normalized with respect to the room temperature yield stress σ_{y20}. Note that the stress-strain curve non-linearity increases significantly with the temperature (for T=20/100 ºC, the constitutive law is bi-linear – elastic-perfectly plastic material). The stress-strain curves prescribed in EC3:1-2 are divided into three regions, associated with distinct strain ranges[7]. Note that the stress-strain curve proportionality limit strain ($\varepsilon_{pT}=\sigma_{pT}/E_T$) and non-linear shape are considerably influenced by the temperature.

For elevated temperatures, the first part of the well-defined yield plateau exhibited by the T=20/100 °C curve is replaced by a strain-hardening region that becomes gradually more pronounced as the temperature rises. The stress-strain curve (i) is linear elastic, with slope E_T (E_{20}=210 GPa), up to the proportionality limit stress σ_{pT}, then (ii) becomes elliptic in the transition between the elastic and plastic ranges, up to the effective yield stress σ_{yT}, occurring at ε_{yT} (σ_{yT} is taken as the *0.2%* proof strength) and accounting for kinematic strain-hardening, and (iii) ends with a perfectly flat yield plateau, up to the limit strain ε_{uT}=0.15 – in all cases, Prandtl-Reuss's plasticity model (von Mises yield criterion and associated flow rule) is adopted. Finally, since the flexural-torsional post-buckling analyses carried out involve large inelastic strains, the nominal (engineering) static stress-strain curve is replaced by a relation between the true stress and the logarithmic plastic strain, which reads

$$\sigma_T = \begin{cases} \varepsilon \cdot E_T & \text{for } \varepsilon \le \varepsilon_{pT} \\ \sigma_{pT} - c + (b/a)\left[a^2 - \left(\varepsilon_{yT} - \varepsilon\right)^2\right]^{0.5} & \text{for } \varepsilon_{pT} < \varepsilon < \varepsilon_{yT} \\ \sigma_{yT} & \text{for } \varepsilon_{yT} \le \varepsilon \le \varepsilon_{uT} \end{cases} \quad . \qquad (6)$$

$$a^2 = \left(\varepsilon_{yT} - \varepsilon_{pT}\right)\left(\varepsilon_{yT} - \varepsilon_{pT} + c/E_T\right),\ b^2 = c\left(\varepsilon_{yT} - \varepsilon_{pT}\right)E_T + c^2,$$

$$c = \frac{\left(\sigma_{yT} - \sigma_{pT}\right)^2}{\left(\varepsilon_{yT} - \varepsilon_{pT}\right)E_T - 2\left(\sigma_{yT} - \sigma_{pT}\right)}$$

3.2 Validation Studies

In order to validate the use of the ANSYS shell finite element model to determine the FT post-buckling behavior and strength of CFS columns at room and elevated temperatures, a fraction of the numerical simulations reported by Bandula Heva & Mahendran (2012) is first replicated – it concerns lipped channel columns experimentally tested by these authors. Figures 3(a)-(b), taken from the above publication, provide an overall view of the experimental set-up that was specially designed and built at the Queensland University of Technology (QUT) Structural Laboratory, comprising mainly (i) a reaction frame (cross-head), (ii) a three-segment furnace, (iii) a furnace temperature control system and (iv) a bottom hydraulic loading system (see Fig. 3(b)).

Table 2 provides the data concerning the columns considered in the validation study, namely the mean values of their dimensions, lengths, steel grades and maximum initial displacements (expressed as a ratio of column length) adopted by Bandula Heva & Mahendran (2012). It is worth noting that, besides the novel experimental investigation involving a large number of column specimens, these authors also performed an extensive numerical investigation at room and elevated temperatures.

---

[7] Although the EC3:1-2 model further extends the stress-strain relationship, to include strain-hardening, for temperatures below 400 °C, this effect is not considered in this work (such strain-hardening is negligible for temperatures above 400°C).

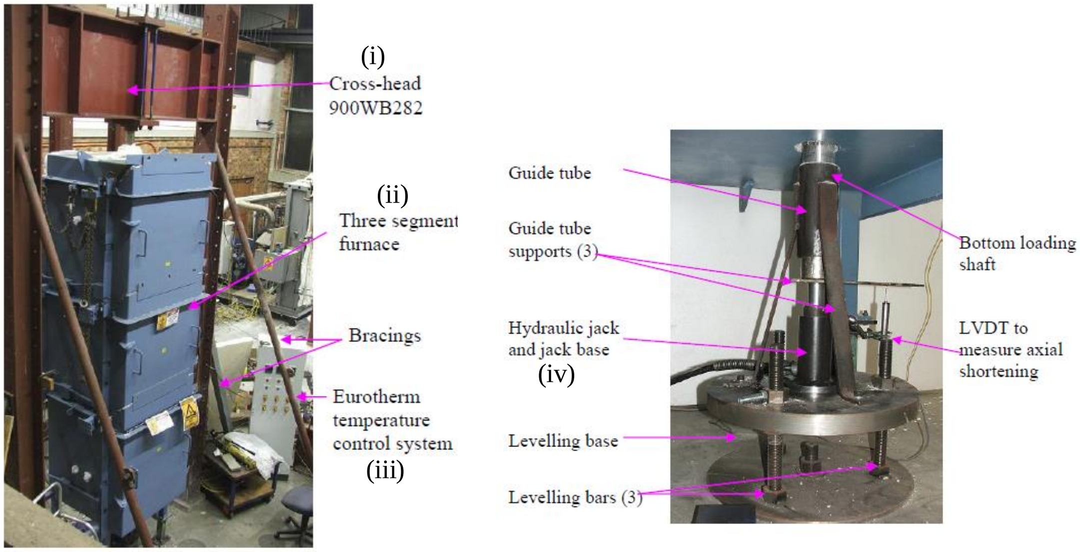

Figure 3. Overall view of the experimental test set-up used by Bandula Heva & Mahendran (2012): (a) three-segment furnace and associated temperature control system, and (b) bottom hydraulic loading system

Table 2: Columns considered in the validation study: (i) geometries and maximum initial displacement amplitudes, and (ii) comparison between the numerical failure loads reported by Bandula Heva & Mahendran (2012) and obtained in this work

T (°C)	b_w (mm)	b_f (mm)	b_l (mm)	*t* (mm)	*L* (mm)	σ_{y20} (MPa)	*Imperfection*	$P_{u.BHM}$ (kN)	$P_{u.TW}$ (kN)	$\frac{P_{u.BHM} - P_{u.TW}}{P_{u.BHM}}$
20	74.92	49.96	15.00	1.95	1740	271	L/3860	90.7	90.1	0.6%
200								84.3	76.2	9.7%
300								62.4	54.8	12.2%
400								41.1	39.9	2.9%
500								26.6	28.6	-7.4%
600								19.0	19.1	-0.4%
700								10.9	10.7	1.9%
20	74.88	49.82	14.81	1.88	1740	515	L/3577	129.0	126.3	2.1%
200								110.0	108.8	1.1%
300								96.4	92.5	4.1%
400								78.0	73.6	5.7%
500								53.4	51.3	3.8%
600								20.5	18.2	11.3%
700								11.3	11.4	-0.9%
20	57.79	36.91	8.82	0.95	1740	615	L/3437	25.4	25.4	-0.1%
200								22.5	22.6	-0.7%
300								19.3	19.7	-1.9%
400								15.8	16.0	-1.2%
600								6.2	6.5	-5.7%
700								4.6	4.3	6.5%

The column analyses (i) were performed in the code ABAQUS (adopting discretizations into fine S4R shell finite element meshes), (ii) accounted for the influence of residual stresses, (iii) included critical-mode (FT) initial geometrical imperfections with the measured amplitudes and (iv) considered steel material properties characterized by σ_{y20}=271-515-615 *MPa*, *E*=188-206-205 *GPa* and $\nu=0.3$, adopting experimentally-based Ramberg-Osgood type constitutive models previously proposed by Ranawaka & Mahendran (2009) and Kankanamge (2009) for columns made of cold-formed steel sheets with nominal thickness 0.95 *mm* (G250 steel grade) and 1.90-1.95 *mm* (G450 and G550 steel grades). As for the numerical analyses carried out in this work, they are similar to those performed by Bandula Heva & Mahendran (2012), except for the fact that (i) the ANSYS code was used (instead of ABAQUS) and (ii) the residual stresses were disregarded. The observation of Table 2 reveals that the percentage differences between the column failure loads reported by Bandula Heva & Mahendran (2012) ($P_{u.BHM}$) and obtained in this work ($P_{u.TW}$), concerning columns with three yield stresses and subjected to different temperatures, never exceed 7.4% and have a mean value equal to 2.76%. In view of this quite good correlation, it seems fair argue that the shell finite element model employed in this work may be deemed adequately validated.

4 Flexural-Torsional Response under Elevated Temperature

4.1 Elastic-Plastic Post-Buckling Behavior

The influence of the (elevated) temperature on the FT elastic-plastic post-buckling behavior and failure load of cold-formed steel C and R columns is addressed in this section. Figs. 4(a)-(b) show the equilibrium paths P/P_{crFT} *vs.* θ, where $P_{crFT}=Af_{crFT}$ and θ is the major-axis bending rotation of the mid-span cross-section, of the C_2 and R_2 columns with the L_3 lengths (corresponding to λ_{FT}=1.5) subjected to the temperatures *T*=20/100-200-300-400-500-600-700-800 *ºC*. The white circles identify the failure loads $P_{uT}=Af_{uT}$ and the room temperature elastic curves are also shown for comparative purposes. As for Figs. 5(a)-(b), they display the deformed configurations and von Mises stress contours, at collapse ($P=P_{uT}$), of the columns subjected to the temperatures *T*=20/100-300-500-700 *ºC* – in order to ensure a better visualization, only half of each column is displayed. The observation of these post-buckling results prompts the following remarks:

(i) Since the C_2 and R_2 column behaviors are, qualitatively, virtually identical, the remarks included in the next items are valid for both of them.

(ii) Naturally, the various column equilibrium paths "move down" as the temperature rises, since the strength and failure load decrease. The drop is particularly large between 500 and 600 *ºC*.

(iii) Since the thermal action effects are negligible (uniform temperature and free-to-deform columns), the FT failure modes do not depend on the temperature and, therefore, are virtually identical for all the columns analyzed. The columns always collapse after the full yielding of the top web-flange corners at the mid-height region. However, note that, at the highest temperatures ($T > 500$ *ºC*), the spread of plasticity in the columns mid-height region is less pronounced, which stems from the temperature dependence of the stress-strain curve shape – recall that k_p drops significantly for temperatures higher than 500 *ºC*. Quantitatively speaking, the stresses obviously decrease as the temperature rises and continuously erodes the steel material behavior.

(iv) As already mentioned, the equilibrium paths of the columns subjected to temperatures $T\geq600$ *ºC* are clearly below the remaining ones, this reflecting the sudden increase in the rate of the steel material behavior degradation occurring between 500 and 600 *ºC*. This is felt mostly via the proportionality limit strain and smoothness of the elliptic transition between the elastic and plastic ranges (see Figs. 2(a)-(b)). For $T\geq600$ ºC, the steel stress-strain curve exhibits again a well-defined yield plateau.

(v) No clear trend was observed concerning the influence of the temperature, geometry or yield stress on the amount of elastic-plastic strength reserve and ductility prior to failure.

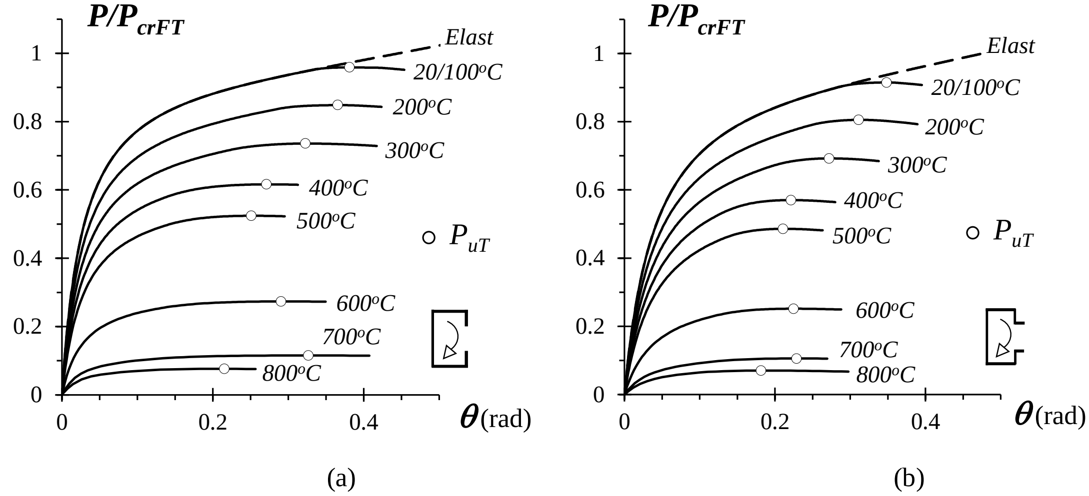

Figure 4. (a) $C_2(L_3)$ and (b) $R_2(L_3)$ columns flexural-torsional post-buckling equilibrium paths for λ_{FT}=1.5 and temperatures T=20/100-200-300-400-500-600-700-800 *ºC*

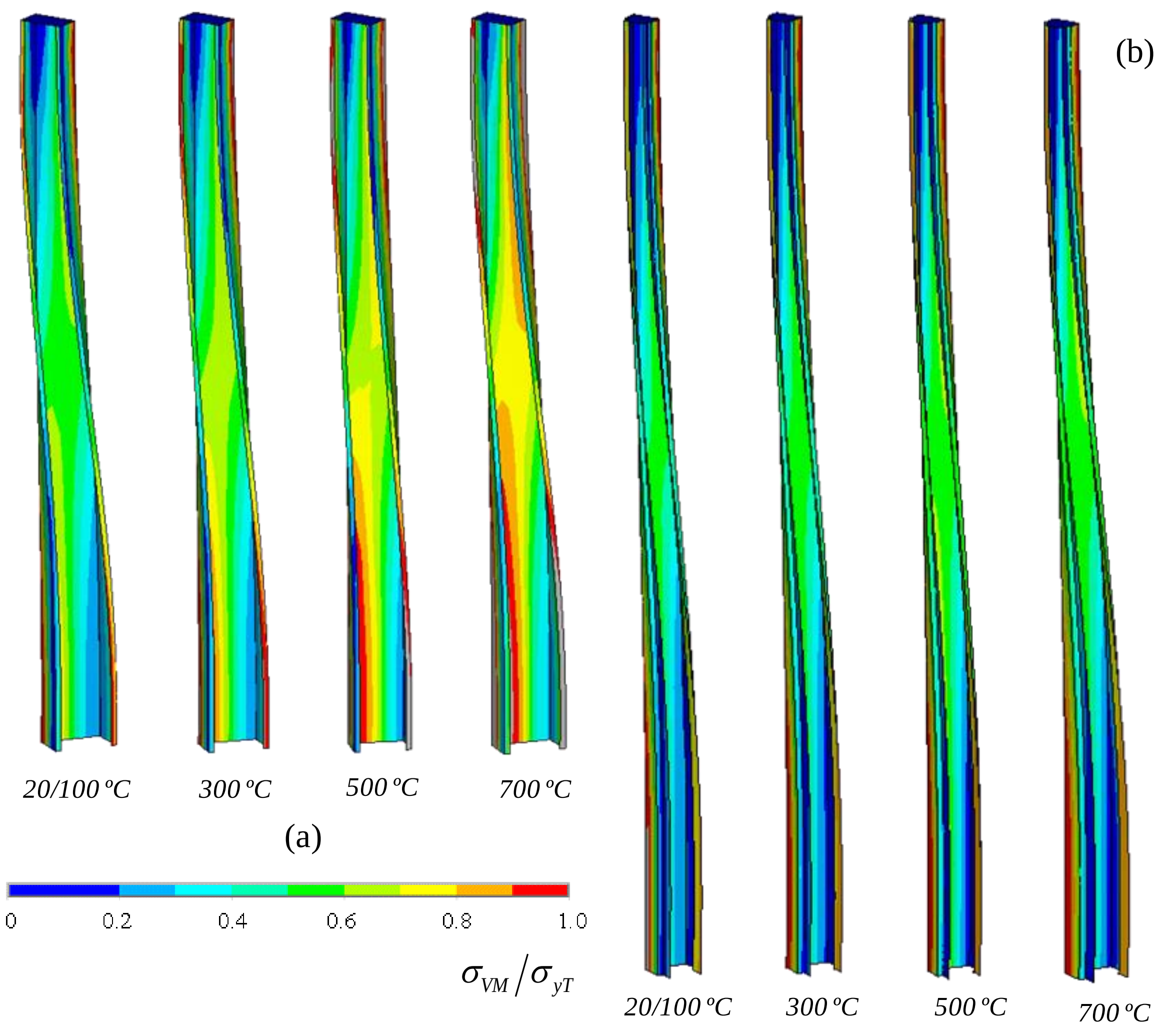

Figure 5. (a) $C_2(L_3)$ and (b) $R_2(L_3)$ columns deformed configurations and von Mises stress contours at collapse, for λ_{FT}=1.5 and temperatures T=20/100-300-500-700 *ºC*

4.2 Failure Load Data

This section presents the output of a parametric study carried out to gather the failure load data that will be used to develop and assess the merits of a DSM-based design approach intended to handle column FT failures under elevated temperatures. A total of 2400 columns are analyzed, corresponding to all possible combinations of (i) the 60 geometries (cross-section dimensions and lengths) defined in Table 1, (ii) 8 uniform temperatures (T=20/100-200-300-400-500-600-700-800 *ºC*), intended to simulate fire conditions, and (iii) 5 room temperature yield stresses (σ_{y20}=75-150-300-450-600 *MPa*), which enable covering wide FT slenderness ranges, comprised between 0.42 and 4.0. The numerical failure loads obtained in this parametric study are given in 25 tables included in Annex A: Tables A1.1 to A5.5 – the tables are divided in five sets (Table set A1 to A5), each one containing five tables. Each table set concerns all the columns with two cross-sections considered in this word (one C and one R, both sharing the same "order" – see Table 1) and their six lengths – the tables belonging to the one set only differ in the room temperature yield stress σ_{y20}. The tables also include several values related to the DSM-based prediction of the numerical failure loads that are addressed in Section 5. Figure 6 plots, against the slenderness $\lambda_{FT.T} =(\sigma_{yT} /f_{crFT.T})^{0.5}$ and for each temperature value, the ratios between the column ultimate strengths and yield stresses (f_{uT}/σ_{yT}) concerning (i) the 2400 columns analyzed in this work and (ii) the numerical (312) and experimental (39) values reported by Bandula Heva & Mahendran (2012), solely for lipped channel columns. The joint observation of these plots makes leads the following conclusions:

(i) Regardless of the temperature, the f_{uT} /σ_{yT} vs. $\lambda_{FT.T}$ "clouds" follows the trend of "Winter-type" strength curves, even if there exists some "vertical dispersion" along the whole slenderness range considered. As previously reported by Dinis *et al.* (2018, 2019a,b), in the context of column FT failures at room temperature, the R columns (black dots) exhibit lower f_{uT}/σ_{yT} values than the C ones (white dots) – this is clearly visible in the whole FT slenderness range and for all temperatures.

(ii) All f_{uT} /σ_{yT} values concerning the C and R columns with low-to-moderate slenderness ($\lambda_{FT.T}\leq 1.5$) at elevated temperatures ($T>100$ *ºC*) are below those concerning the same columns at room/moderate temperatures ($T\leq 100$ *ºC*). This is not perceptible in the moderate and high FT slenderness ranges ($\lambda_{FT.T}>1.5$). Moreover, the drop caused by the temperature increase does not follow the "logical" temperature sequence, *i.e.*, the decrease with the temperature is not monotonic. Indeed, the reduction is ordered in the sequence T=20/100-200-300-<u>800</u>-400-<u>700</u>-500-600 *ºC* (the "out of sequence" values are underlined). This unexpected finding has no obvious mechanical explanation, on the basis of the EC3:1-2 CFS temperature-dependence constitutive model, and must be investigated.

(iii) The numerical (yellow diamonds) and experimental (yellow triangles) values reported by Bandula Heva & Mahendran (2012), involving only lipped channel columns at temperatures up to 700 *ºC*, also align along a "Winter-type" curves and "mingle" fairly well with those obtained in this work. Nevertheless, they are a bit higher and exhibit more "vertical dispersion", specially the experimental ones. Recall also that the numerical ultimate strengths were obtained with experimentally-based Ramberg-Osgood constitutive models, which are quite different from the EC3:1-2 one adopted in this work. This issue will be further addressed in Section 5.

(iv) The above results are promising with respect to the possibility of developing an efficient (safe and reliable) DSM-based design approach to estimate the FT failure loads of columns subjected to elevated temperatures. Nevertheless, such results also show very clearly that the FT failure load predictions for columns at room and elevated temperatures must be handled separately in the low-to-moderate slenderness range (at least when adopting the EC3:1-2 temperature-dependence model) – the DSM design of C and R columns failing in FT modes at elevated temperatures is addressed next.

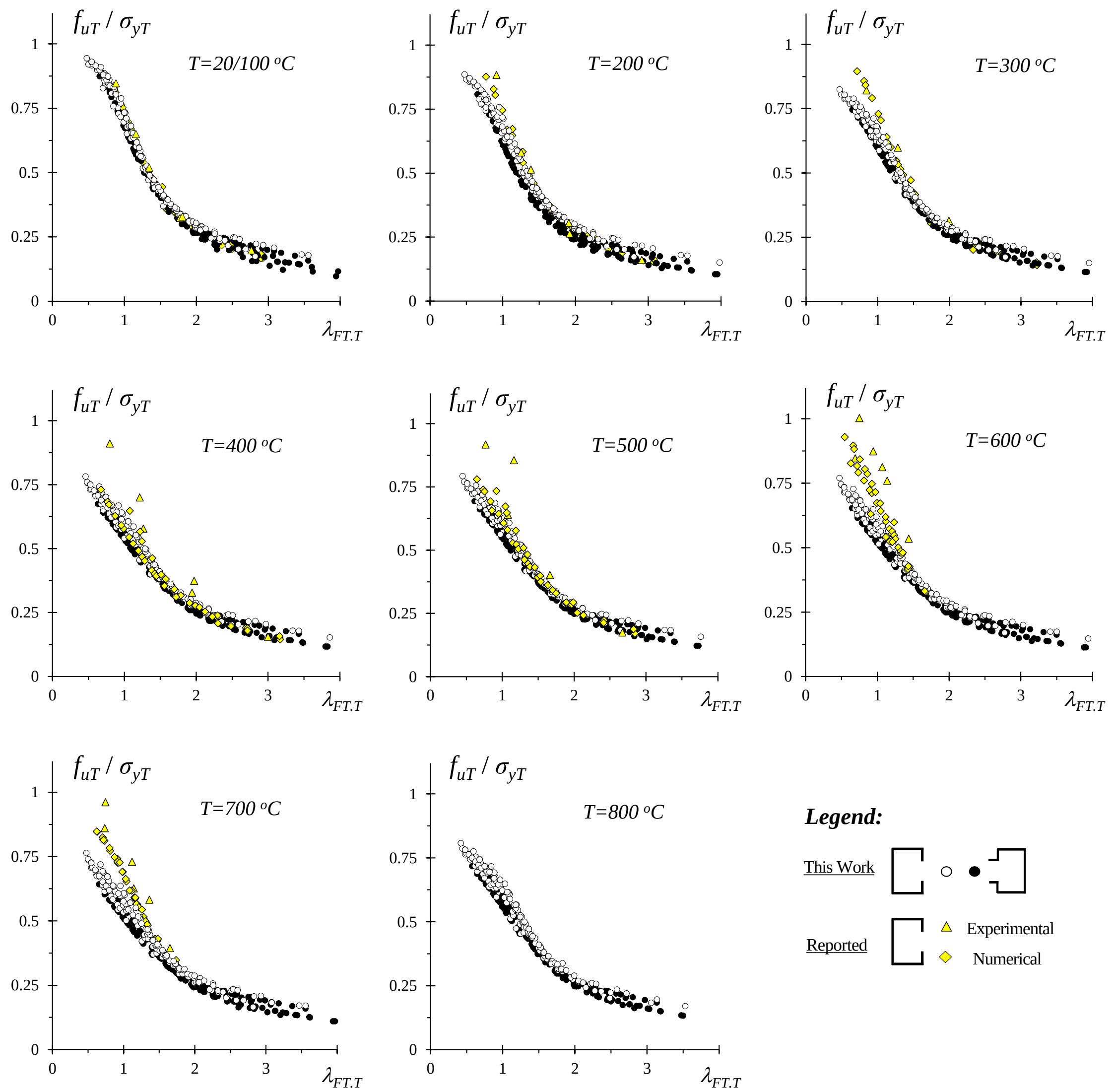

Figure 6. Plots f_{uT}/σ_{yT} vs. $\lambda_{FT.T}$ concerning the failure loads obtained in this work and reported by Bandula Heva & Mahendran (2012) for the temperatures T=20/100-200-300-400-500-600-700-800 *ºC*

5 DSM Design at Elevated Temperatures

The DSM-based prediction of the FT failure loads gathered in the previous section, concerning C and R columns at elevated temperatures, is addressed in this section. The first step consist of assessing the adequacy of the available strength curves, developed in the context of room temperature, namely (i) the current DSM global design curve, and (ii) the FT strength curve proposed by Dinis *et al.* (2019b), defined in Eqs. (1) and (3)-(5), respectively. Naturally, these strength curves must include the temperature effects associated with the EC3:1-2 constitutive, through the FT buckling (f_{crFT}) and yield (σ_{yT}) stresses. This approach was already explored by other researchers, namely Bandula Heva & Mahendran (2012) and Landesmann *et al.* (2019) (for columns buckling and failing in FT and distortional modes, respectively), but always involving solely the currently codified DSM design curves.

The influence of the temperature on f_{crFT} is felt through the Young's modulus, which decreases as the temperature rises. Therefore, the modification of Eqs. (1) and (3) consists of replacing f_{crFT} and $\sigma_{y}\equiv\sigma_{y20}$ by

$f_{crFT.T}$ and σ_{yT}, which implies that λ_{FT} also varies with T ($\lambda_{FT.T}$). Then, the nominal ultimate strengths of the CFS columns failing in FT modes are given, respectively, by the expressions

$$f_{nG.T} = \begin{cases} f_{yT} \left(0.658^{\lambda_{FT.T}^2}\right) & \text{if} \quad \lambda_{\mathrm{FT.T}} \leq 1.5 \\ f_{yT} \left(\dfrac{0.877}{\lambda_{FT.T}^2}\right) & \text{if} \quad \lambda_{\mathrm{FT.T}} > 1.5 \end{cases} , \quad (7)$$

$$f_{nFT.T} = \begin{cases} f_{yT} \left(0.658^{\lambda_{FT.T}^2}\right) & \text{if} \quad \lambda_{\mathrm{FT.T}} \leq 1.5 \\ f_{yT} \left(\dfrac{a}{\lambda_{FT.T}^b}\right) & \text{if} \quad \lambda_{\mathrm{FT.T}} > 1.5 \end{cases} , \quad (8)$$

where $\lambda_{FT.T}=(\sigma_{yT}/f_{crFT.T})^{0.5}$ and σ_{yT} and $f_{crFT.T}$ are the yield and FT buckling stresses at a given (elevated) temperature T. Parameters a and b are still given by the same functions of the geometric parameter β_{FT} (see Eqs. (4)-(5)) and, therefore, are independent of the temperature.

The plots shown in Fig. 7 make it possible to compare the (i) f_{uT}/σ_{yT} values previously displayed in Fig. 6 with (ii) the available DSM FT strength curves, including the temperature effects (black and red solid lines, respectively), for the temperatures T=20/100-200-300-400-500-600-700-800 ºC. Moreover, Tables A1.1 to A5.5, included in Annex A, provide the values of the ultimate strength ratios $f_{uT}/f_{nG.T}$ and $f_{uT}/f_{nFT.T}$ for the columns numerically analyzed in this work. As for Figs. 8 and 9, they plot, against $\lambda_{FT.T}$, all the $f_{uT}/f_{nG.T}$ and $f_{uT}/f_{nFT.T}$ values, enabling a quick and visual quantitative assessment of the quality (accuracy and safety) of the ultimate strength predictions provided by the DSM strength curves. The $f_{uT}/f_{nG.T}$ and $f_{uT}/f_{nFT.T}$ statistical indicators (averages, standard deviations and maximum/minimum values) of the whole set of columns gathered in this work are given in Tables 3 to 5, together with the numbers of "clearly unsafe" ultimate strength predictions, in the sense that $f_{uT}/f_{nG.T}$<0.95 or $f_{uT}/f_{nFT.T}$<0.95. The observation of the results presented in these figures and tables prompts the following comments:

(i) Concerning the ultimate strengths at room/moderate temperatures ($T\leq$100 ºC), it is observed that the most slender columns ($\lambda_{FT.T}$>1.5) are visibly underestimated by the current DSM design curve – the $f_{uT}/f_{nG.T}$ average, standard deviation, maximum and minimum values equal (i_1) 1.44-0.26-2.76-1.0, for the columns analyzed in this work (see Table 3), (i_2) 1.37-0.24-1.72-1.16, for the columns tested by Bandula Heva & Mahendran (2012) (see Table 4), and (i_3) 1.29-0.15-1.76-1.02, for the columns numerically analyzed by these authors (see Table 5). Only the stockier column ($\lambda_{FT.T}\leq$ 1.5) ultimate strengths are predicted accurately – the $f_{uT}/f_{nG.T}$ statistical indicators are equal to 1.06-0.03-1.15-0.99, 1.14-0.02-1.17-1.11 and 1.09-0.02-1.13-1.03, as displayed by Tables 3, 4 and 5, respectively.

(ii) Similar findings were reported by Dinis *et al.* (2019b), on the basis of the numerical failure load data gathered by them, and prompted the proposal of the strength curve set defined in Eqs. (3)-(5). It is readily observed that the ultimate strength prediction quality improves substantially for $\lambda_{FT.T}$ > 1.5, as attested by the $f_{uT}/f_{nFT.T}$ average, standard deviation and maximum/minimum values: 1.05-0.03-1.15-0.92, 1.03-0.03-1.06-1.00 and 1.00-0.04-1.16-0.90, respectively (see Tables 3 to 5).

(iii) Concerning the ultimate strength predictions yielded by Eqs. (7) and (8) for the columns subjected to elevated temperatures ($T\geq$200 ºC), it is observed the only safe and reasonably accurate ones are the $f_{nFT.T}$ values in the moderate and high slenderness range ($\lambda_{FT.T}$>1.5) and regardless of the temperature.

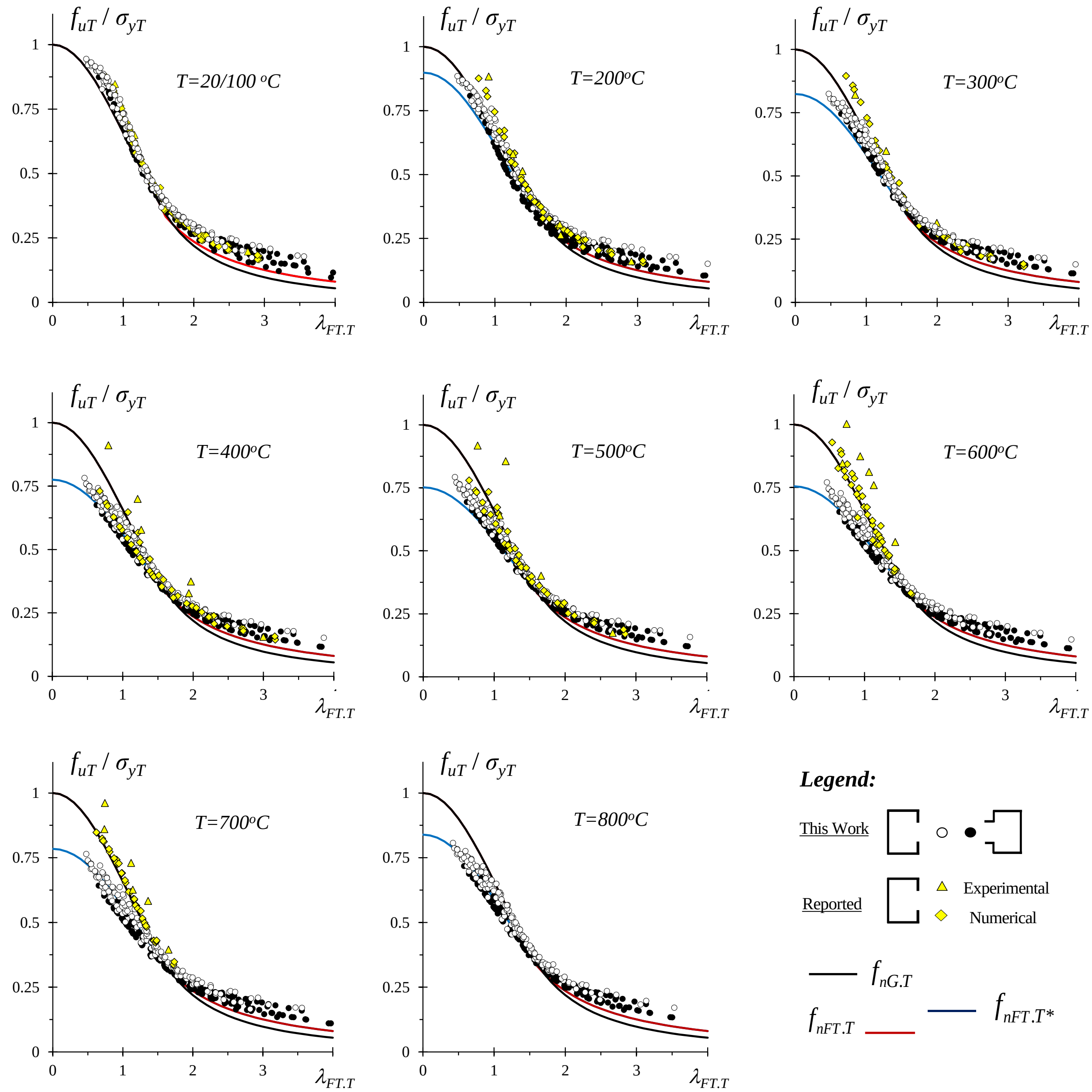

Figure 7. Comparison between the f_{uT}/σ_{yT} values and the DSM FT strength curves (T=20/100-200-300-400-500-600-700-800 ºC)

Thus, it is concluded that the DSM-based strength curve set defined in Eq. (8) constitutes an efficient design approach for columns such that $\lambda_{FT.T}>1.5$, both at room/moderate and elevated temperatures – see the red solid lines in Fig 7.

(iv) On the other hand, most of the ultimate strengths concerning columns such that $\lambda_{FT.T}\leq 1.5$ are visibly overestimated by the available DSM design curve (note that $f_{nG.T}$ and $f_{nFT.T}$ coincide for $\lambda_{FT.T}\leq 1.5$).

(v) The observation of the $f_{uT}/f_{nG.T}$ vs. $\lambda_{FT.T}$ and $f_{uT}/f_{nFT.T}$ vs. $\lambda_{FT.T}$ plots, depicted in Figs. 8 and 9, confirms that several ultimate strength predictions are excessively unsafe for the stockier columns subjected to temperatures exceeding 100 ºC ($T\geq 200$ ºC) – the numbers of such predictions increase with T. Indeed, the $f_{uT}/f_{nG.T}$ and $f_{uT}/f_{nFT.T}$ indicators provided in Table 3 show that the number of “clearly unsafe” ultimate strength predictions ($f_{uT}/f_{nG.T}<0.95$ or $f_{uT}/f_{nFT.T}<0.95$) varies between 35 (T=200 ºC
unsafe” ultimate strength predictions ($f_{uT}/f_{nG.T}<0.95$ or $f_{uT}/f_{nFT.T}<0.95$) varies between 35 (T=200 ºC –

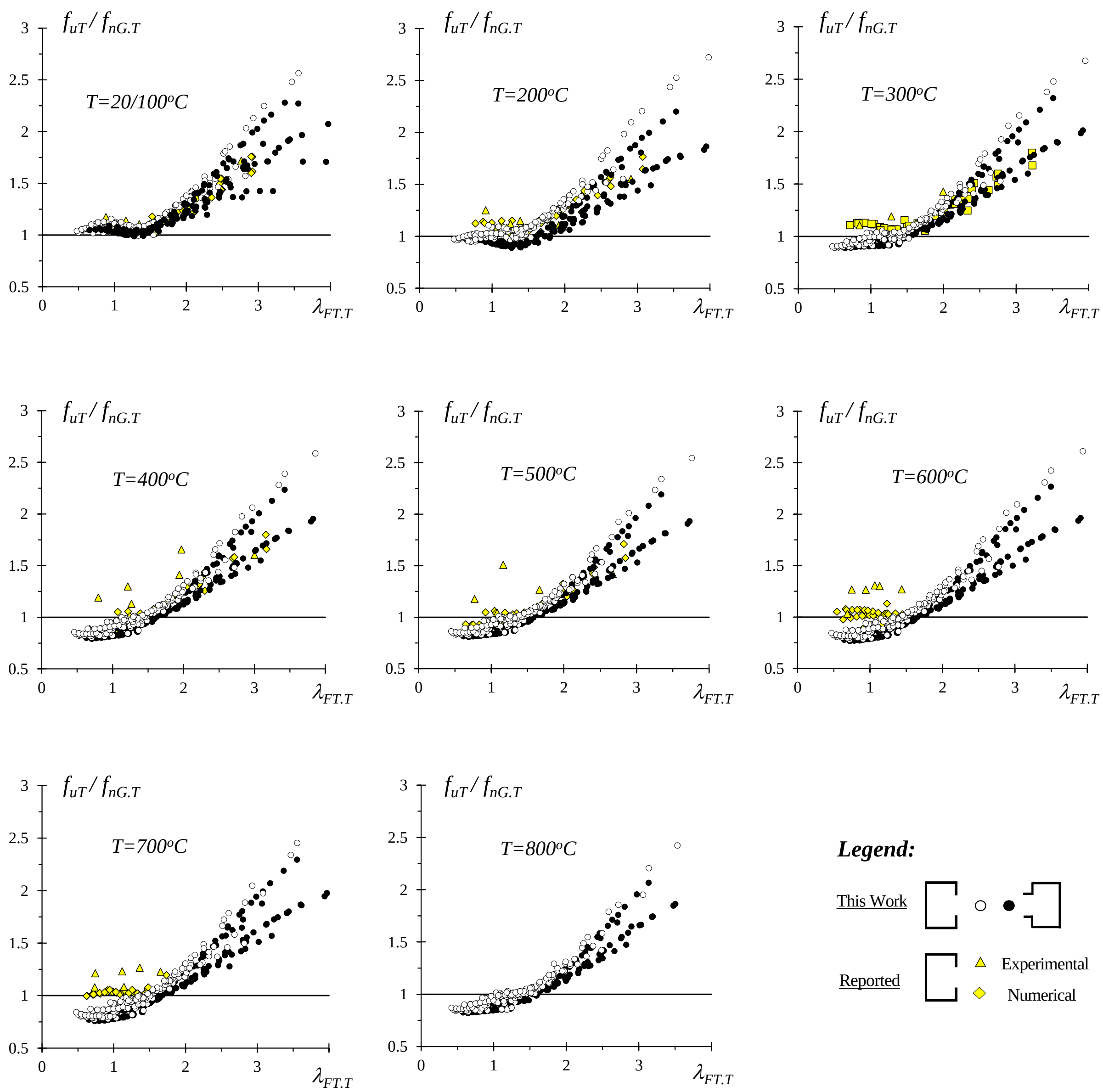

Figure 8. $f_{uT}/f_{nG.T}$ *vs.* $\lambda_{FT.T}$ plots for all the available column ultimate strengths (T=20/100-200-300-400-500-600-700-800 ºC)

25% of *140*) and 119 (T=700 ºC – *86%* of *139*). Note that, the above overestimation is slightly different for C and R columns – recall that R columns exhibit slightly lower FT ultimate strengths than the C ones (compare the black and white dots in Figs. 8 and 9).

(vi) The ultimate strength prediction quality is not significantly affected by the steel constitutive model (stress-strain-temperature curves), since, in general, the estimates of the numerical ultimate strengths reported by Bandula Heva & Mahendran (2012) "mingle" quite well with those obtained in this work. However, the ultimate strengths of the columns with $\lambda_{FT.T} \leq 1.5$ subjected to T=600 ºC and T=700 ºC are almost perfectly predicted by Eqs. (7) or (8), in contrast with the overestimations observed for the ultimate strengths of similar columns analyzed in this work. This is probably be due to the distinct steel constitutive models used – recall that Bandula Heva & Mahendran (2012) employed different constitutive models for the G250, G450 and G550 steel grades.

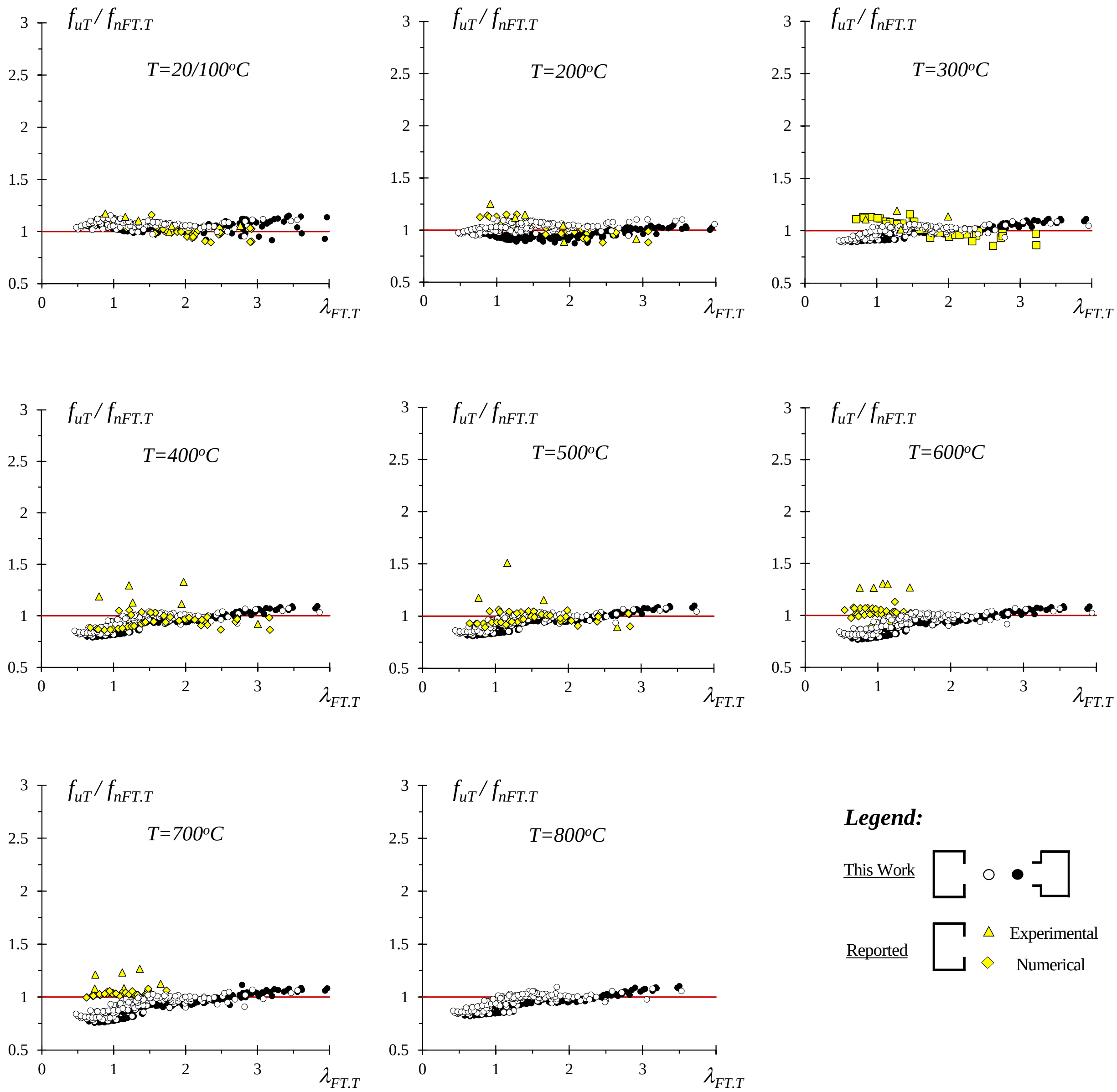

Figure 9. $f_{uT}/f_{nFT.T}$ *vs.* $\lambda_{FT.T}$ plots for all the available column ultimate strengths (T=20/100-200-300-400-500-600-700-800 ºC)

(vii) Virtually all the experimental ultimate strengths reported by Bandula Heva & Mahendran (2012) concerning columns such that $\lambda_{FT.T} \leq 1.5$ are safely and reasonably accurately predicted by Eqs. (7) and (8), identical for this slenderness range. Indeed, the $f_{uT}/f_{nG.T}$ or $f_{uT}/f_{nFT.T}$ average, standard deviation and maximum/minimum values vary between 1.10 (300 ºC) and 1.24 (500 ºC), 0.02 (20 ºC) and 0.18 (500 ºC), 1.17 (20 ºC) and 1.51 (500 ºC), 1.01 (300 ºC) and 1.13 (400 ºC), respectively (see Table 4).

(viii) In order to quantify the impact of the temperature-dependent steel constitutive model on the column FT ultimate strength, one single column (column C_2 with length L_3) is analyzed for yield stresses such that $\lambda_{FT.20}$=0.75-1.5-2.5, subjected to temperatures T=20-300-500-700 ºC and considering the three steel constitutive models (EC3:1-2, G250, G450 and G550). Fig. 10 compares the f_{uT}/σ_{yT} values obtained (also given in Table 6) with Eq. (8) and shows that there is little difference between the f_{uT}/σ_{yT} values obtained with the four steel constitutive models for $\lambda_{FT.20}$=1.5-2.5, regardless of the

Table 3: $f_{uT}/f_{nG.T}$, $f_{uT}/f_{nFT.T}$ and $f_{uT}/f_{nFT.T^*}$ statistical indicators for C and R columns numerically analyzed in this work at T=20/100-200-300-400-500-600-700-800 *°C*

T (°C)		*20/100*		*200*		*300*		*400*		*500*		*600*		*700*		*800*	
$\lambda_{FT.T}$		≤1.5	>1.5	≤1.5	>1.5	≤1.5	>1.5	≤1.5	>1.5	≤1.5	>1.5	≤1.5	>1.5	≤1.5	>1.5	≤1.5	>1.5
n		139	161	140	160	142	158	147	153	151	149	142	158	139	161	163	137
$f_{uT}/f_{nG.T}$	*Avr*	1.06	1.44	0.99	1.37	0.96	1.40	0.89	1.35	0.90	1.34	0.87	1.35	0.86	1.36	0.91	1.30
	SD	0.03	0.26	0.04	0.25	0.04	0.26	0.06	0.25	0.05	0.24	0.06	0.26	0.06	0.26	0.05	0.21
	Max	1.15	2.76	1.11	2.72	1.06	2.67	1.04	2.58	1.04	2.54	1.02	2.61	1.02	2.63	1.05	2.42
	Min	0.99	1.00	0.89	0.93	0.89	0.98	0.79	0.95	0.81	0.96	0.77	0.94	0.76	0.93	0.82	0.99
	<0.95	0	0	35	3	63	0	112	0	109	0	118	1	119	2	113	0
$f_{uT}/f_{nFT.T}$	*Avr*	1.06	1.05	0.99	0.99	0.96	1.02	0.89	0.99	0.90	1.00	0.87	0.99	0.86	0.98	0.91	1.00
	SD	0.03	0.03	0.04	0.05	0.04	0.03	0.06	0.03	0.05	0.03	0.06	0.04	0.06	0.04	0.05	0.03
	Max	1.15	1.15	1.11	1.10	1.06	1.11	1.04	1.09	1.04	1.10	1.02	1.09	1.02	1.11	1.05	1.10
	Min	0.99	0.92	0.89	0.87	0.89	0.94	0.79	0.92	0.81	0.93	0.77	0.90	0.76	0.90	0.82	0.94
	<0.95	0	4	35	47	63	1	112	22	109	14	118	37	119	44	113	5
$f_{uT}/f_{nFT.T^*}$	*Avr*	1.06	1.05	1.05	0.99	1.07	1.02	1.03	0.99	1.07	1.00	1.02	0.99	0.99	0.98	1.01	1.00
	SD	0.03	0.03	0.05	0.05	0.04	0.03	0.04	0.03	0.04	0.03	0.05	0.04	0.05	0.04	0.04	0.03
	Max	1.15	1.15	1.18	1.10	1.18	1.11	1.14	1.09	1.18	1.10	1.14	1.09	1.10	1.11	1.12	1.10
	Min	0.99	0.92	0.91	0.87	0.97	0.94	0.93	0.92	0.96	0.93	0.92	0.90	0.89	0.90	0.92	0.94
	<0.95	0	4	10	47	0	1	10	22	0	14	24	37	40	44	21	5

Table 4: $f_{uT}/f_{nG.T}$, $f_{uT}/f_{nFT.T}$ and $f_{uT}/f_{nFT.T^*}$ statistical indicators for the C columns tested by Bandula Heva & Mahendran (2012) at T=20-200-300-400-500-600-700 *°C*

T (°C)		*20*		*200*		*300*		*400*		*500*		*600*		*700*	
$\lambda_{FT.T}$		≤1.5	>1.5	≤1.5	>1.5	≤1.5	>1.5	≤1.5	>1.5	≤1.5	>1.5	≤1.5	>1.5	≤1.5	>1.5
n		3	3	3	3	3	1	3	3	3	2	6	0	5	1
$f_{uT}/f_{nG.T}$	*Avr*	1.14	1.37	1.17	1.31	1.10	1.43	1.21	1.56	1.24	1.34	1.24	0.00	1.17	1.23
	SD	0.02	0.24	0.05	0.16	0.06	0.00	0.06	0.10	0.18	0.08	0.07	0.00	0.07	0.00
	Max	1.17	1.72	1.25	1.55	1.19	1.43	1.30	1.66	1.51	1.42	1.31	0.00	1.27	1.23
	Min	1.11	1.16	1.12	1.11	1.01	1.43	1.13	1.41	1.04	1.27	1.03	0.00	1.08	1.23
	<0.95	0	0	0	0	0	0	0	0	0	0	0	0	0	0
$f_{uT}/f_{nFT.T}$	*Avr*	1.14	1.03	1.17	0.95	1.10	1.14	1.21	1.12	1.24	1.02	1.24	0.00	1.17	1.12
	SD	0.02	0.03	0.05	0.06	0.06	0.00	0.06	0.14	0.18	0.13	0.07	0.00	0.07	0.00
	Max	1.17	1.06	1.25	1.04	1.19	1.14	1.30	1.33	1.51	1.15	1.31	0.00	1.27	1.12
	Min	1.11	1.00	1.12	0.89	1.01	1.14	1.13	0.92	1.04	0.90	1.03	0.00	1.08	1.12
	<0.95	0	0	0	2	0	0	0	1	0	1	0	0	0	0
$f_{uT}/f_{nFT.T^*}$	*Avr*	1.14	1.03	1.23	0.95	1.21	1.14	1.39	1.12	1.48	1.02	1.47	0.00	1.36	1.12
	SD	0.02	0.03	0.08	0.06	0.09	0.00	0.09	0.14	0.18	0.13	0.09	0.00	0.07	0.00
	Max	1.17	1.06	1.34	1.04	1.28	1.14	1.46	1.33	1.74	1.15	1.58	0.00	1.47	1.12
	Min	1.11	1.00	1.16	0.89	1.08	1.14	1.25	0.92	1.23	0.90	1.30	0.00	1.23	1.12
	<0.95	0	0	0	2	0	0	0	1	0	1	0	0	0	0

Table 5: $f_{uT}/f_{nG.T}$, $f_{uT}/f_{nFT.T}$ and $f_{uT}/f_{nFT.T*}$ statistical indicators for the C columns numerically analyzed by Bandula Heva & Mahendran (2012) at T=20-200-300-400-500-600-700 *ºC*

	T (ºC)	*20*		*200*		*300*		*400*		*500*		*600*		*700*	
	$\lambda_{FT.T}$	≤1.5	>1.5	≤1.5	>1.5	≤1.5	>1.5	≤1.5	>1.5	≤1.5	>1.5	≤1.5	>1.5	≤1.5	>1.5
	n	34	44	16	23	16	23	18	21	22	17	37	2	37	2
$f_{uT}/f_{nG.T}$	*Avr*	1.09	1.29	1.09	1.31	1.09	1.33	0.92	1.32	0.97	1.28	1.02	1.04	1.03	1.17
	SD	0.02	0.15	0.03	0.16	0.03	0.17	0.05	0.17	0.05	0.15	0.03	0.00	0.01	0.03
	Max	1.13	1.76	1.15	1.76	1.16	1.80	1.06	1.80	1.06	1.71	1.13	1.05	1.08	1.19
	Min	1.03	1.02	1.03	1.04	1.00	1.06	0.86	0.98	0.89	1.01	0.89	1.04	1.00	1.14
	<0.95	0	0	0	0	0	0	14	0	11	0	3	0	0	0
$f_{uT}/f_{nFT.T}$	*Avr*	1.09	1.00	1.09	0.98	1.09	0.97	0.92	0.96	0.97	0.99	1.02	0.96	1.03	1.04
	SD	0.02	0.04	0.03	0.04	0.03	0.04	0.05	0.03	0.05	0.03	0.03	0.00	0.01	0.03
	Max	1.13	1.16	1.15	1.06	1.16	1.09	1.06	1.03	1.06	1.05	1.13	0.96	1.08	1.06
	Min	1.03	0.90	1.03	0.88	1.00	0.86	0.86	0.86	0.89	0.90	0.89	0.95	1.00	1.01
	<0.95	0	8	0	4	0	8	14	7	11	3	3	0	0	0
$f_{uT}/f_{nFT.T*}$	*Avr*	1.09	1.00	1.15	0.98	1.20	0.97	1.05	0.96	1.13	0.99	1.20	0.96	1.17	1.04
	SD	0.02	0.04	0.05	0.04	0.06	0.04	0.05	0.03	0.05	0.03	0.08	0.00	0.05	0.03
	Max	1.13	1.16	1.23	1.06	1.31	1.09	1.22	1.03	1.27	1.05	1.36	0.96	1.24	1.06
	Min	1.03	0.90	1.06	0.88	1.07	0.86	1.00	0.86	1.05	0.90	1.03	0.95	1.08	1.01
	<0.95	0	8	0	4	0	8	0	7	0	3	0	0	0	0

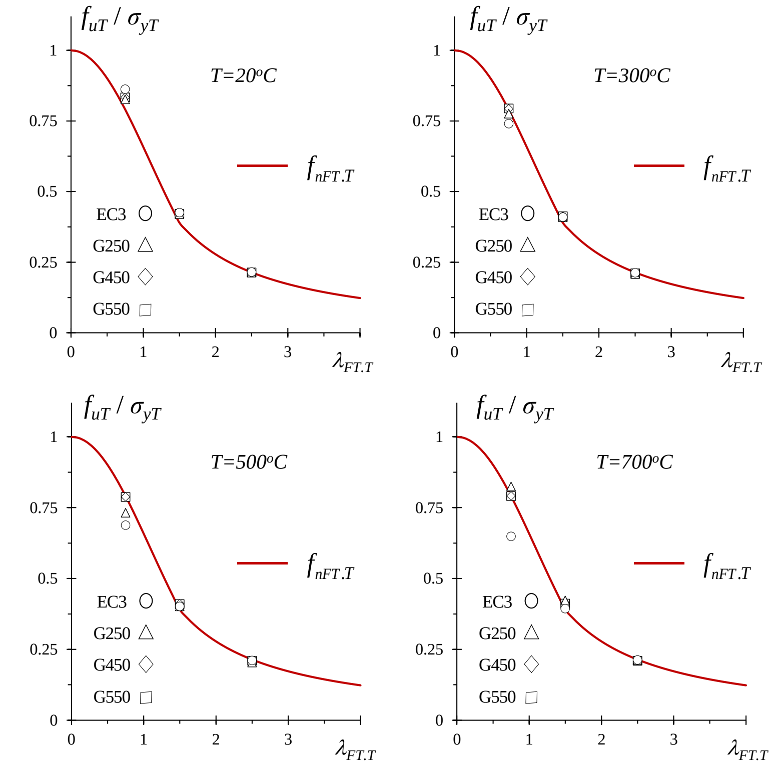

Figure 10. Comparison between the design curve given by Eq. (8) and f_{uT}/σ_{yT} values of column C_2 with length L_3 and $\lambda_{FT.20}$=0.75-1.5-2.5 under T=20-300-500-700*ºC*, obtained with the EC3:1-2, G250, G450 and G550 constitutive models

Table 6: Influence of steel constitutive model adopted on the f_{uT}/σ_{yT} values of columns C_2 with length L_3 and $\lambda_{FT.20}$=0.75-1.5-2.5 under T=20-300-500-700 ºC

$\lambda_{FT.F}$	*Model*	f_{uT}/σ_{yT} 20 ºC	300 ºC	500 ºC	700 ºC
0.75	EC3	0.86	0.74	0.69	0.65
	G250	0.83	0.78	0.73	0.82
	G450	0.83	0.79	0.79	0.79
	G550	0.83	0.79	0.79	0.79
1.5	EC3	0.43	0.41	0.40	0.39
	G250	0.42	0.41	0.40	0.42
	G450	0.42	0.41	0.41	0.41
	G550	0.42	0.41	0.41	0.41
2.5	EC3	0.22	0.21	0.21	0.21
	G250	0.21	0.21	0.20	0.21
	G450	0.21	0.21	0.21	0.21
	G550	0.21	0.21	0.21	0.21

temperature. However, the picture changes for $\lambda_{FT.20}$=0.75, since the f_{uT}/σ_{yT} values obtained with the EC3:1-2 model are visibly apart from the remaining ones, particularly for T=500 ºC and T=700 ºC – they are ordered according to the constitutive model sequence EC3:1-2-G250-G450-G550.

(ix) In view of the findings reported in the above items, it is clear that the available DSM design curve is not able to predict adequately the FT ultimate strengths of columns such that $\lambda_{FT.T}\leq 1.5$ (low-to-moderate slenderness) at elevated temperatures – a large number these ultimate strength predictions are substantially unsafe. In order to improve them, it is necessary to modify/lower the existing strength curve (Eq. (7) or (8)) valid for low-to-moderate slenderness range. This issue will be addressed in the next section (Section 5.1).

5.1 Modification/lowering of the DSM design curve (low-to-moderate slenderness range)

On the basis of the numerical failure load data gathered in this work (see Section 4.2), a first attempt is now made to modify/lower the available DSM design curve valid for the low-to-moderate slenderness range ($\lambda_{FT.T}\leq 1.5$), so that it is able to predict adequately the ultimate strengths of C and R columns failing in FT modes at elevated temperatures. The main idea behind this attempt is to incorporate a temperature-dependence reduction factor (η) in the expressions providing the DSM strength curve for $\lambda_{FT.T}\leq 1.5$, while retaining Eq. (8) for $\lambda_{FT.T}>1.5$. A "trial- and-error" curve fitting procedure led to the sought expression, termed $f_{nFT.T^*}$ (the asterisk identifies the presence of the modification for $\lambda_{FT.T}\leq 1.5$),

$$f_{nFT.T^*}=\begin{cases} f_{yT}\ \left(\eta\cdot 0.658\right)^{\eta\cdot\lambda_{FT.T}^2} & \text{if}\quad \lambda_{FT.T}\leq 1.5 \\ f_{yT}\ \left(\dfrac{a}{\lambda_{FT.T}^{b}}\right) & \text{if}\quad \lambda_{FT.T}>1.5 \end{cases}\quad \text{with}\quad \eta=1.3\cdot 10^{-6}T^2-1.4\cdot 10^{-3}T+1.127\leq 1\ . \quad (9)$$

These strength curve set differs from Eq. (8) in the presence of factor η factor multiplying both (i) the coefficient 0.658 and (ii) the exponent $\lambda_{FT.T}^2$. The DSM-based FT design curves provided by Eq. (9) are displayed in Fig. 11 (and also plotted in Fig. 7, as solid blue lines). It is worth mentioning that the room/moderate temperature ($T\leq 100$ ºC) curve remains unchanged (η=1). Since the modification of the current design curve is based on the numerical ultimate strengths obtained in this work, adopting the

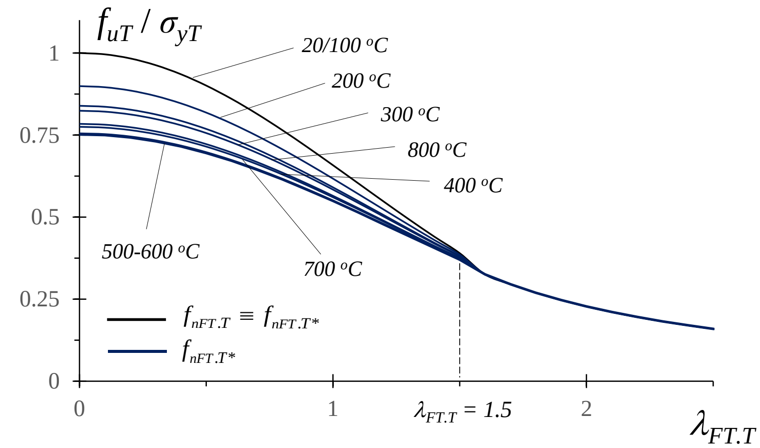

Figure 11. Modified/lowered DSM-based FT strength curves for columns under T=20/100-200-300-400-500-600-700-800*ºC*

EC3:1-2 steel constitutive model, it is just logical that the new design curves (for $\lambda_{FT.T} \leq 1.5$) are ordered according to their previous predictions, *i.e.*, in the sequence T=20/100-200-300-800-400-700-500-600*ºC*.

In order to assess the quality of the ultimate strength predictions provided by the $f_{uT}/f_{nFT.T^*}$ values, Fig. 12 plot the ratios $f_{uT}/f_{nFT.T^*}$ against $\lambda_{FT.T}$ – the associated statistical indicators are provided in Tables 3 to 5 and the $f_{uT}/f_{nFT.T^*}$ values (for the columns analyzed in this work) are given in Tables A1.1 to A5.5, included in Annex A. The observation of these ultimate strength predictions leads to the following conclusions:

(i) Despite the inherent simplicity of the modification, the ultimate strength prediction quality improved considerably for the stockier ($\lambda_{FT.T} \leq 1.5$) columns analyzed in this work. Naturally, the estimates of the experimental and numerical ultimate strengths reported by Bandula Heva & Mahendran (2012) are now a bit safer, but still reasonably accurate, as attested by the $f_{uT}/f_{nFT.T^*}$ statistical indicators provided in Tables 4 and 5. Indeed, the averages, standard deviations and maximum/minimum values vary between 1.05 and 1.48, 0.02 and 0.18, 1.13 and 1.74, and 1.00 and 1.30, respectively.

(ii) The $f_{uT}/f_{nFT.T^*}$ statistical indicators concerning the ultimate strengths obtained in this work for columns with $\lambda_{FT.T} \leq 1.5$, given in Table 3, become also fairly good and are similar for all the temperatures considered. Indeed, the average, standard deviation and maximum/minimum values vary from 0.99 to 1.07, 0.03 to 0.05, 1.10 to 1.18 and 0.89 to 0.99, respectively. Although the numbers of unsafe ultimate strength predictions are still substantial for columns under at $T \geq 600$ºC, the amounts of overestimation are considerably reduced – they never exceed 8%.

The fact that the quite small proposed modification was shown to improve visibly the ultimate strength prediction quality, for columns with $\lambda_{FT.T} \leq 1.5$), provides encouragement to proceed along this path in the search for an efficient DSM-based design approach for columns exhibiting FT failures at elevated temperatures. The next step of this ongoing investigation consists of looking for additional experimental and numerical ultimate strength data available in the literature. This is by no means an easy task, since, to the authors' best knowledge, the number of works dealing specifically with column FT failures under elevated temperature is very scarce – indeed, it is expected that the available ultimate strength data will be dispersed among studies having different focuses. Then, the merits of the strength curves defined in Eq. (9) in predicting these additional ultimate strengths will be assessed – such assessment will provide either additional evidence on the adequacy of these strength curves or guidelines on how to improve them. It is also worth noting that the authors are also planning, for the near future, the performance of a test campaign involving lipped channel columns failing in FT modes at both room and elevated temperatures.

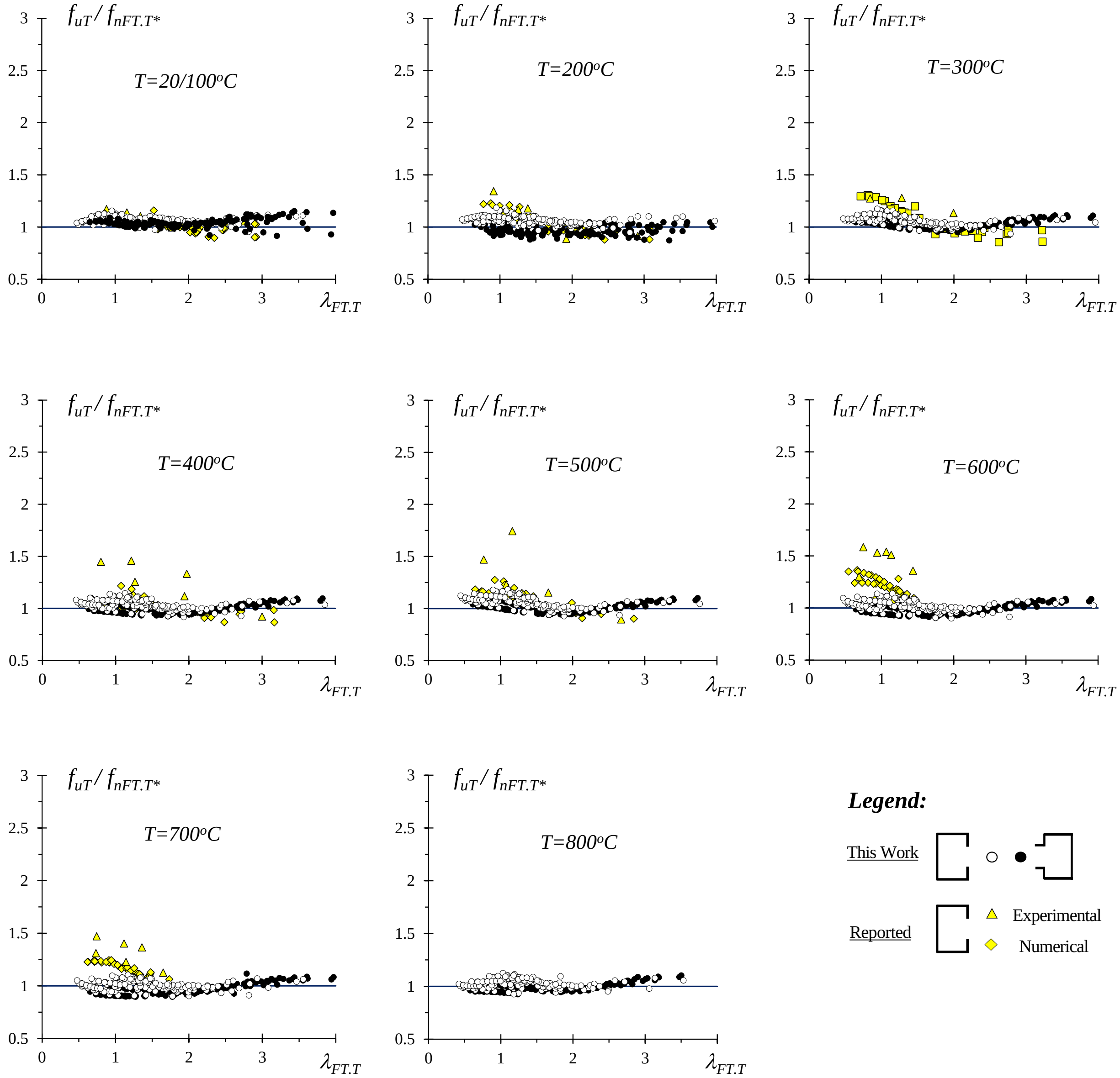

Figure 12. $f_{uT}/f_{nFT.T*}$ *vs.* $\lambda_{FT.T}$ plots of the ultimate strengths considered in this work (*T*=20/100-200-300-400-500-600-700-800 ºC)

6 Concluding Remarks

This paper reported the most recent results of an ongoing investigation, initiated by the authors a few years ago, on the post-buckling behavior, ultimate strength and DSM design of cold-formed steel columns failing in flexural-torsional modes. Its scope has been extended in this work to cover columns subjected to elevated temperatures, typically caused by fire conditions. After addressing the column geometry selection and the influence of the temperature on the column flexural-torsional post-buckling behavior, numerical ultimate strengths were obtained for 2400 columns exhibiting (i) two cross-section shapes (lipped channels and racks) with various dimensions and lengths (60 geometries per cross-section shape), (ii) 5 room temperature yield stresses, chosen to enable covering wide flexural-torsional slenderness ranges ($0.42 \leq \lambda_{FT.T} \leq 4.0$), and (iii) eight uniform temperatures (up to 800 ºC).

The flexural-torsional ultimate strength obtained in this work, together with the 39 experimental and 312 numerical values reported by Bandula Heva & Mahendran (2012), were subsequently used to propose a first contribution towards the development of an efficient DSM-based design approach for columns failing in flexural-torsional modes at elevated temperatures. Out of the various findings reported in this work, the following ones deserve to be specially mentioned:

(i) Regardless of the temperature, the f_{uT}/σ_{yT} vs. $\lambda_{FT.T}$ "clouds" follow "Winter-type" curve trends, even if there exists some "vertical dispersion" in the low-to-moderate slenderness range ($\lambda_{FT.T}\leq 1.5$) – this dispersion was found to be higher for the columns tested and numerically analyzed by Bandula Heva & Mahendran (2012). No such visible vertical dispersion was observed for columns with $\lambda_{FT.T}>1.5$.

(ii) All f_{uT}/σ_{yT} values of columns with $\lambda_{FT.T}\leq 1.5$ at elevated temperatures ($T>100$ ºC) were found to fall below those concerning the same columns at room/moderate temperatures ($T\leq 100$ ºC). This did not happen for the columns with $\lambda_{FT.T}>1.5$.

(iii) Concerning the ultimate strengths at room/moderate temperatures ($T\leq 100$ ºC), it was observed that those concerning columns with $\lambda_{FT.T}>1.5$ are visibly underestimated by the current DSM design curve (AISI 2016). This observation led to the proposal, by Dinis *et al.* (2019b), of a novel DSM-based flexural-torsional design curve set, which was shown to improve substantially the ultimate strength prediction quality. On the other hand, most ultimate strengths of columns with $\lambda_{FT.T}\leq 1.5$ under elevated temperatures ($T\geq 200$ ºC) are visibly overestimated by the available DSM FT design curve – recall that the curves of Dinis *et al.* (2019b) coincide with the codified one for $\lambda_{FT.T}\leq 1.5$.

(iv) The DSM FT design curve set proposed by Dinis *et al.* (2019b), including temperature-dependent critical (FT) buckling and squash stresses loads, was used to predict the ultimate strengths of columns at elevated temperatures. Fairly accurate and mostly safe ultimate strength predictions are provided only for columns with $\lambda_{FT.T}>1.5$. In the low-to-moderate slenderness range ($\lambda_{FT.T}\leq 1.5$), several column ultimate strengths are clearly overestimated, thus showing that some modification is needed.

(v) The existing FT strength curve for columns with $\lambda_{FT.T}\leq 1.5$, which is the currently codified one (it was not altered by the proposal of Dinis et al. (2019b)), was modified through the multiplication by a temperature-dependent reduction factor η. In spite of the inherent simplicity of this modification, the ensuing DSM-based temperature-dependent "lowered" strength curve set improves considerable the column ultimate strength prediction quality, thus providing encouragement to proceed along this path in the search for with an efficient DSM-based design approach for columns failing in FT modes at elevated temperatures.

The next steps of this ongoing investigation consist of (i) conducting a test campaign involving lipped channel columns, carefully selected to fail in FT modes at room and elevated temperatures, and (ii) performing parametric studies to gather failure load data concerning columns with a wide variety of cross-section shapes and dimensions and also failing in FT modes at room and elevated temperatures – *e.g.*, those considered by Dinis *et al.* 2019b: plain channels, hat-sections, return lipped channels, web-stiffened lipped channels and web/flange-stiffened lipped channels.

References

ABNT (Brazilian Standards Association) (2010). *Brazilian Standard on Design of Cold-Formed Steel Structures* (ABNT NBR 14762:2010), Rio de Janeiro. (Portuguese)

AISC (American Institute of Steel Construction) (1986). *Load and Resistance Factor Design Specification for Structural Steel Buildings* (AISC 328:1986), Chicago IL.

AISI (American Iron and Steel Institute) (1996). *Cold-Formed Steel Design Manual*, Washington DC.

AISI (American Iron and Steel Institute) (2016). *North American Specification (NAS) for the Design of Cold-Formed Steel Structural Members* (AISI-S100-16) + respective *Commentary*, Washington DC.

AS/NZS (Standards of Australia – SA – and Standards of New Zealand – SNZ) (2018). *Cold-Formed Steel Structures* (AS/NZS 4600:2018 – 3rd ed.), Sydney-Wellington.

Bandula Heva Y (2009). *Behaviour and Design of Cold-formed Steel Compression Members at Elevated Temperatures*, PhD Thesis, Queensland University of Technology, Brisbane, Australia.

Bandula Heva Y, Mahendran M (2012). Flexural-torsional buckling tests of cold-formed steel compression members at elevated temperatures, *Steel and Composite Structures*, **14**(3), 205-227.

Bebiano R, Camotim D, Gonçalves R (2018). GBTUL 2.0 – a second-generation code for the GBT-based buckling and vibration analysis of thin-walled members, *Thin-Walled Structures*, **124**(March), 235-257.

Camotim D, Dinis PB, Martins AD (2016). Direct Strength Method (DSM) – a general approach for the design of cold-formed steel structures, *Recent Trends in Cold-Formed Steel Construction*, C. Yu (ed.), Woodhead Publishing (Series in Civil and Structural Engineering), Amsterdam, 69-105.

Comité Européen de Normalisation (CEN) (2005). *Eurocode 3: Design of Steel Structures – Part 1.2: General Rules – Structural Fire Design*, Brussels.

Dinis PB, Camotim D, Martins AD (2018). On the accuracy of the current Direct Strength Method (DSM) design curve for columns failing in global modes, *Website Proceedings of Structural Stability Research Council (SSRC) Annual Stability Conference* (Baltimore, 10-13/4).

Dinis PB, Camotim D, Landesmann A, Martins AD (2019a). On the Direct Strength Method design of columns against global failure, *Thin-Walled Structures*, **139**(June), 242-270.

Dinis PB, Camotim D, Landesmann A, Martins AD (2019b). Improving the Direct Strength Method prediction of column flexural-torsional failure loads, *Thin-Walled Structures*, in press. (https://doi.org/10.1016/j.tws.2019.106461)

Ellobody E, Young B (2005). Behavior of cold-formed steel plain angle columns, *Journal of Structural Engineering* (ASCE), **131**(3), 469-478.

Kankanamge ND (2009). *Flexural Behaviour of Cold-formed Steel Beams at Elevated Temperatures*, PhD thesis, Queensland University of Technology (QUT), Brisbane, Australia.

Landesmann A, Camotim D (2011). On the distortional buckling, post-buckling and strength of cold-formed steel lipped channel columns under fire conditions, *Journal of Structural Fire Engineering*, **2**(1), 1-19.

Landesmann A, Camotim D, Silva FCM (2019). DSM design of cold-formed steel columns failing in distortional modes at elevated temperatures, *International Journal of Steel Structures*, **19**(3), 1023-1041.

Li Z, Abreu JCB, Leng J, Ádány S, Schafer BW (2014). Review: constrained finite strip method developments and applications in cold-formed steel design, *Thin-Walled Structures*, **81**(August), 2-18.

Peköz T, Sümer O (1992), *Design Provisions for Cold-Formed Steel Columns and Beam-Column*, Research Report RP92-1, American Iron and Steel Institute, Washington DC.

Ranawaka T, Mahendran M (2009). Experimental study of the mechanical properties of light gauge cold-formed steels at elevated temperatures, *Fire Safety Journal*, **147**(2), 219-229.

SAS (Swanson Analysis Systems Inc.) (2009). *ANSYS Reference Manual* (version 12).

Schafer B.W. (2019). Advances in the Direct Strength Method of cold-formed steel design, *Thin-Walled Structures*, **140**(July), 533-541.

Ziemian R (editor) (2010). *Guide to Stability Design Criteria for Metal Structures* (6th edition), John Wiley & Sons, Hoboken.

ANNEX A – Data Concerning C and R Columns at Room and Elevated Temperatures

The sets of Tables A1 to A5 provide information concerning the column numerical failure loads, at room and elevated temperatures (T=20/100 to T=800 $ºC$), and their DSM-based estimates. Each table shows the results of all the columns with two cross-sections dealt with in this work (one C and one R, both sharing the same "order" – see Table 1) – recall that six lengths are considered for each cross-section (L_1 to L_6 – see Table 1). Each set comprises five tables, one per yield stress considered (σ_{y20} =75-150-300-450-600 MPa), which leads to a total of 25 tables. The values presented are (i) FT slenderness values ($\lambda_{FT.T}$), (ii) ratios between FT ultimate strengths and yield stresses (f_{uT}/σ_{yT}), and (iii) three numerical-to-predicted ultimate strength ratios ($f_{uT}/f_{nG.T}$, $f_{uT}/f_{nFT.T}$, and $f_{uT}/f_{nF.FT*}$).

Table A1.1: Numerical failure loads and their DSM estimates concerning the **C₁** and **R₁** columns with σ_{y20}=**75 *MPa***.

L	T (ºC)	**C_1**					**R_1**				
		$\lambda_{FT.T}$	f_{uT}/σ_{yT}	$f_{uT}/f_{nG.T}$	$f_{uT}/f_{nFT.T}$	$f_{uT}/f_{nF.FT^*}$	$\lambda_{FT.T}$	f_{uT}/σ_{yT}	$f_{uT}/f_{nG.T}$	$f_{uT}/f_{nFT.T}$	$f_{uT}/f_{nF.FT^*}$
L_1	20/100	0.545	0.916	1.038	1.038	1.038	0.735	0.842	1.055	1.055	1.055
	200	0.542	0.857	0.969	0.969	1.065	0.731	0.773	0.967	0.967	1.052
	300	0.538	0.787	0.889	0.889	1.056	0.726	0.716	0.892	0.892	1.042
	400	0.525	0.731	0.821	0.821	1.032	0.708	0.640	0.790	0.790	0.972
	500	0.513	0.745	0.831	0.831	1.076	0.691	0.661	0.807	0.807	1.021
	600	0.536	0.715	0.806	0.806	1.037	0.723	0.615	0.766	0.766	0.961
	700	0.545	0.706	0.800	0.800	0.993	0.735	0.603	0.755	0.755	0.918
	800	0.481	0.763	0.841	0.841	0.987	0.648	0.687	0.819	0.819	0.949
L_2	20/100	0.734	0.839	1.051	1.051	1.051	0.873	0.764	1.051	1.051	1.051
	200	0.730	0.788	0.985	0.985	1.071	0.868	0.701	0.961	0.961	1.036
	300	0.725	0.721	0.898	0.898	1.048	0.862	0.662	0.903	0.903	1.038
	400	0.707	0.651	0.802	0.802	0.988	0.841	0.595	0.800	0.800	0.965
	500	0.690	0.671	0.818	0.818	1.036	0.820	0.616	0.816	0.816	1.012
	600	0.722	0.627	0.779	0.779	0.979	0.859	0.567	0.772	0.772	0.947
	700	0.734	0.614	0.770	0.770	0.935	0.873	0.553	0.760	0.760	0.905
	800	0.647	0.697	0.831	0.831	0.962	0.770	0.646	0.827	0.827	0.948
L_3	20/100	0.921	0.728	1.038	1.038	1.038	1.010	0.672	1.030	1.030	1.030
	200	0.916	0.693	0.985	0.985	1.057	1.004	0.608	0.928	0.928	0.989
	300	0.909	0.643	0.908	0.908	1.037	0.997	0.599	0.909	0.909	1.025
	400	0.887	0.584	0.811	0.811	0.972	0.973	0.549	0.815	0.815	0.962
	500	0.865	0.605	0.828	0.828	1.019	0.949	0.567	0.827	0.827	1.002
	600	0.906	0.557	0.786	0.786	0.957	0.993	0.519	0.785	0.785	0.940
	700	0.921	0.544	0.776	0.776	0.917	1.010	0.506	0.775	0.775	0.902
	800	0.812	0.637	0.839	0.839	0.956	0.890	0.601	0.838	0.838	0.947
L_4	20/100	1.036	0.650	1.019	1.019	1.019	1.144	0.579	1.002	1.002	1.002
	200	1.031	0.625	0.976	0.976	1.037	1.138	0.527	0.906	0.906	0.954
	300	1.023	0.587	0.910	0.910	1.022	1.130	0.534	0.911	0.911	1.006
	400	0.999	0.540	0.820	0.820	0.964	1.102	0.495	0.824	0.824	0.948
	500	0.974	0.562	0.836	0.836	1.007	1.075	0.517	0.838	0.838	0.988
	600	1.020	0.514	0.794	0.794	0.945	1.126	0.472	0.802	0.802	0.933
	700	1.036	0.501	0.786	0.786	0.910	1.144	0.457	0.791	0.791	0.896
	800	0.914	0.596	0.845	0.845	0.952	1.009	0.554	0.849	0.849	0.945
L_5	20/100	1.258	0.516	1.001	1.001	1.001	1.276	0.499	0.987	0.987	0.987
	200	1.251	0.502	0.967	0.967	1.007	1.269	0.453	0.889	0.889	0.924
	300	1.242	0.481	0.917	0.917	0.993	1.260	0.470	0.913	0.913	0.985
	400	1.212	0.455	0.843	0.843	0.947	1.229	0.445	0.838	0.838	0.938
	500	1.183	0.475	0.853	0.853	0.981	1.199	0.465	0.849	0.849	0.972
	600	1.238	0.434	0.825	0.825	0.933	1.255	0.424	0.819	0.819	0.923
	700	1.258	0.422	0.818	0.818	0.904	1.276	0.411	0.813	0.813	0.895
	800	1.110	0.512	0.857	0.857	0.940	1.125	0.503	0.854	0.854	0.935
L_6	20/100	1.416	0.443	1.025	1.025	1.025	1.404	0.434	0.992	0.992	0.992
	200	1.408	0.432	0.991	0.991	1.014	1.396	0.395	0.893	0.893	0.915
	300	1.398	0.416	0.944	0.944	0.992	1.387	0.413	0.924	0.924	0.974
	400	1.364	0.400	0.871	0.871	0.943	1.353	0.399	0.858	0.858	0.931
	500	1.331	0.417	0.875	0.875	0.968	1.320	0.418	0.866	0.866	0.962
	600	1.393	0.381	0.859	0.859	0.933	1.381	0.380	0.844	0.844	0.919
	700	1.416	0.370	0.857	0.857	0.912	1.404	0.368	0.841	0.841	0.897
	800	1.249	0.453	0.871	0.871	0.934	1.238	0.453	0.861	0.861	0.925

Table A1.2: Numerical failure loads and their DSM estimates concerning the **C_1** and **R_1** columns with σ_{y20}**=150** ***MPa***.

L	*T* (ºC)	C_1					R_1				
		$\lambda_{FT.T}$	f_{uT}/σ_{yT}	$f_{uT}/f_{nG.T}$	$f_{uT}/f_{nFT.T}$	$f_{uT}/f_{nF.FT*}$	$\lambda_{FT.T}$	f_{uT}/σ_{yT}	$f_{uT}/f_{nG.T}$	$f_{uT}/f_{nFT.T}$	$f_{uT}/f_{nF.FT*}$
L_1	20/100	0.771	0.848	1.087	1.087	1.087	1.039	0.685	1.077	1.077	1.077
	200	0.767	0.743	0.950	0.950	1.031	1.033	0.627	0.981	0.981	1.043
	300	0.761	0.744	0.948	0.948	1.103	1.026	0.622	0.966	0.966	1.085
	400	0.743	0.686	0.864	0.864	1.058	1.001	0.575	0.874	0.874	1.027
	500	0.725	0.703	0.876	0.876	1.103	0.977	0.596	0.889	0.889	1.070
	600	0.759	0.666	0.847	0.847	1.057	1.022	0.549	0.851	0.851	1.013
	700	0.771	0.655	0.840	0.840	1.015	1.039	0.536	0.842	0.842	0.974
	800	0.680	0.727	0.882	0.882	1.019	0.916	0.631	0.896	0.896	1.009
L_2	20/100	1.038	0.677	1.062	1.062	1.062	1.234	0.545	1.031	1.031	1.031
	200	1.032	0.636	0.993	0.993	1.056	1.227	0.494	0.928	0.928	0.969
	300	1.025	0.620	0.962	0.962	1.081	1.219	0.517	0.963	0.963	1.048
	400	1.000	0.577	0.877	0.877	1.029	1.189	0.493	0.891	0.891	1.006
	500	0.976	0.598	0.890	0.890	1.073	1.160	0.514	0.904	0.904	1.045
	600	1.021	0.553	0.855	0.855	1.018	1.214	0.471	0.873	0.873	0.994
	700	1.038	0.539	0.846	0.846	0.979	1.234	0.457	0.865	0.865	0.962
	800	0.915	0.632	0.897	0.897	1.010	1.089	0.550	0.903	0.903	0.994
L_3	20/100	1.302	0.507	1.031	1.031	1.031	1.428	0.437	1.025	1.025	1.025
	200	1.295	0.488	0.984	0.984	1.020	1.420	0.393	0.915	0.915	0.935
	300	1.286	0.482	0.963	0.963	1.035	1.410	0.423	0.971	0.971	1.018
	400	1.255	0.465	0.899	0.899	1.000	1.376	0.414	0.915	0.915	0.987
	500	1.224	0.485	0.908	0.908	1.033	1.342	0.433	0.920	0.920	1.014
	600	1.281	0.445	0.884	0.884	0.989	1.405	0.396	0.903	0.903	0.977
	700	1.302	0.432	0.879	0.879	0.962	1.428	0.384	0.901	0.901	0.956
	800	1.148	0.524	0.910	0.910	0.992	1.259	0.472	0.917	0.917	0.982
L_4	20/100	1.466	0.432	1.061	1.061	1.061	1.618	0.347	1.035	0.987	0.987
	200	1.458	0.416	1.013	1.013	1.030	1.609	0.329	0.970	0.929	0.929
	300	1.447	0.412	0.991	0.991	1.031	1.598	0.351	1.021	0.982	0.982
	400	1.412	0.403	0.928	0.928	0.992	1.559	0.344	0.954	0.931	0.931
	500	1.378	0.420	0.930	0.930	1.016	1.521	0.364	0.959	0.950	0.950
	600	1.442	0.385	0.920	0.920	0.984	1.592	0.333	0.961	0.926	0.926
	700	1.466	0.374	0.920	0.920	0.966	1.618	0.323	0.963	0.919	0.919
	800	1.293	0.458	0.922	0.922	0.982	1.427	0.400	0.937	0.937	0.974
L_5	20/100	1.779	0.339	1.225	1.038	1.038	1.804	0.310	1.151	1.026	1.026
	200	1.769	0.326	1.163	0.990	0.990	1.794	0.268	0.983	0.879	0.879
	300	1.757	0.322	1.134	0.972	0.972	1.782	0.298	1.079	0.969	0.969
	400	1.715	0.315	1.055	0.926	0.926	1.739	0.297	1.023	0.933	0.933
	500	1.672	0.328	1.045	0.940	0.940	1.696	0.311	1.019	0.944	0.944
	600	1.750	0.301	1.053	0.906	0.906	1.775	0.284	1.021	0.920	0.920
	700	1.779	0.294	1.062	0.900	0.900	1.804	0.276	1.024	0.913	0.913
	800	1.569	0.358	1.005	0.962	0.962	1.591	0.342	0.987	0.951	0.951
L_6	20/100	2.002	0.300	1.370	1.035	1.035	1.986	0.273	1.229	1.033	1.033
	200	1.991	0.287	1.297	0.985	0.985	1.975	0.241	1.070	0.902	0.902
	300	1.977	0.283	1.264	0.967	0.967	1.961	0.259	1.136	0.962	0.962
	400	1.930	0.276	1.170	0.916	0.916	1.914	0.259	1.081	0.930	0.930
	500	1.882	0.286	1.155	0.926	0.926	1.867	0.270	1.074	0.938	0.938
	600	1.970	0.265	1.173	0.900	0.900	1.954	0.249	1.083	0.919	0.919
	700	2.002	0.261	1.192	0.901	0.901	1.986	0.242	1.087	0.913	0.913
	800	1.766	0.310	1.103	0.942	0.942	1.751	0.297	1.041	0.945	0.945

Table A1.3: Numerical failure loads and their DSM estimates concerning the **C_1** and **R_1** columns with $\boldsymbol{\sigma_{y20}}$**=300** ***MPa***.

L	T (ºC)	C_1					R_1				
		$\lambda_{FT.T}$	f_{uT}/σ_{yT}	$f_{uT}/f_{nG.T}$	$f_{uT}/f_{nFT.T}$	$f_{uT}/f_{nF.FT*}$	$\lambda_{FT.T}$	f_{uT}/σ_{yT}	$f_{uT}/f_{nG.T}$	$f_{uT}/f_{nFT.T}$	$f_{uT}/f_{nF.FT*}$
L_1	20/100	1.091	0.632	1.039	1.039	1.039	1.470	0.414	1.023	1.023	1.023
	200	1.085	0.629	1.029	1.029	1.089	1.461	0.374	0.914	0.914	0.929
	300	1.077	0.615	0.999	0.999	1.113	1.451	0.410	0.990	0.990	1.029
	400	1.051	0.590	0.937	0.937	1.090	1.416	0.413	0.957	0.957	1.022
	500	1.025	0.611	0.949	0.949	1.131	1.381	0.432	0.960	0.960	1.047
	600	1.073	0.568	0.920	0.920	1.082	1.446	0.396	0.950	0.950	1.015
	700	1.091	0.555	0.913	0.913	1.046	1.470	0.384	0.948	0.948	0.995
	800	0.962	0.648	0.954	0.954	1.068	1.296	0.477	0.963	0.963	1.025
L_2	20/100	1.468	0.430	1.059	1.059	1.059	1.746	0.320	1.112	1.012	1.012
	200	1.460	0.427	1.041	1.041	1.058	1.736	0.292	1.004	0.917	0.917
	300	1.450	0.421	1.014	1.014	1.054	1.724	0.316	1.070	0.982	0.982
	400	1.415	0.419	0.968	0.968	1.034	1.682	0.319	1.030	0.959	0.959
	500	1.380	0.437	0.969	0.969	1.058	1.641	0.334	1.026	0.971	0.971
	600	1.444	0.402	0.962	0.962	1.029	1.717	0.306	1.029	0.946	0.946
	700	1.468	0.391	0.963	0.963	1.011	1.746	0.297	1.033	0.940	0.940
	800	1.295	0.478	0.965	0.965	1.027	1.539	0.371	1.002	0.986	0.986
L_3	20/100	1.841	0.327	1.264	1.036	1.036	2.019	0.265	1.233	1.026	1.026
	200	1.831	0.322	1.231	1.014	1.014	2.008	0.243	1.119	0.934	0.934
	300	1.818	0.315	1.187	0.985	0.985	1.994	0.259	1.173	0.983	0.983
	400	1.774	0.312	1.120	0.951	0.951	1.946	0.259	1.117	0.951	0.951
	500	1.731	0.323	1.104	0.961	0.961	1.898	0.270	1.108	0.957	0.957
	600	1.811	0.302	1.130	0.941	0.941	1.986	0.249	1.122	0.943	0.943
	700	1.841	0.296	1.145	0.938	0.938	2.019	0.243	1.130	0.940	0.940
	800	1.624	0.352	1.059	0.980	0.980	1.781	0.297	1.075	0.966	0.966
L_4	20/100	2.073	0.291	1.425	1.041	1.041	2.288	0.200	1.196	0.921	0.921
	200	2.061	0.286	1.388	1.019	1.019	2.275	0.212	1.254	0.969	0.969
	300	2.047	0.281	1.343	0.993	0.993	2.259	0.222	1.290	1.001	1.001
	400	1.997	0.279	1.267	0.960	0.960	2.205	0.222	1.229	0.968	0.968
	500	1.948	0.286	1.237	0.960	0.960	2.151	0.230	1.213	0.971	0.971
	600	2.039	0.272	1.291	0.958	0.958	2.251	0.213	1.232	0.958	0.958
	700	2.073	0.268	1.314	0.960	0.960	2.288	0.209	1.250	0.962	0.962
	800	1.828	0.306	1.165	0.961	0.961	2.018	0.250	1.163	0.968	0.968
L_5	20/100	2.516	0.248	1.787	1.082	1.082	2.552	0.205	1.519	1.094	1.094
	200	2.502	0.245	1.746	1.063	1.063	2.537	0.189	1.387	1.002	1.002
	300	2.485	0.241	1.694	1.038	1.038	2.520	0.198	1.433	1.040	1.040
	400	2.425	0.239	1.605	1.007	1.007	2.459	0.197	1.355	0.998	0.998
	500	2.365	0.245	1.561	1.004	1.004	2.398	0.203	1.334	0.998	0.998
	600	2.475	0.234	1.637	1.007	1.007	2.510	0.190	1.367	0.994	0.994
	700	2.516	0.230	1.663	1.007	1.007	2.552	0.186	1.382	0.995	0.995
	800	2.219	0.257	1.444	0.987	0.987	2.250	0.220	1.270	0.988	0.988
L_6	20/100	2.832	0.222	2.031	1.097	1.097	2.809	0.184	1.651	1.121	1.121
	200	2.816	0.219	1.983	1.077	1.077	2.793	0.169	1.505	1.025	1.025
	300	2.796	0.216	1.925	1.052	1.052	2.773	0.178	1.559	1.066	1.066
	400	2.729	0.215	1.824	1.021	1.021	2.706	0.177	1.475	1.024	1.024
	500	2.662	0.220	1.778	1.020	1.020	2.640	0.183	1.452	1.023	1.023
	600	2.786	0.210	1.857	1.019	1.019	2.763	0.171	1.489	1.020	1.020
	700	2.832	0.206	1.886	1.019	1.019	2.809	0.167	1.505	1.021	1.021
	800	2.498	0.222	1.581	0.964	0.964	2.477	0.197	1.379	1.011	1.011

Table A1.4: Numerical failure loads and their DSM estimates concerning the **C1** and **R1** columns with σ_{y20}=**450** ***MPa***.

L	*T* (ºC)	***C1***					***R1***				
		$\lambda_{FT.T}$	f_{uT}/σ_{yT}	$f_{uT}/f_{nG.T}$	$f_{uT}/f_{nFT.T}$	$f_{uT}/f_{nF.FT*}$	$\lambda_{FT.T}$	f_{uT}/σ_{yT}	$f_{uT}/f_{nG.T}$	$f_{uT}/f_{nFT.T}$	$f_{uT}/f_{nF.FT*}$
L_1	20/100	1.336	0.471	0.993	0.993	0.993	1.800	0.299	1.103	0.985	0.985
	200	1.328	0.469	0.981	0.981	1.013	1.790	0.274	1.002	0.898	0.898
	300	1.319	0.470	0.973	0.973	1.039	1.777	0.295	1.061	0.955	0.955
	400	1.287	0.477	0.955	0.955	1.054	1.734	0.300	1.027	0.939	0.939
	500	1.255	0.498	0.962	0.962	1.087	1.692	0.314	1.024	0.950	0.950
	600	1.314	0.459	0.946	0.946	1.050	1.771	0.288	1.028	0.927	0.927
	700	1.336	0.448	0.945	0.945	1.026	1.800	0.280	1.033	0.923	0.923
	800	1.178	0.547	0.978	0.978	1.061	1.587	0.351	1.008	0.973	0.973
L_2	20/100	1.798	0.332	1.224	1.026	1.026	2.138	0.244	1.274	1.023	1.023
	200	1.788	0.329	1.198	1.010	1.010	2.126	0.226	1.167	0.940	0.940
	300	1.775	0.324	1.165	0.989	0.989	2.111	0.239	1.214	0.983	0.983
	400	1.733	0.324	1.110	0.965	0.965	2.060	0.241	1.167	0.959	0.959
	500	1.690	0.335	1.091	0.971	0.971	2.009	0.250	1.151	0.961	0.961
	600	1.769	0.316	1.127	0.960	0.960	2.103	0.234	1.178	0.956	0.956
	700	1.798	0.310	1.144	0.959	0.959	2.138	0.228	1.191	0.956	0.956
	800	1.586	0.366	1.048	0.993	0.993	1.885	0.274	1.109	0.963	0.963
L_3	20/100	2.255	0.270	1.565	1.054	1.054	2.473	0.202	1.411	1.036	1.036
	200	2.243	0.268	1.535	1.039	1.039	2.459	0.184	1.269	0.935	0.935
	300	2.227	0.265	1.499	1.022	1.022	2.442	0.201	1.363	1.009	1.009
	400	2.173	0.265	1.428	0.997	0.997	2.383	0.203	1.315	0.988	0.988
	500	2.119	0.271	1.389	0.993	0.993	2.324	0.211	1.299	0.991	0.991
	600	2.218	0.260	1.459	0.998	0.998	2.433	0.196	1.321	0.980	0.980
	700	2.255	0.257	1.488	1.002	1.002	2.473	0.191	1.332	0.978	0.978
	800	1.989	0.286	1.290	0.981	0.981	2.181	0.229	1.240	0.983	0.983
L_4	20/100	2.539	0.246	1.808	1.085	1.085	2.802	0.183	1.636	1.112	1.112
	200	2.525	0.244	1.775	1.072	1.072	2.787	0.169	1.495	1.020	1.020
	300	2.507	0.242	1.735	1.054	1.054	2.767	0.179	1.562	1.070	1.070
	400	2.446	0.242	1.655	1.030	1.030	2.701	0.179	1.493	1.038	1.038
	500	2.386	0.248	1.608	1.025	1.025	2.634	0.185	1.466	1.035	1.035
	600	2.497	0.238	1.690	1.031	1.031	2.757	0.174	1.510	1.037	1.037
	700	2.539	0.234	1.723	1.034	1.034	2.802	0.171	1.528	1.038	1.038
	800	2.239	0.260	1.487	1.008	1.008	2.472	0.200	1.390	1.021	1.021
L_5	20/100	3.082	0.207	2.245	1.117	1.117	3.125	0.154	1.710	1.086	1.086
	200	3.065	0.206	2.203	1.102	1.102	3.108	0.148	1.632	1.041	1.041
	300	3.043	0.204	2.153	1.084	1.084	3.086	0.158	1.715	1.098	1.098
	400	2.970	0.205	2.060	1.062	1.062	3.011	0.159	1.642	1.067	1.067
	500	2.897	0.210	2.010	1.062	1.062	2.937	0.164	1.615	1.066	1.066
	600	3.032	0.200	2.095	1.059	1.059	3.074	0.154	1.659	1.065	1.065
	700	3.082	0.182	1.972	0.981	0.981	3.125	0.151	1.676	1.065	1.065
	800	2.718	0.220	1.855	1.042	1.042	2.756	0.177	1.534	1.053	1.053
L_6	20/100	3.468	0.181	2.481	1.101	1.101	3.440	0.143	1.923	1.152	1.152
	200	3.449	0.180	2.437	1.087	1.087	3.421	0.131	1.742	1.047	1.047
	300	3.425	0.178	2.379	1.069	1.069	3.397	0.140	1.843	1.112	1.112
	400	3.342	0.179	2.280	1.049	1.049	3.315	0.141	1.768	1.083	1.083
	500	3.260	0.184	2.235	1.053	1.053	3.233	0.146	1.743	1.085	1.085
	600	3.412	0.174	2.307	1.040	1.040	3.384	0.137	1.783	1.079	1.079
	700	3.468	0.171	2.339	1.038	1.038	3.440	0.133	1.799	1.077	1.077
	800	3.059	0.183	1.951	0.978	0.978	3.034	0.159	1.664	1.077	1.077

Table A1.5: Numerical failure loads and their DSM estimates concerning the **C1** and **R1** columns with σ_{y20}=**600** ***MPa***.

L	*T* (ºC)	***C1***					***R1***				
		$\lambda_{FT.T}$	f_{uT}/σ_{yT}	$f_{uT}/f_{nG.T}$	$f_{uT}/f_{nFT.T}$	$f_{uT}/f_{nF.FT^*}$	$\lambda_{FT.T}$	f_{uT}/σ_{yT}	$f_{uT}/f_{nG.T}$	$f_{uT}/f_{nFT.T}$	$f_{uT}/f_{nF.FT^*}$
L_1	20/100	1.542	0.369	1.000	0.973	0.973	2.078	0.240	1.183	0.967	0.967
	200	1.534	0.369	0.989	0.967	0.967	2.067	0.218	1.062	0.871	0.871
	300	1.523	0.371	0.980	0.965	0.965	2.052	0.240	1.154	0.950	0.950
	400	1.486	0.383	0.966	0.966	1.013	2.003	0.245	1.122	0.939	0.939
	500	1.450	0.400	0.965	0.965	1.032	1.953	0.256	1.112	0.944	0.944
	600	1.517	0.369	0.969	0.958	0.958	2.044	0.236	1.126	0.929	0.929
	700	1.542	0.359	0.975	0.948	0.948	2.078	0.230	1.132	0.925	0.925
	800	1.360	0.451	0.978	0.978	1.029	1.833	0.279	1.070	0.945	0.945
L_2	20/100	2.076	0.288	1.417	1.034	1.034	2.469	0.204	1.418	1.042	1.042
	200	2.065	0.287	1.394	1.022	1.022	2.455	0.186	1.275	0.941	0.941
	300	2.050	0.285	1.366	1.008	1.008	2.438	0.202	1.372	1.016	1.016
	400	2.001	0.287	1.308	0.989	0.989	2.379	0.205	1.323	0.994	0.994
	500	1.951	0.294	1.275	0.988	0.988	2.320	0.212	1.301	0.993	0.993
	600	2.042	0.281	1.336	0.990	0.990	2.428	0.199	1.335	0.991	0.991
	700	2.076	0.277	1.360	0.992	0.992	2.469	0.194	1.347	0.990	0.990
	800	1.831	0.311	1.190	0.980	0.980	2.177	0.229	1.237	0.982	0.982
L_3	20/100	2.604	0.240	1.854	1.086	1.086	2.856	0.176	1.638	1.100	1.100
	200	2.589	0.239	1.825	1.075	1.075	2.840	0.162	1.491	1.005	1.005
	300	2.571	0.237	1.790	1.061	1.061	2.820	0.174	1.577	1.067	1.067
	400	2.509	0.239	1.716	1.042	1.042	2.752	0.176	1.518	1.043	1.043
	500	2.447	0.244	1.669	1.038	1.038	2.684	0.182	1.491	1.041	1.041
	600	2.562	0.234	1.753	1.044	1.044	2.809	0.171	1.536	1.042	1.042
	700	2.604	0.231	1.785	1.046	1.046	2.856	0.167	1.554	1.044	1.044
	800	2.296	0.257	1.545	1.022	1.022	2.518	0.196	1.415	1.027	1.027
L_4	20/100	2.931	0.217	2.129	1.112	1.112	3.236	0.150	1.796	1.117	1.117
	200	2.915	0.216	2.096	1.101	1.101	3.218	0.140	1.652	1.031	1.031
	300	2.895	0.215	2.056	1.087	1.087	3.195	0.151	1.754	1.099	1.099
	400	2.825	0.217	1.975	1.069	1.069	3.118	0.153	1.692	1.076	1.076
	500	2.755	0.222	1.924	1.067	1.067	3.041	0.158	1.666	1.076	1.076
	600	2.884	0.212	2.014	1.068	1.068	3.183	0.148	1.709	1.074	1.074
	700	2.931	0.209	2.046	1.069	1.069	3.236	0.145	1.726	1.073	1.073
	800	2.585	0.235	1.788	1.054	1.054	2.854	0.171	1.587	1.066	1.066
L_5	20/100	3.559	0.178	2.565	1.110	1.110	3.609	0.132	1.965	1.142	1.142
	200	3.539	0.177	2.526	1.099	1.099	3.588	0.121	1.775	1.035	1.035
	300	3.514	0.176	2.478	1.086	1.086	3.563	0.131	1.899	1.113	1.113
	400	3.429	0.178	2.389	1.072	1.072	3.477	0.133	1.837	1.093	1.093
	500	3.345	0.184	2.341	1.076	1.076	3.391	0.138	1.813	1.095	1.095
	600	3.501	0.173	2.423	1.065	1.065	3.550	0.129	1.852	1.087	1.087
	700	3.559	0.170	2.453	1.062	1.062	3.609	0.126	1.866	1.085	1.085
	800	3.139	0.196	2.205	1.078	1.078	3.182	0.150	1.738	1.092	1.092
L_6	20/100	4.005	0.151	2.763	1.067	1.067	3.972	0.115	2.073	1.136	1.136
	200	3.983	0.151	2.724	1.057	1.057	3.950	0.105	1.864	1.025	1.025
	300	3.955	0.150	2.674	1.045	1.045	3.922	0.115	2.011	1.111	1.111
	400	3.859	0.152	2.584	1.034	1.034	3.828	0.117	1.951	1.094	1.094
	500	3.764	0.157	2.545	1.043	1.043	3.733	0.121	1.931	1.099	1.099
	600	3.940	0.147	2.610	1.023	1.023	3.907	0.113	1.962	1.086	1.086
	700	4.005	0.144	2.634	1.017	1.017	3.972	0.110	1.974	1.082	1.082
	800	3.532	0.170	2.422	1.056	1.056	3.503	0.133	1.862	1.102	1.102

Table A2.1: Numerical failure loads and their DSM estimates concerning the **C2** and **R2** columns with σ_{y20}=**75** ***MPa***.

L	T (ºC)	C_2					R_2				
		$\lambda_{FT.T}$	f_{uT}/σ_{yT}	$f_{uT}/f_{nG.T}$	$f_{uT}/f_{nFT.T}$	$f_{uT}/f_{nF.FT*}$	$\lambda_{FT.T}$	f_{uT}/σ_{yT}	$f_{uT}/f_{nG.T}$	$f_{uT}/f_{nFT.T}$	$f_{uT}/f_{nF.FT*}$
L_1	20/100	0.501	0.920	1.022	1.022	1.022	0.656	0.874	1.046	1.046	1.046
	200	0.498	0.866	0.961	0.961	1.058	0.652	0.808	0.965	0.965	1.054
	300	0.495	0.806	0.893	0.893	1.064	0.648	0.745	0.888	0.888	1.045
	400	0.483	0.759	0.837	0.837	1.057	0.632	0.675	0.798	0.798	0.992
	500	0.471	0.771	0.846	0.846	1.099	0.616	0.693	0.813	0.813	1.039
	600	0.493	0.746	0.826	0.826	1.067	0.645	0.653	0.778	0.778	0.987
	700	0.501	0.739	0.821	0.821	1.024	0.656	0.642	0.769	0.769	0.944
	800	0.442	0.786	0.853	0.853	1.003	0.578	0.717	0.825	0.825	0.961
L_2	20/100	0.560	0.921	1.051	1.051	1.051	0.744	0.834	1.051	1.051	1.051
	200	0.557	0.860	0.980	0.980	1.076	0.740	0.769	0.967	0.967	1.051
	300	0.553	0.791	0.899	0.899	1.067	0.735	0.715	0.896	0.896	1.045
	400	0.540	0.734	0.829	0.829	1.041	0.717	0.643	0.798	0.798	0.980
	500	0.527	0.748	0.840	0.840	1.085	0.699	0.663	0.814	0.814	1.028
	600	0.551	0.717	0.814	0.814	1.045	0.732	0.618	0.774	0.774	0.970
	700	0.560	0.708	0.808	0.808	1.001	0.744	0.606	0.764	0.764	0.927
	800	0.494	0.767	0.850	0.850	0.996	0.656	0.690	0.826	0.826	0.956
L_3	20/100	0.626	0.898	1.058	1.058	1.058	0.820	0.792	1.050	1.050	1.050
	200	0.622	0.839	0.987	0.987	1.080	0.816	0.728	0.962	0.962	1.040
	300	0.618	0.769	0.902	0.902	1.064	0.810	0.686	0.902	0.902	1.043
	400	0.603	0.705	0.820	0.820	1.023	0.791	0.617	0.801	0.801	0.975
	500	0.588	0.721	0.834	0.834	1.070	0.771	0.638	0.818	0.818	1.023
	600	0.615	0.684	0.802	0.802	1.022	0.807	0.591	0.776	0.776	0.961
	700	0.626	0.674	0.794	0.794	0.978	0.820	0.577	0.765	0.765	0.918
	800	0.552	0.744	0.845	0.845	0.987	0.724	0.667	0.830	0.830	0.955
L_4	20/100	0.702	0.827	1.017	1.017	1.017	0.907	0.739	1.043	1.043	1.043
	200	0.698	0.796	0.976	0.976	1.064	0.902	0.677	0.951	0.951	1.022
	300	0.693	0.739	0.904	0.904	1.059	0.895	0.648	0.907	0.907	1.037
	400	0.677	0.674	0.817	0.817	1.009	0.874	0.586	0.807	0.807	0.969
	500	0.660	0.693	0.831	0.831	1.057	0.852	0.608	0.824	0.824	1.016
	600	0.691	0.651	0.795	0.795	1.003	0.892	0.560	0.781	0.781	0.954
	700	0.702	0.640	0.786	0.786	0.959	0.907	0.546	0.771	0.771	0.912
	800	0.619	0.718	0.843	0.843	0.979	0.800	0.639	0.836	0.836	0.954
L_5	20/100	0.848	0.757	1.023	1.023	1.023	0.991	0.684	1.032	1.032	1.032
	200	0.843	0.728	0.980	0.980	1.058	0.986	0.624	0.938	0.938	1.001
	300	0.837	0.680	0.912	0.912	1.051	0.979	0.610	0.911	0.911	1.030
	400	0.817	0.622	0.822	0.822	0.996	0.955	0.556	0.815	0.815	0.965
	500	0.797	0.642	0.838	0.838	1.043	0.932	0.578	0.831	0.831	1.009
	600	0.834	0.597	0.798	0.798	0.984	0.975	0.530	0.789	0.789	0.948
	700	0.848	0.583	0.788	0.788	0.941	0.991	0.516	0.779	0.779	0.909
	800	0.748	0.671	0.848	0.848	0.973	0.874	0.611	0.841	0.841	0.952
L_6	20/100	0.950	0.716	1.044	1.044	1.044	1.084	0.621	1.016	1.016	1.016
	200	0.945	0.688	0.999	0.999	1.070	1.078	0.566	0.920	0.920	0.974
	300	0.938	0.644	0.930	0.930	1.058	1.071	0.565	0.913	0.913	1.018
	400	0.915	0.590	0.838	0.838	0.999	1.045	0.521	0.823	0.823	0.958
	500	0.893	0.612	0.854	0.854	1.045	1.019	0.543	0.838	0.838	1.000
	600	0.934	0.564	0.813	0.813	0.984	1.067	0.496	0.799	0.799	0.942
	700	0.950	0.549	0.801	0.801	0.942	1.084	0.483	0.790	0.790	0.906
	800	0.838	0.645	0.865	0.865	0.983	0.956	0.578	0.847	0.847	0.949

Table A2.2: Numerical failure loads and their DSM estimates concerning the $\mathbf{C_2}$ and $\mathbf{R_2}$ columns with σ_{y20}=**150** ***MPa***.

L	*T* (ºC)	***C2***					***R2***				
		$\lambda_{FT.T}$	f_{uT}/σ_{yT}	$f_{uT}/f_{nG.T}$	$f_{uT}/f_{nFT.T}$	$f_{uT}/f_{nF.FT*}$	$\lambda_{FT.T}$	f_{uT}/σ_{yT}	$f_{uT}/f_{nG.T}$	$f_{uT}/f_{nFT.T}$	$f_{uT}/f_{nF.FT*}$
L_1	20/100	0.708	0.880	1.086	1.086	1.086	0.928	0.761	1.090	1.090	1.090
	200	0.705	0.769	0.947	0.947	1.031	0.922	0.699	0.998	0.998	1.070
	300	0.700	0.770	0.945	0.945	1.106	0.916	0.676	0.961	0.961	1.096
	400	0.683	0.718	0.873	0.873	1.078	0.894	0.620	0.866	0.866	1.037
	500	0.666	0.733	0.882	0.882	1.121	0.872	0.640	0.880	0.880	1.082
	600	0.697	0.702	0.860	0.860	1.084	0.913	0.596	0.844	0.844	1.026
	700	0.708	0.693	0.855	0.855	1.042	0.928	0.583	0.835	0.835	0.986
	800	0.625	0.754	0.888	0.888	1.030	0.818	0.671	0.888	0.888	1.011
L_2	20/100	0.792	0.860	1.119	1.119	1.119	1.052	0.673	1.069	1.069	1.069
	200	0.788	0.775	1.004	1.004	1.088	1.046	0.615	0.972	0.972	1.032
	300	0.782	0.746	0.963	0.963	1.117	1.039	0.614	0.964	0.964	1.080
	400	0.764	0.686	0.876	0.876	1.070	1.014	0.571	0.878	0.878	1.029
	500	0.745	0.704	0.887	0.887	1.114	0.989	0.592	0.891	0.891	1.071
	600	0.779	0.666	0.859	0.859	1.069	1.035	0.546	0.855	0.855	1.015
	700	0.792	0.655	0.852	0.852	1.027	1.052	0.532	0.845	0.845	0.976
	800	0.699	0.729	0.894	0.894	1.031	0.928	0.626	0.898	0.898	1.010
L_3	20/100	0.885	0.803	1.114	1.114	1.114	1.160	0.597	1.049	1.049	1.049
	200	0.880	0.732	1.013	1.013	1.090	1.154	0.543	0.949	0.949	0.997
	300	0.873	0.707	0.973	0.973	1.117	1.146	0.557	0.964	0.964	1.063
	400	0.852	0.649	0.880	0.880	1.061	1.118	0.524	0.884	0.884	1.014
	500	0.831	0.669	0.893	0.893	1.106	1.090	0.547	0.899	0.899	1.057
	600	0.870	0.627	0.860	0.860	1.054	1.141	0.502	0.865	0.865	1.003
	700	0.885	0.614	0.852	0.852	1.013	1.160	0.489	0.858	0.858	0.969
	800	0.780	0.698	0.900	0.900	1.030	1.023	0.583	0.904	0.904	1.004
L_4	20/100	0.993	0.696	1.052	1.052	1.052	1.282	0.521	1.036	1.036	1.036
	200	0.988	0.656	0.987	0.987	1.053	1.275	0.473	0.933	0.933	0.969
	300	0.981	0.640	0.957	0.957	1.082	1.266	0.494	0.966	0.966	1.042
	400	0.957	0.597	0.875	0.875	1.036	1.236	0.474	0.898	0.898	1.004
	500	0.934	0.617	0.888	0.888	1.079	1.205	0.494	0.908	0.908	1.038
	600	0.977	0.574	0.855	0.855	1.027	1.261	0.455	0.886	0.886	0.997
	700	0.993	0.561	0.848	0.848	0.989	1.282	0.441	0.877	0.877	0.964
	800	0.876	0.648	0.894	0.894	1.011	1.131	0.534	0.911	0.911	0.997
L_5	20/100	1.199	0.570	1.041	1.041	1.041	1.402	0.457	1.041	1.041	1.041
	200	1.192	0.547	0.992	0.992	1.039	1.394	0.416	0.938	0.938	0.961
	300	1.184	0.540	0.970	0.970	1.062	1.384	0.438	0.977	0.977	1.030
	400	1.155	0.516	0.902	0.902	1.026	1.351	0.426	0.915	0.915	0.994
	500	1.127	0.536	0.913	0.913	1.064	1.318	0.445	0.920	0.920	1.022
	600	1.180	0.494	0.884	0.884	1.015	1.379	0.408	0.903	0.903	0.985
	700	1.199	0.481	0.879	0.879	0.984	1.402	0.396	0.900	0.900	0.962
	800	1.057	0.574	0.917	0.917	1.014	1.236	0.484	0.917	0.917	0.986
L_6	20/100	1.343	0.495	1.053	1.053	1.053	1.533	0.402	1.077	1.057	1.057
	200	1.336	0.478	1.009	1.009	1.040	1.525	0.366	0.969	0.956	0.956
	300	1.326	0.474	0.989	0.989	1.054	1.514	0.386	1.010	1.002	1.002
	400	1.294	0.461	0.929	0.929	1.023	1.478	0.379	0.946	0.946	0.994
	500	1.262	0.480	0.936	0.936	1.055	1.441	0.396	0.946	0.946	1.013
	600	1.321	0.438	0.910	0.910	1.008	1.509	0.364	0.943	0.939	0.939
	700	1.343	0.431	0.917	0.917	0.993	1.533	0.352	0.944	0.927	0.927
	800	1.185	0.474	0.852	0.852	0.924	1.352	0.434	0.933	0.933	0.983

Table A2.3: Numerical failure loads and their DSM estimates concerning the **C2** and **R2** columns with σ_{y20}**=450** ***MPa***.

L	*T* (ºC)	***C2***					***R2***				
		$\lambda_{FT.T}$	f_{uT}/σ_{yT}	$f_{uT}/f_{nG.T}$	$f_{uT}/f_{nFT.T}$	$f_{uT}/f_{nF.FT^*}$	$\lambda_{FT.T}$	f_{uT}/σ_{yT}	$f_{uT}/f_{nG.T}$	$f_{uT}/f_{nFT.T}$	$f_{uT}/f_{nF.FT^*}$
L_1	20/100	1.002	0.735	1.118	1.118	1.118	1.312	0.511	1.051	1.051	1.051
	200	0.996	0.717	1.087	1.087	1.159	1.305	0.462	0.942	0.942	0.975
	300	0.989	0.681	1.026	1.026	1.159	1.295	0.495	1.000	1.000	1.073
	400	0.965	0.641	0.947	0.947	1.119	1.264	0.487	0.950	0.950	1.054
	500	0.942	0.661	0.957	0.957	1.161	1.233	0.507	0.957	0.957	1.087
	600	0.986	0.620	0.931	0.931	1.116	1.291	0.466	0.936	0.936	1.046
	700	1.002	0.607	0.924	0.924	1.076	1.312	0.453	0.932	0.932	1.017
	800	0.884	0.692	0.959	0.959	1.085	1.157	0.549	0.961	0.961	1.047
L_2	20/100	1.121	0.652	1.103	1.103	1.103	1.488	0.422	1.065	1.065	1.065
	200	1.114	0.641	1.078	1.078	1.138	1.480	0.383	0.957	0.957	0.970
	300	1.106	0.618	1.032	1.032	1.144	1.469	0.413	1.019	1.019	1.055
	400	1.080	0.589	0.960	0.960	1.110	1.434	0.411	0.972	0.972	1.033
	500	1.053	0.611	0.972	0.972	1.152	1.398	0.430	0.974	0.974	1.057
	600	1.102	0.567	0.942	0.942	1.102	1.464	0.394	0.966	0.966	1.027
	700	1.121	0.553	0.935	0.935	1.065	1.488	0.384	0.970	0.970	1.013
	800	0.988	0.649	0.976	0.976	1.090	1.312	0.471	0.969	0.969	1.029
L_3	20/100	1.251	0.558	1.075	1.075	1.075	1.641	0.366	1.123	1.043	1.043
	200	1.244	0.552	1.055	1.055	1.099	1.632	0.333	1.011	0.943	0.943
	300	1.235	0.539	1.020	1.020	1.107	1.620	0.358	1.071	1.005	1.005
	400	1.206	0.525	0.965	0.965	1.086	1.581	0.358	1.019	0.976	0.976
	500	1.176	0.546	0.974	0.974	1.123	1.542	0.374	1.013	0.990	0.990
	600	1.231	0.504	0.950	0.950	1.078	1.614	0.343	1.019	0.959	0.959
	700	1.251	0.489	0.942	0.942	1.043	1.641	0.333	1.024	0.951	0.951
	800	1.103	0.588	0.979	0.979	1.075	1.447	0.412	0.989	0.989	1.023
L_4	20/100	1.405	0.471	1.076	1.076	1.076	1.813	0.320	1.201	1.028	1.028
	200	1.397	0.467	1.056	1.056	1.082	1.803	0.294	1.089	0.936	0.936
	300	1.387	0.459	1.026	1.026	1.081	1.790	0.312	1.141	0.987	0.987
	400	1.354	0.455	0.979	0.979	1.063	1.747	0.311	1.083	0.956	0.956
	500	1.320	0.474	0.983	0.983	1.091	1.704	0.324	1.074	0.967	0.967
	600	1.382	0.436	0.970	0.970	1.056	1.784	0.300	1.087	0.943	0.943
	700	1.405	0.424	0.967	0.967	1.032	1.813	0.292	1.096	0.938	0.938
	800	1.239	0.517	0.983	0.983	1.057	1.599	0.358	1.043	0.989	0.989
L_5	20/100	1.696	0.358	1.175	1.061	1.061	1.983	0.289	1.293	1.029	1.029
	200	1.686	0.355	1.150	1.043	1.043	1.971	0.268	1.186	0.948	0.948
	300	1.674	0.349	1.116	1.018	1.018	1.958	0.280	1.224	0.984	0.984
	400	1.634	0.348	1.060	0.987	0.987	1.910	0.278	1.159	0.950	0.950
	500	1.594	0.362	1.050	0.998	0.998	1.863	0.289	1.144	0.957	0.957
	600	1.668	0.335	1.064	0.974	0.974	1.950	0.269	1.167	0.941	0.941
	700	1.696	0.327	1.072	0.968	0.968	1.983	0.263	1.179	0.938	0.938
	800	1.496	0.398	1.015	1.015	1.040	1.748	0.315	1.099	0.969	0.969
L_6	20/100	1.900	0.313	1.289	1.060	1.060	2.169	0.262	1.407	1.040	1.040
	200	1.889	0.309	1.259	1.041	1.041	2.157	0.244	1.296	0.962	0.962
	300	1.876	0.304	1.220	1.014	1.014	2.141	0.254	1.329	0.993	0.993
	400	1.831	0.303	1.156	0.981	0.981	2.090	0.252	1.255	0.956	0.956
	500	1.785	0.314	1.142	0.989	0.989	2.038	0.260	1.234	0.959	0.959
	600	1.869	0.292	1.164	0.970	0.970	2.133	0.244	1.269	0.950	0.950
	700	1.900	0.284	1.168	0.961	0.961	2.169	0.240	1.285	0.950	0.950
	800	1.675	0.343	1.097	1.001	1.001	1.913	0.282	1.174	0.962	0.962

Table A2.4: Numerical failure loads and their DSM estimates concerning the **C2** and **R2** columns with $\boldsymbol{\sigma_{y20}}$**=450** ***MPa***.

L	T (ºC)	**C_2**					**R_2**				
		$\lambda_{FT.T}$	f_{uT}/σ_{yT}	$f_{uT}/f_{nG.T}$	$f_{uT}/f_{nFT.T}$	$f_{uT}/f_{nF.FT^*}$	$\lambda_{FT.T}$	f_{uT}/σ_{yT}	$f_{uT}/f_{nG.T}$	$f_{uT}/f_{nFT.T}$	$f_{uT}/f_{nF.FT^*}$
L_1	20/100	1.227	0.562	1.056	1.056	1.056	1.607	0.369	1.085	1.025	1.025
	200	1.220	0.561	1.047	1.047	1.094	1.598	0.337	0.979	0.930	0.930
	300	1.212	0.556	1.028	1.028	1.120	1.586	0.365	1.047	0.999	0.999
	400	1.182	0.549	0.986	0.986	1.116	1.548	0.370	1.010	0.984	0.984
	500	1.153	0.571	0.996	0.996	1.154	1.510	0.387	1.005	0.999	0.999
	600	1.207	0.528	0.972	0.972	1.109	1.581	0.355	1.011	0.968	0.968
	700	1.227	0.515	0.967	0.967	1.076	1.607	0.345	1.016	0.959	0.959
	800	1.082	0.615	1.004	1.004	1.106	1.417	0.429	0.994	0.994	1.035
L_2	20/100	1.372	0.482	1.060	1.060	1.060	1.822	0.314	1.190	1.014	1.014
	200	1.365	0.481	1.049	1.049	1.079	1.812	0.290	1.086	0.930	0.930
	300	1.355	0.477	1.030	1.030	1.092	1.799	0.308	1.138	0.980	0.980
	400	1.322	0.479	0.995	0.995	1.089	1.756	0.310	1.091	0.958	0.958
	500	1.290	0.499	1.001	1.001	1.120	1.713	0.323	1.080	0.968	0.968
	600	1.350	0.460	0.986	0.986	1.083	1.793	0.300	1.099	0.949	0.949
	700	1.372	0.447	0.983	0.983	1.057	1.822	0.293	1.110	0.946	0.946
	800	1.210	0.546	1.008	1.008	1.088	1.607	0.356	1.050	0.991	0.991
L_3	20/100	1.532	0.407	1.089	1.069	1.069	2.010	0.282	1.297	1.020	1.020
	200	1.524	0.405	1.071	1.057	1.057	1.998	0.262	1.192	0.942	0.942
	300	1.513	0.401	1.046	1.038	1.038	1.984	0.275	1.235	0.982	0.982
	400	1.476	0.404	1.005	1.005	1.056	1.937	0.277	1.183	0.959	0.959
	500	1.440	0.421	1.002	1.002	1.074	1.889	0.286	1.164	0.963	0.963
	600	1.507	0.388	1.006	1.002	1.002	1.977	0.269	1.197	0.955	0.955
	700	1.532	0.378	1.012	0.994	0.994	2.010	0.263	1.213	0.954	0.954
	800	1.351	0.462	0.991	0.991	1.045	1.772	0.311	1.115	0.972	0.972
L_4	20/100	1.720	0.353	1.190	1.062	1.062	2.221	0.254	1.430	1.037	1.037
	200	1.711	0.350	1.167	1.047	1.047	2.208	0.238	1.322	0.963	0.963
	300	1.699	0.346	1.137	1.026	1.026	2.193	0.249	1.366	1.000	1.000
	400	1.658	0.347	1.088	1.001	1.001	2.140	0.249	1.302	0.973	0.973
	500	1.617	0.361	1.076	1.011	1.011	2.087	0.257	1.276	0.973	0.973
	600	1.692	0.335	1.094	0.990	0.990	2.185	0.243	1.323	0.972	0.972
	700	1.720	0.326	1.102	0.983	0.983	2.221	0.239	1.343	0.973	0.973
	800	1.517	0.386	1.012	1.002	1.002	1.959	0.276	1.208	0.971	0.971
L_5	20/100	2.077	0.280	1.376	1.052	1.052	2.428	0.233	1.569	1.058	1.058
	200	2.065	0.277	1.350	1.036	1.036	2.415	0.218	1.452	0.983	0.983
	300	2.051	0.274	1.316	1.016	1.016	2.398	0.228	1.496	1.019	1.019
	400	2.001	0.275	1.258	0.991	0.991	2.340	0.229	1.430	0.994	0.994
	500	1.952	0.285	1.237	0.995	0.995	2.282	0.235	1.398	0.991	0.991
	600	2.043	0.265	1.261	0.977	0.977	2.389	0.224	1.454	0.993	0.993
	700	2.077	0.262	1.288	0.984	0.984	2.428	0.220	1.477	0.995	0.995
	800	1.832	0.337	1.291	1.094	1.094	2.141	0.251	1.314	0.981	0.981
L_6	20/100	2.327	0.244	1.503	1.046	1.046	2.656	0.213	1.710	1.071	1.071
	200	2.314	0.242	1.476	1.032	1.032	2.641	0.200	1.592	1.001	1.001
	300	2.297	0.239	1.440	1.012	1.012	2.623	0.210	1.645	1.041	1.041
	400	2.242	0.240	1.377	0.988	0.988	2.559	0.211	1.573	1.015	1.015
	500	2.187	0.248	1.355	0.992	0.992	2.496	0.216	1.537	1.013	1.013
	600	2.289	0.233	1.393	0.982	0.982	2.613	0.205	1.598	1.014	1.014
	700	2.327	0.229	1.412	0.983	0.983	2.656	0.202	1.622	1.016	1.016
	800	2.052	0.269	1.291	0.996	0.996	2.342	0.230	1.441	1.000	1.000

Table A2.5: Numerical failure loads and their DSM estimates concerning the **C_2** and **R_2** columns with **σ_{y20}=600*MPa***.

L	T (ºC)	***C_2***					***R_2***				
		$\lambda_{FT.T}$	f_{uT}/σ_{yT}	$f_{uT}/f_{nG.T}$	$f_{uT}/f_{nFT.T}$	$f_{uT}/f_{nF.FT^*}$	$\lambda_{FT.T}$	f_{uT}/σ_{yT}	$f_{uT}/f_{nG.T}$	$f_{uT}/f_{nFT.T}$	$f_{uT}/f_{nF.FT^*}$
L_1	20/100	1.417	0.440	1.020	1.020	1.020	1.855	0.304	1.193	1.002	1.002
	200	1.409	0.443	1.018	1.018	1.041	1.845	0.282	1.094	0.923	0.923
	300	1.399	0.445	1.010	1.010	1.061	1.832	0.300	1.148	0.974	0.974
	400	1.365	0.455	0.993	0.993	1.075	1.788	0.303	1.103	0.955	0.955
	500	1.332	0.475	0.998	0.998	1.104	1.744	0.313	1.086	0.960	0.960
	600	1.394	0.437	0.986	0.986	1.070	1.825	0.294	1.118	0.952	0.952
	700	1.417	0.425	0.985	0.985	1.048	1.855	0.289	1.132	0.951	0.951
	800	1.250	0.525	1.009	1.009	1.082	1.636	0.344	1.051	0.979	0.979
L_2	20/100	1.585	0.385	1.101	1.052	1.052	2.104	0.266	1.341	1.016	1.016
	200	1.576	0.383	1.084	1.040	1.040	2.093	0.248	1.238	0.943	0.943
	300	1.565	0.382	1.066	1.029	1.029	2.078	0.262	1.290	0.987	0.987
	400	1.527	0.389	1.034	1.018	1.018	2.028	0.264	1.237	0.966	0.966
	500	1.489	0.406	1.027	1.027	1.085	1.978	0.272	1.213	0.967	0.967
	600	1.559	0.374	1.037	1.004	1.004	2.070	0.258	1.258	0.966	0.966
	700	1.585	0.364	1.042	0.995	0.995	2.104	0.253	1.277	0.967	0.967
	800	1.398	0.449	1.018	1.018	1.063	1.856	0.294	1.153	0.968	0.968
L_3	20/100	1.769	0.337	1.204	1.050	1.050	2.320	0.241	1.481	1.036	1.036
	200	1.759	0.336	1.184	1.038	1.038	2.308	0.226	1.372	0.964	0.964
	300	1.747	0.333	1.160	1.022	1.022	2.291	0.238	1.425	1.007	1.007
	400	1.705	0.337	1.117	1.004	1.004	2.236	0.240	1.366	0.985	0.985
	500	1.663	0.350	1.102	1.012	1.012	2.181	0.247	1.338	0.985	0.985
	600	1.740	0.326	1.128	0.997	0.997	2.283	0.234	1.392	0.987	0.987
	700	1.769	0.319	1.140	0.994	0.994	2.320	0.230	1.413	0.988	0.988
	800	1.560	0.384	1.066	1.031	1.031	2.046	0.264	1.261	0.977	0.977
L_4	20/100	1.987	0.296	1.330	1.055	1.055	2.564	0.220	1.646	1.061	1.061
	200	1.975	0.294	1.308	1.042	1.042	2.550	0.205	1.522	0.986	0.986
	300	1.962	0.292	1.281	1.026	1.026	2.532	0.217	1.585	1.032	1.032
	400	1.914	0.295	1.232	1.007	1.007	2.471	0.218	1.520	1.010	1.010
	500	1.867	0.305	1.211	1.010	1.010	2.410	0.225	1.488	1.009	1.009
	600	1.954	0.286	1.247	1.002	1.002	2.523	0.213	1.548	1.011	1.011
	700	1.987	0.281	1.262	1.001	1.001	2.564	0.210	1.572	1.013	1.013
	800	1.752	0.330	1.155	1.016	1.016	2.262	0.239	1.396	0.997	0.997
L_5	20/100	2.398	0.235	1.544	1.048	1.048	2.804	0.191	1.710	1.025	1.025
	200	2.385	0.234	1.519	1.036	1.036	2.788	0.188	1.665	1.002	1.002
	300	2.368	0.233	1.488	1.021	1.021	2.768	0.199	1.739	1.053	1.053
	400	2.311	0.235	1.432	1.002	1.002	2.702	0.201	1.671	1.032	1.032
	500	2.254	0.243	1.408	1.006	1.006	2.635	0.206	1.635	1.030	1.030
	600	2.359	0.228	1.448	0.996	0.996	2.758	0.196	1.699	1.031	1.031
	700	2.398	0.224	1.466	0.995	0.995	2.804	0.192	1.723	1.032	1.032
	800	2.115	0.262	1.336	1.006	1.006	2.473	0.220	1.535	1.019	1.019
L_6	20/100	2.686	0.202	1.661	1.026	1.026	3.067	0.175	1.881	1.047	1.047
	200	2.672	0.202	1.642	1.019	1.019	3.050	0.170	1.805	1.009	1.009
	300	2.653	0.201	1.609	1.005	1.005	3.028	0.181	1.896	1.066	1.066
	400	2.589	0.203	1.553	0.990	0.990	2.955	0.183	1.825	1.047	1.047
	500	2.525	0.211	1.532	0.997	0.997	2.882	0.189	1.788	1.047	1.047
	600	2.643	0.197	1.566	0.981	0.981	3.017	0.178	1.851	1.044	1.044
	700	2.686	0.192	1.579	0.976	0.976	3.067	0.175	1.875	1.044	1.044
	800	2.369	0.228	1.460	1.001	1.001	2.705	0.202	1.685	1.039	1.039

Table A3.1: Numerical failure loads and their DSM estimates concerning the **C3** and **R3** columns with σ_{y20}=75 ***MPa***.

L	*T* (ºC)	***C3***					***R3***				
		$\lambda_{FT.T}$	f_{uT}/σ_{yT}	$f_{uT}/f_{nG.T}$	$f_{uT}/f_{nFT.T}$	$f_{uT}/f_{nF.FT*}$	$\lambda_{FT.T}$	f_{uT}/σ_{yT}	$f_{uT}/f_{nG.T}$	$f_{uT}/f_{nFT.T}$	$f_{uT}/f_{nF.FT*}$
L_1	20/100	0.478	0.944	1.039	1.039	1.039	0.797	0.815	1.064	1.064	1.064
	200	0.476	0.885	0.973	0.973	1.072	0.792	0.747	0.971	0.971	1.052
	300	0.472	0.825	0.906	0.906	1.081	0.787	0.695	0.900	0.900	1.044
	400	0.461	0.782	0.855	0.855	1.081	0.768	0.622	0.796	0.796	0.972
	500	0.450	0.792	0.862	0.862	1.123	0.749	0.644	0.814	0.814	1.021
	600	0.471	0.770	0.845	0.845	1.094	0.784	0.596	0.770	0.770	0.958
	700	0.478	0.764	0.840	0.840	1.050	0.797	0.582	0.760	0.760	0.915
	800	0.422	0.807	0.869	0.869	1.023	0.703	0.672	0.826	0.826	0.952
L_2	20/100	0.546	0.929	1.053	1.053	1.053	0.920	0.737	1.051	1.051	1.051
	200	0.543	0.870	0.984	0.984	1.081	0.915	0.672	0.954	0.954	1.025
	300	0.540	0.804	0.908	0.908	1.079	0.909	0.644	0.909	0.909	1.038
	400	0.527	0.751	0.843	0.843	1.060	0.887	0.581	0.807	0.807	0.967
	500	0.514	0.764	0.853	0.853	1.104	0.865	0.603	0.825	0.825	1.015
	600	0.537	0.735	0.829	0.829	1.066	0.906	0.554	0.780	0.780	0.950
	700	0.546	0.727	0.823	0.823	1.022	0.920	0.539	0.769	0.769	0.908
	800	0.482	0.782	0.862	0.862	1.011	0.812	0.634	0.836	0.836	0.953
L_3	20/100	0.611	0.912	1.066	1.066	1.066	1.043	0.651	1.027	1.027	1.027
	200	0.607	0.854	0.996	0.996	1.091	1.037	0.593	0.930	0.930	0.989
	300	0.603	0.786	0.915	0.915	1.081	1.030	0.588	0.916	0.916	1.028
	400	0.589	0.725	0.838	0.838	1.047	1.005	0.537	0.820	0.820	0.962
	500	0.574	0.741	0.851	0.851	1.093	0.980	0.560	0.836	0.836	1.007
	600	0.601	0.706	0.821	0.821	1.048	1.026	0.511	0.794	0.794	0.945
	700	0.611	0.696	0.814	0.814	1.003	1.043	0.497	0.784	0.784	0.906
	800	0.539	0.762	0.861	0.861	1.006	0.920	0.594	0.845	0.845	0.952
L_4	20/100	0.671	0.893	1.078	1.078	1.078	1.162	0.569	1.003	1.003	1.003
	200	0.668	0.836	1.008	1.008	1.100	1.156	0.518	0.906	0.906	0.952
	300	0.663	0.768	0.923	0.923	1.085	1.148	0.527	0.915	0.915	1.008
	400	0.647	0.703	0.837	0.837	1.038	1.120	0.491	0.831	0.831	0.953
	500	0.631	0.721	0.851	0.851	1.086	1.093	0.513	0.846	0.846	0.994
	600	0.660	0.681	0.817	0.817	1.035	1.144	0.468	0.810	0.810	0.938
	700	0.671	0.670	0.809	0.809	0.990	1.162	0.455	0.801	0.801	0.904
	800	0.592	0.745	0.862	0.862	1.004	1.025	0.549	0.853	0.853	0.947
L_5	20/100	0.728	0.871	1.087	1.087	1.087	1.280	0.498	0.989	0.989	0.989
	200	0.724	0.818	1.018	1.018	1.108	1.272	0.453	0.892	0.892	0.927
	300	0.719	0.751	0.932	0.932	1.089	1.264	0.470	0.917	0.917	0.990
	400	0.701	0.683	0.840	0.840	1.035	1.233	0.447	0.845	0.845	0.945
	500	0.684	0.703	0.855	0.855	1.084	1.203	0.467	0.855	0.855	0.979
	600	0.716	0.658	0.816	0.816	1.025	1.259	0.426	0.827	0.827	0.931
	700	0.728	0.647	0.808	0.808	0.982	1.280	0.413	0.820	0.820	0.902
	800	0.642	0.730	0.867	0.867	1.005	1.129	0.504	0.859	0.859	0.940
L_6	20/100	0.781	0.847	1.093	1.093	1.093	1.394	0.442	0.996	0.996	0.996
	200	0.776	0.798	1.027	1.027	1.113	1.386	0.401	0.896	0.896	0.919
	300	0.771	0.734	0.941	0.941	1.093	1.376	0.420	0.927	0.927	0.978
	400	0.752	0.666	0.845	0.845	1.033	1.343	0.405	0.861	0.861	0.938
	500	0.734	0.687	0.861	0.861	1.083	1.310	0.423	0.867	0.867	0.965
	600	0.768	0.641	0.820	0.820	1.023	1.371	0.386	0.848	0.848	0.926
	700	0.781	0.627	0.809	0.809	0.977	1.394	0.374	0.844	0.844	0.903
	800	0.688	0.716	0.873	0.873	1.008	1.229	0.460	0.865	0.865	0.932

Table A3.2: Numerical failure loads and their DSM estimates concerning the **C_3** and **R_3** columns with σ_{y20}**=150*MPa***.

L	T (ºC)	C_3					R_3				
		$\lambda_{FT.T}$	f_{uT}/σ_{yT}	$f_{uT}/f_{nG.T}$	$f_{uT}/f_{nFT.T}$	$f_{uT}/f_{nF.FT^*}$	$\lambda_{FT.T}$	f_{uT}/σ_{yT}	$f_{uT}/f_{nG.T}$	$f_{uT}/f_{nFT.T}$	$f_{uT}/f_{nF.FT^*}$
L_1	20/100	0.676	0.909	1.101	1.101	1.101	1.127	0.620	1.055	1.055	1.055
	200	0.673	0.789	0.953	0.953	1.040	1.121	0.563	0.953	0.953	1.005
	300	0.668	0.789	0.951	0.951	1.117	1.113	0.578	0.970	0.970	1.074
	400	0.652	0.742	0.887	0.887	1.099	1.086	0.542	0.888	0.888	1.025
	500	0.636	0.755	0.895	0.895	1.141	1.059	0.563	0.901	0.901	1.066
	600	0.665	0.727	0.875	0.875	1.108	1.109	0.517	0.865	0.865	1.010
	700	0.676	0.719	0.871	0.871	1.066	1.127	0.504	0.857	0.857	0.975
	800	0.597	0.775	0.899	0.899	1.046	0.994	0.601	0.908	0.908	1.013
L_2	20/100	0.773	0.872	1.119	1.119	1.119	1.302	0.504	1.025	1.025	1.025
	200	0.768	0.785	1.005	1.005	1.091	1.295	0.457	0.921	0.921	0.955
	300	0.763	0.757	0.966	0.966	1.123	1.285	0.483	0.965	0.965	1.037
	400	0.745	0.702	0.886	0.886	1.085	1.254	0.467	0.903	0.903	1.005
	500	0.726	0.719	0.896	0.896	1.128	1.223	0.488	0.913	0.913	1.039
	600	0.760	0.683	0.870	0.870	1.086	1.281	0.446	0.887	0.887	0.993
	700	0.773	0.673	0.864	0.864	1.044	1.302	0.434	0.881	0.881	0.964
	800	0.681	0.745	0.904	0.904	1.045	1.148	0.528	0.917	0.917	1.001
L_3	20/100	0.864	0.824	1.126	1.126	1.126	1.474	0.417	1.036	1.036	1.036
	200	0.859	0.750	1.021	1.021	1.101	1.466	0.379	0.931	0.931	0.946
	300	0.853	0.724	0.982	0.982	1.129	1.456	0.404	0.981	0.981	1.019
	400	0.832	0.668	0.892	0.892	1.079	1.421	0.398	0.927	0.927	0.989
	500	0.812	0.687	0.905	0.905	1.124	1.386	0.416	0.930	0.930	1.013
	600	0.850	0.646	0.874	0.874	1.075	1.451	0.381	0.919	0.919	0.981
	700	0.864	0.634	0.866	0.866	1.033	1.474	0.369	0.918	0.918	0.962
	800	0.762	0.715	0.911	0.911	1.045	1.300	0.456	0.925	0.925	0.984
L_4	20/100	0.949	0.768	1.121	1.121	1.121	1.644	0.355	1.095	1.033	1.033
	200	0.944	0.708	1.029	1.029	1.102	1.635	0.308	0.939	0.889	0.889
	300	0.937	0.687	0.992	0.992	1.129	1.623	0.344	1.034	0.983	0.983
	400	0.915	0.635	0.901	0.901	1.074	1.584	0.341	0.976	0.943	0.943
	500	0.892	0.655	0.915	0.915	1.120	1.545	0.356	0.970	0.952	0.952
	600	0.934	0.611	0.880	0.880	1.066	1.617	0.327	0.974	0.928	0.928
	700	0.949	0.598	0.872	0.872	1.025	1.644	0.317	0.977	0.922	0.922
	800	0.837	0.694	0.930	0.930	1.058	1.450	0.392	0.945	0.945	0.978
L_5	20/100	1.029	0.710	1.106	1.106	1.106	1.810	0.300	1.119	0.994	0.994
	200	1.024	0.664	1.030	1.030	1.096	1.800	0.271	1.000	0.891	0.891
	300	1.016	0.648	0.998	0.998	1.122	1.787	0.300	1.091	0.977	0.977
	400	0.992	0.604	0.911	0.911	1.072	1.744	0.297	1.030	0.936	0.936
	500	0.967	0.625	0.925	0.925	1.116	1.701	0.310	1.023	0.945	0.945
	600	1.013	0.579	0.889	0.889	1.060	1.780	0.284	1.028	0.923	0.923
	700	1.029	0.566	0.882	0.882	1.022	1.810	0.276	1.032	0.916	0.916
	800	0.908	0.660	0.932	0.932	1.051	1.596	0.342	0.993	0.954	0.954
L_6	20/100	1.104	0.654	1.090	1.090	1.090	1.971	0.268	1.186	0.998	0.998
	200	1.098	0.621	1.028	1.028	1.087	1.960	0.255	1.117	0.943	0.943
	300	1.090	0.609	1.001	1.001	1.113	1.946	0.267	1.154	0.979	0.979
	400	1.064	0.574	0.922	0.922	1.069	1.899	0.264	1.084	0.934	0.934
	500	1.037	0.596	0.935	0.935	1.112	1.853	0.275	1.077	0.942	0.942
	600	1.086	0.550	0.900	0.900	1.057	1.939	0.253	1.084	0.921	0.921
	700	1.104	0.538	0.895	0.895	1.023	1.971	0.246	1.088	0.916	0.916
	800	0.974	0.634	0.942	0.942	1.053	1.738	0.302	1.042	0.949	0.949

Table A3.3: Numerical failure loads and their DSM estimates concerning the **C3** and **R3** columns with σ_{y20}**=300** ***MPa***.

L	*T* (ºC)	***C3***					***R3***				
		$\lambda_{FT.T}$	f_{uT}/σ_{yT}	$f_{uT}/f_{nG.T}$	$f_{uT}/f_{nFT.T}$	$f_{uT}/f_{nF.FT*}$	$\lambda_{FT.T}$	f_{uT}/σ_{yT}	$f_{uT}/f_{nG.T}$	$f_{uT}/f_{nFT.T}$	$f_{uT}/f_{nF.FT*}$
L_1	20/100	0.957	0.787	1.155	1.155	1.155	1.594	0.364	1.053	1.013	1.013
	200	0.951	0.757	1.106	1.106	1.184	1.585	0.330	0.944	0.912	0.912
	300	0.945	0.712	1.034	1.034	1.175	1.574	0.361	1.019	0.988	0.988
	400	0.922	0.668	0.954	0.954	1.136	1.536	0.366	0.983	0.968	0.968
	500	0.899	0.687	0.963	0.963	1.178	1.498	0.383	0.979	0.979	1.031
	600	0.941	0.648	0.939	0.939	1.136	1.568	0.356	0.997	0.969	0.969
	700	0.957	0.636	0.933	0.933	1.095	1.594	0.340	0.984	0.946	0.946
	800	0.844	0.716	0.965	0.965	1.096	1.406	0.424	0.969	0.969	1.011
L_2	20/100	1.093	0.680	1.121	1.121	1.121	1.841	0.300	1.158	1.017	1.017
	200	1.087	0.665	1.090	1.090	1.154	1.831	0.274	1.047	0.924	0.924
	300	1.079	0.638	1.038	1.038	1.157	1.818	0.293	1.105	0.979	0.979
	400	1.053	0.607	0.965	0.965	1.122	1.774	0.295	1.059	0.952	0.952
	500	1.027	0.628	0.976	0.976	1.163	1.730	0.309	1.054	0.963	0.963
	600	1.075	0.585	0.948	0.948	1.116	1.811	0.284	1.060	0.941	0.941
	700	1.093	0.571	0.941	0.941	1.077	1.841	0.275	1.065	0.935	0.935
	800	0.964	0.664	0.979	0.979	1.097	1.624	0.342	1.027	0.976	0.976
L_3	20/100	1.222	0.584	1.091	1.091	1.091	2.085	0.258	1.278	1.039	1.039
	200	1.215	0.576	1.069	1.069	1.117	2.074	0.238	1.167	0.951	0.951
	300	1.206	0.562	1.032	1.032	1.126	2.059	0.251	1.212	0.993	0.993
	400	1.177	0.546	0.974	0.974	1.104	2.009	0.250	1.151	0.957	0.957
	500	1.148	0.567	0.984	0.984	1.142	1.960	0.260	1.138	0.962	0.962
	600	1.202	0.524	0.960	0.960	1.096	2.051	0.241	1.157	0.950	0.950
	700	1.222	0.511	0.954	0.954	1.064	2.085	0.235	1.167	0.948	0.948
	800	1.077	0.609	0.990	0.990	1.091	1.839	0.285	1.100	0.967	0.967
L_4	20/100	1.343	0.508	1.080	1.080	1.080	2.325	0.229	1.410	1.070	1.070
	200	1.335	0.503	1.061	1.061	1.094	2.312	0.211	1.288	0.981	0.981
	300	1.326	0.494	1.031	1.031	1.099	2.296	0.222	1.331	1.018	1.018
	400	1.294	0.488	0.983	0.983	1.083	2.240	0.220	1.259	0.977	0.977
	500	1.262	0.508	0.990	0.990	1.116	2.185	0.228	1.242	0.979	0.979
	600	1.321	0.468	0.972	0.972	1.077	2.287	0.213	1.268	0.972	0.972
	700	1.343	0.456	0.969	0.969	1.050	2.325	0.208	1.281	0.972	0.972
	800	1.184	0.553	0.994	0.994	1.078	2.050	0.248	1.187	0.975	0.975
L_5	20/100	1.456	0.449	1.091	1.091	1.091	2.559	0.206	1.538	1.098	1.098
	200	1.448	0.445	1.071	1.071	1.090	2.545	0.190	1.403	1.005	1.005
	300	1.437	0.439	1.042	1.042	1.086	2.527	0.199	1.449	1.043	1.043
	400	1.403	0.437	0.996	0.996	1.068	2.466	0.197	1.369	1.001	1.001
	500	1.368	0.456	0.998	0.998	1.093	2.405	0.204	1.349	1.002	1.002
	600	1.432	0.420	0.990	0.990	1.063	2.518	0.191	1.381	0.997	0.997
	700	1.456	0.408	0.991	0.991	1.044	2.559	0.187	1.396	0.997	0.997
	800	1.284	0.500	0.996	0.996	1.062	2.257	0.221	1.284	0.993	0.993
L_6	20/100	1.561	0.403	1.120	1.088	1.088	2.788	0.187	1.654	1.119	1.119
	200	1.552	0.400	1.099	1.071	1.071	2.772	0.172	1.504	1.022	1.022
	300	1.541	0.395	1.069	1.048	1.048	2.753	0.181	1.559	1.064	1.064
	400	1.504	0.395	1.020	1.017	1.017	2.686	0.179	1.475	1.022	1.022
	500	1.467	0.413	1.016	1.016	1.080	2.620	0.186	1.453	1.022	1.022
	600	1.536	0.380	1.021	1.003	1.003	2.742	0.173	1.488	1.017	1.017
	700	1.561	0.369	1.026	0.996	0.996	2.788	0.186	1.646	1.114	1.114
	800	1.377	0.452	1.000	1.000	1.049	2.458	0.200	1.382	1.012	1.012

Table A3.4: Numerical failure loads and their DSM estimates concerning the **C3** and **R3** columns with σ_{y20}=**450** ***MPa***.

L	T (ºC)	C_3					R_3				
		$\lambda_{FT.T}$	f_{uT}/σ_{yT}	$f_{uT}/f_{nG.T}$	$f_{uT}/f_{nFT.T}$	$f_{uT}/f_{nF.FT*}$	$\lambda_{FT.T}$	f_{uT}/σ_{yT}	$f_{uT}/f_{nG.T}$	$f_{uT}/f_{nFT.T}$	$f_{uT}/f_{nF.FT*}$
L_1	20/100	1.172	0.617	1.096	1.096	1.096	1.952	0.272	1.180	0.999	0.999
	200	1.165	0.614	1.084	1.084	1.139	1.941	0.250	1.076	0.915	0.915
	300	1.157	0.601	1.053	1.053	1.158	1.927	0.267	1.130	0.965	0.965
	400	1.129	0.586	0.999	0.999	1.143	1.881	0.269	1.083	0.939	0.939
	500	1.101	0.607	1.009	1.009	1.183	1.835	0.279	1.070	0.943	0.943
	600	1.153	0.565	0.985	0.985	1.138	1.920	0.260	1.092	0.935	0.935
	700	1.172	0.551	0.979	0.979	1.103	1.952	0.254	1.103	0.934	0.934
	800	1.033	0.649	1.014	1.014	1.125	1.721	0.308	1.042	0.955	0.955
L_2	20/100	1.338	0.510	1.080	1.080	1.080	2.255	0.233	1.348	1.043	1.043
	200	1.331	0.507	1.065	1.065	1.099	2.242	0.215	1.235	0.959	0.959
	300	1.322	0.501	1.041	1.041	1.111	2.226	0.228	1.287	1.004	1.004
	400	1.290	0.500	1.002	1.002	1.106	2.173	0.228	1.229	0.973	0.973
	500	1.258	0.520	1.009	1.009	1.139	2.119	0.236	1.210	0.973	0.973
	600	1.317	0.480	0.993	0.993	1.101	2.218	0.221	1.242	0.970	0.970
	700	1.338	0.468	0.989	0.989	1.073	2.255	0.217	1.256	0.972	0.972
	800	1.180	0.567	1.015	1.015	1.102	1.988	0.256	1.156	0.968	0.968
L_3	20/100	1.496	0.432	1.102	1.102	1.102	2.554	0.204	1.516	1.084	1.084
	200	1.488	0.430	1.085	1.085	1.099	2.540	0.189	1.387	0.995	0.995
	300	1.477	0.425	1.060	1.060	1.096	2.522	0.199	1.445	1.042	1.042
	400	1.442	0.428	1.021	1.021	1.084	2.461	0.200	1.379	1.010	1.010
	500	1.406	0.446	1.021	1.021	1.106	2.400	0.206	1.355	1.008	1.008
	600	1.472	0.412	1.020	1.020	1.081	2.512	0.194	1.395	1.008	1.008
	700	1.496	0.400	1.022	1.022	1.065	2.554	0.190	1.412	1.010	1.010
	800	1.319	0.490	1.016	1.016	1.077	2.252	0.223	1.288	0.997	0.997
L_4	20/100	1.644	0.377	1.163	1.088	1.088	2.847	0.181	1.671	1.116	1.116
	200	1.635	0.375	1.143	1.074	1.074	2.832	0.167	1.523	1.021	1.021
	300	1.624	0.371	1.117	1.054	1.054	2.812	0.177	1.593	1.073	1.073
	400	1.585	0.374	1.071	1.029	1.029	2.744	0.177	1.523	1.041	1.041
	500	1.546	0.390	1.061	1.038	1.038	2.676	0.183	1.497	1.040	1.040
	600	1.618	0.360	1.074	1.016	1.016	2.801	0.172	1.540	1.039	1.039
	700	1.644	0.345	1.064	0.996	0.996	2.847	0.164	1.513	1.010	1.010
	800	1.450	0.436	1.051	1.051	1.087	2.511	0.198	1.421	1.027	1.027
L_5	20/100	1.783	0.337	1.222	1.078	1.078	3.134	0.153	1.710	1.075	1.075
	200	1.773	0.335	1.201	1.064	1.064	3.117	0.148	1.636	1.033	1.033
	300	1.761	0.332	1.173	1.044	1.044	3.095	0.158	1.723	1.092	1.092
	400	1.718	0.334	1.126	1.020	1.020	3.020	0.159	1.650	1.062	1.062
	500	1.676	0.348	1.113	1.027	1.027	2.946	0.164	1.625	1.063	1.063
	600	1.754	0.323	1.133	1.012	1.012	3.083	0.154	1.666	1.058	1.058
	700	1.783	0.314	1.140	1.006	1.006	3.134	0.150	1.682	1.058	1.058
	800	1.572	0.379	1.070	1.034	1.034	2.764	0.178	1.548	1.053	1.053
L_6	20/100	1.912	0.305	1.270	1.066	1.066	3.414	0.144	1.910	1.138	1.138
	200	1.901	0.303	1.249	1.053	1.053	3.395	0.131	1.725	1.031	1.031
	300	1.888	0.300	1.220	1.034	1.034	3.371	0.141	1.830	1.099	1.099
	400	1.842	0.303	1.172	1.010	1.010	3.290	0.142	1.756	1.071	1.071
	500	1.797	0.315	1.159	1.017	1.017	3.209	0.148	1.734	1.074	1.074
	600	1.881	0.292	1.178	1.001	1.001	3.359	0.138	1.770	1.065	1.065
	700	1.912	0.282	1.175	0.987	0.987	3.414	0.134	1.784	1.063	1.063
	800	1.686	0.345	1.118	1.028	1.028	3.011	0.160	1.659	1.070	1.070

Table A3.5: Numerical failure loads and their DSM estimates concerning the **C3** and **R3** columns with $\boldsymbol{\sigma_{y20}}$**=600*MPa***.

L	*T* (ºC)	***C3***					***R3***				
		$\lambda_{FT.T}$	f_{uT}/σ_{yT}	$f_{uT}/f_{nG.T}$	$f_{uT}/f_{nFT.T}$	$f_{uT}/f_{nF.FT*}$	$\lambda_{FT.T}$	f_{uT}/σ_{yT}	$f_{uT}/f_{nG.T}$	$f_{uT}/f_{nFT.T}$	$f_{uT}/f_{nF.FT*}$
L_1	20/100	1.353	0.489	1.052	1.052	1.052	2.254	0.219	1.271	0.983	0.983
	200	1.345	0.491	1.047	1.047	1.079	2.241	0.198	1.132	0.879	0.879
	300	1.336	0.491	1.036	1.036	1.103	2.226	0.220	1.242	0.969	0.969
	400	1.304	0.497	1.012	1.012	1.112	2.172	0.224	1.206	0.955	0.955
	500	1.272	0.518	1.019	1.019	1.146	2.118	0.233	1.194	0.961	0.961
	600	1.331	0.478	1.002	1.002	1.107	2.217	0.216	1.212	0.948	0.948
	700	1.353	0.464	0.999	0.999	1.080	2.254	0.210	1.218	0.943	0.943
	800	1.193	0.567	1.029	1.029	1.114	1.988	0.254	1.145	0.959	0.959
L_2	20/100	1.545	0.408	1.110	1.086	1.086	2.604	0.193	1.490	1.053	1.053
	200	1.537	0.407	1.095	1.076	1.076	2.589	0.175	1.338	0.949	0.949
	300	1.526	0.405	1.074	1.060	1.060	2.571	0.192	1.447	1.030	1.030
	400	1.489	0.411	1.039	1.039	1.088	2.509	0.194	1.395	1.009	1.009
	500	1.452	0.428	1.035	1.035	1.106	2.447	0.201	1.374	1.010	1.010
	600	1.520	0.396	1.042	1.032	1.032	2.561	0.188	1.407	1.004	1.004
	700	1.545	0.385	1.048	1.026	1.026	2.604	0.183	1.418	1.002	1.002
	800	1.363	0.473	1.028	1.028	1.081	2.296	0.217	1.306	0.999	0.999
L_3	20/100	1.728	0.351	1.194	1.078	1.078	2.949	0.170	1.687	1.102	1.102
	200	1.718	0.349	1.176	1.066	1.066	2.933	0.156	1.526	1.000	1.000
	300	1.706	0.347	1.153	1.051	1.051	2.912	0.168	1.628	1.072	1.072
	400	1.665	0.352	1.113	1.032	1.032	2.842	0.170	1.568	1.049	1.049
	500	1.624	0.366	1.101	1.039	1.039	2.772	0.176	1.543	1.048	1.048
	600	1.700	0.340	1.121	1.025	1.025	2.901	0.165	1.586	1.047	1.047
	700	1.728	0.332	1.131	1.021	1.021	2.949	0.162	1.602	1.046	1.046
	800	1.524	0.403	1.066	1.053	1.053	2.601	0.190	1.467	1.038	1.038
L_4	20/100	1.899	0.309	1.272	1.073	1.073	3.288	0.150	1.843	1.125	1.125
	200	1.888	0.308	1.253	1.062	1.062	3.270	0.137	1.665	1.020	1.020
	300	1.875	0.306	1.228	1.046	1.046	3.247	0.148	1.777	1.093	1.093
	400	1.830	0.311	1.186	1.027	1.027	3.168	0.150	1.715	1.071	1.071
	500	1.785	0.322	1.171	1.033	1.033	3.090	0.155	1.691	1.073	1.073
	600	1.868	0.300	1.194	1.019	1.019	3.235	0.145	1.730	1.067	1.067
	700	1.899	0.293	1.205	1.017	1.017	3.288	0.142	1.745	1.065	1.065
	800	1.675	0.335	1.073	0.991	0.991	2.900	0.172	1.647	1.088	1.088
L_5	20/100	2.059	0.276	1.333	1.061	1.061	3.619	0.114	1.708	0.981	0.981
	200	2.047	0.275	1.314	1.050	1.050	3.599	0.119	1.764	1.017	1.017
	300	2.033	0.273	1.288	1.034	1.034	3.574	0.130	1.895	1.097	1.097
	400	1.984	0.277	1.243	1.016	1.016	3.488	0.132	1.834	1.078	1.078
	500	1.935	0.288	1.229	1.023	1.023	3.402	0.137	1.813	1.083	1.083
	600	2.025	0.267	1.250	1.007	1.007	3.560	0.128	1.847	1.072	1.072
	700	2.059	0.261	1.262	1.005	1.005	3.619	0.124	1.860	1.068	1.068
	800	1.816	0.315	1.185	1.033	1.033	3.192	0.150	1.743	1.084	1.084
L_6	20/100	2.208	0.245	1.359	1.029	1.029	3.942	0.096	1.707	0.929	0.929
	200	2.195	0.244	1.343	1.021	1.021	3.920	0.105	1.832	1.001	1.001
	300	2.180	0.244	1.320	1.008	1.008	3.893	0.115	1.984	1.088	1.088
	400	2.127	0.248	1.278	0.993	0.993	3.799	0.117	1.925	1.073	1.073
	500	2.075	0.258	1.265	1.001	1.001	3.705	0.122	1.908	1.080	1.080
	600	2.172	0.238	1.282	0.982	0.982	3.878	0.113	1.935	1.064	1.064
	700	2.208	0.233	1.294	0.979	0.979	3.942	0.110	1.945	1.059	1.059
	800	1.947	0.283	1.222	1.013	1.013	3.477	0.134	1.845	1.087	1.087

Table A4.1: Numerical failure loads and their DSM estimates concerning the **C4** and **R4** columns with σ_{y20}=75 ***MPa***.

L	T (ºC)	***C4***					***R4***				
		$\lambda_{FT.T}$	f_{uT}/σ_{yT}	$f_{uT}/f_{nG.T}$	$f_{uT}/f_{nFT.T}$	$f_{uT}/f_{nF.FT*}$	$\lambda_{FT.T}$	f_{uT}/σ_{yT}	$f_{uT}/f_{nG.T}$	$f_{uT}/f_{nFT.T}$	$f_{uT}/f_{nF.FT*}$
L_1	20/100	0.547	0.930	1.054	1.054	1.054	0.800	0.810	1.060	1.060	1.060
	200	0.544	0.870	0.985	0.985	1.082	0.796	0.743	0.969	0.969	1.049
	300	0.540	0.804	0.908	0.908	1.078	0.790	0.695	0.902	0.902	1.046
	400	0.527	0.749	0.842	0.842	1.058	0.771	0.621	0.797	0.797	0.972
	500	0.514	0.763	0.852	0.852	1.103	0.752	0.642	0.814	0.814	1.021
	600	0.538	0.733	0.828	0.828	1.064	0.787	0.595	0.771	0.771	0.958
	700	0.547	0.725	0.822	0.822	1.020	0.800	0.581	0.760	0.760	0.915
	800	0.482	0.781	0.861	0.861	1.010	0.706	0.671	0.826	0.826	0.952
L_2	20/100	0.603	0.915	1.065	1.065	1.065	0.868	0.769	1.054	1.054	1.054
	200	0.600	0.856	0.995	0.995	1.090	0.864	0.705	0.964	0.964	1.039
	300	0.595	0.787	0.913	0.913	1.080	0.858	0.667	0.907	0.907	1.043
	400	0.581	0.727	0.837	0.837	1.046	0.837	0.598	0.802	0.802	0.969
	500	0.567	0.742	0.849	0.849	1.092	0.816	0.620	0.820	0.820	1.017
	600	0.593	0.708	0.820	0.820	1.047	0.854	0.572	0.776	0.776	0.954
	700	0.603	0.698	0.813	0.813	1.003	0.868	0.557	0.764	0.764	0.910
	800	0.532	0.763	0.859	0.859	1.005	0.766	0.650	0.831	0.831	0.953
L_3	20/100	0.656	0.898	1.075	1.075	1.075	0.936	0.726	1.048	1.048	1.048
	200	0.652	0.841	1.005	1.005	1.098	0.931	0.664	0.954	0.954	1.024
	300	0.648	0.773	0.921	0.921	1.084	0.924	0.638	0.912	0.912	1.039
	400	0.632	0.707	0.836	0.836	1.039	0.902	0.574	0.807	0.807	0.965
	500	0.617	0.725	0.850	0.850	1.087	0.880	0.598	0.826	0.826	1.014
	600	0.645	0.686	0.817	0.817	1.036	0.921	0.548	0.782	0.782	0.950
	700	0.656	0.675	0.808	0.808	0.991	0.936	0.534	0.771	0.771	0.909
	800	0.579	0.749	0.861	0.861	1.004	0.825	0.629	0.837	0.837	0.952
L_4	20/100	0.706	0.880	1.084	1.084	1.084	1.002	0.679	1.035	1.035	1.035
	200	0.702	0.825	1.014	1.014	1.104	0.997	0.620	0.940	0.940	1.002
	300	0.697	0.757	0.928	0.928	1.086	0.990	0.607	0.915	0.915	1.033
	400	0.681	0.689	0.837	0.837	1.034	0.966	0.552	0.816	0.816	0.964
	500	0.664	0.709	0.852	0.852	1.083	0.942	0.574	0.832	0.832	1.009
	600	0.695	0.666	0.815	0.815	1.028	0.986	0.526	0.790	0.790	0.947
	700	0.706	0.652	0.804	0.804	0.980	1.002	0.512	0.780	0.780	0.908
	800	0.623	0.735	0.864	0.864	1.003	0.884	0.605	0.839	0.839	0.948
L_5	20/100	0.754	0.859	1.090	1.090	1.090	1.068	0.633	1.020	1.020	1.020
	200	0.750	0.807	1.022	1.022	1.110	1.062	0.576	0.924	0.924	0.980
	300	0.744	0.742	0.935	0.935	1.090	1.055	0.575	0.915	0.915	1.024
	400	0.726	0.674	0.840	0.840	1.032	1.029	0.528	0.823	0.823	0.961
	500	0.708	0.694	0.856	0.856	1.081	1.004	0.550	0.838	0.838	1.004
	600	0.741	0.648	0.815	0.815	1.021	1.051	0.503	0.798	0.798	0.944
	700	0.754	0.635	0.806	0.806	0.976	1.068	0.488	0.787	0.787	0.905
	800	0.665	0.722	0.869	0.869	1.005	0.942	0.584	0.847	0.847	0.951
L_6	20/100	0.798	0.837	1.092	1.092	1.092	1.133	0.588	1.007	1.007	1.007
	200	0.794	0.789	1.027	1.027	1.113	1.127	0.535	0.911	0.911	0.960
	300	0.788	0.726	0.942	0.942	1.092	1.119	0.542	0.915	0.915	1.013
	400	0.769	0.659	0.845	0.845	1.031	1.092	0.504	0.829	0.829	0.956
	500	0.750	0.681	0.861	0.861	1.081	1.065	0.525	0.843	0.843	0.997
	600	0.785	0.632	0.818	0.818	1.018	1.114	0.479	0.806	0.806	0.939
	700	0.798	0.619	0.808	0.808	0.973	1.133	0.466	0.797	0.797	0.906
	800	0.704	0.710	0.874	0.874	1.007	0.999	0.560	0.851	0.851	0.948

Table A4.2: Numerical failure loads and their DSM estimates concerning the **C**4 and **R**4 columns with $\boldsymbol{\sigma_{y20}}$**=150** ***MPa***.

L	T (°C)	***C4***					***R4***				
		$\lambda_{FT.T}$	f_{uT}/σ_{yT}	$f_{uT}/f_{nG.T}$	$f_{uT}/f_{nFT.T}$	$f_{uT}/f_{nF.FT*}$	$\lambda_{FT.T}$	f_{uT}/σ_{yT}	$f_{uT}/f_{nG.T}$	$f_{uT}/f_{nFT.T}$	$f_{uT}/f_{nF.FT*}$
L_1	20/100	0.773	0.873	1.121	1.121	1.121	1.132	0.617	1.054	1.054	1.054
	200	0.769	0.756	0.969	0.969	1.051	1.126	0.561	0.953	0.953	1.005
	300	0.764	0.757	0.967	0.967	1.124	1.118	0.574	0.968	0.968	1.072
	400	0.745	0.701	0.885	0.885	1.083	1.091	0.538	0.885	0.885	1.021
	500	0.727	0.718	0.896	0.896	1.128	1.064	0.561	0.901	0.901	1.065
	600	0.761	0.682	0.869	0.869	1.085	1.113	0.514	0.864	0.864	1.008
	700	0.773	0.672	0.863	0.863	1.043	1.132	0.501	0.856	0.856	0.973
	800	0.682	0.742	0.902	0.902	1.042	0.998	0.597	0.906	0.906	1.009
L_2	20/100	0.853	0.832	1.127	1.127	1.127	1.228	0.550	1.035	1.035	1.035
	200	0.848	0.755	1.019	1.019	1.100	1.221	0.499	0.931	0.931	0.972
	300	0.842	0.728	0.979	0.979	1.128	1.213	0.522	0.966	0.966	1.052
	400	0.822	0.670	0.889	0.889	1.077	1.184	0.498	0.895	0.895	1.013
	500	0.801	0.689	0.902	0.902	1.122	1.154	0.519	0.907	0.907	1.050
	600	0.839	0.649	0.871	0.871	1.073	1.208	0.476	0.876	0.876	0.999
	700	0.853	0.637	0.863	0.863	1.031	1.228	0.463	0.870	0.870	0.968
	800	0.752	0.717	0.909	0.909	1.043	1.083	0.558	0.912	0.912	1.005
L_3	20/100	0.928	0.784	1.124	1.124	1.124	1.324	0.491	1.022	1.022	1.022
	200	0.923	0.720	1.028	1.028	1.103	1.316	0.446	0.920	0.920	0.951
	300	0.916	0.697	0.991	0.991	1.130	1.307	0.472	0.965	0.965	1.033
	400	0.894	0.643	0.898	0.898	1.075	1.275	0.457	0.904	0.904	1.001
	500	0.872	0.663	0.912	0.912	1.120	1.244	0.478	0.913	0.913	1.034
	600	0.913	0.619	0.877	0.877	1.067	1.302	0.437	0.889	0.889	0.990
	700	0.928	0.606	0.869	0.869	1.026	1.324	0.427	0.890	0.890	0.969
	800	0.818	0.694	0.919	0.919	1.047	1.167	0.518	0.916	0.916	0.996
L_4	20/100	0.999	0.732	1.112	1.112	1.112	1.418	0.442	1.025	1.025	1.025
	200	0.993	0.681	1.030	1.030	1.098	1.410	0.401	0.921	0.921	0.942
	300	0.986	0.662	0.995	0.995	1.124	1.400	0.428	0.971	0.971	1.020
	400	0.963	0.615	0.906	0.906	1.071	1.366	0.419	0.916	0.916	0.991
	500	0.939	0.636	0.920	0.920	1.116	1.332	0.438	0.922	0.922	1.019
	600	0.983	0.590	0.884	0.884	1.060	1.395	0.401	0.905	0.905	0.982
	700	0.999	0.576	0.874	0.874	1.019	1.418	0.389	0.902	0.902	0.960
	800	0.881	0.670	0.927	0.927	1.048	1.250	0.478	0.920	0.920	0.987
L_5	20/100	1.066	0.681	1.096	1.096	1.096	1.511	0.401	1.042	1.037	1.037
	200	1.060	0.642	1.027	1.027	1.090	1.502	0.363	0.935	0.933	0.933
	300	1.053	0.627	0.997	0.997	1.115	1.492	0.389	0.987	0.987	1.017
	400	1.027	0.587	0.914	0.914	1.067	1.456	0.385	0.935	0.935	0.988
	500	1.002	0.609	0.927	0.927	1.111	1.420	0.402	0.935	0.935	1.008
	600	1.049	0.563	0.892	0.892	1.056	1.486	0.368	0.927	0.927	0.979
	700	1.066	0.544	0.875	0.875	1.007	1.511	0.357	0.928	0.924	0.924
	800	0.940	0.646	0.935	0.935	1.050	1.332	0.440	0.924	0.924	0.977
L_6	20/100	1.129	0.635	1.082	1.082	1.082	1.602	0.366	1.072	1.031	1.031
	200	1.123	0.604	1.023	1.023	1.079	1.593	0.332	0.962	0.929	0.929
	300	1.115	0.593	0.997	0.997	1.104	1.582	0.356	1.015	0.984	0.984
	400	1.088	0.561	0.920	0.920	1.062	1.544	0.353	0.960	0.944	0.944
	500	1.061	0.583	0.933	0.933	1.104	1.506	0.369	0.955	0.952	0.952
	600	1.111	0.537	0.900	0.900	1.050	1.576	0.339	0.959	0.931	0.931
	700	1.129	0.523	0.892	0.892	1.014	1.602	0.328	0.960	0.923	0.923
	800	0.996	0.622	0.941	0.941	1.049	1.413	0.407	0.938	0.938	0.977

Table A4.3: Numerical failure loads and their DSM estimates concerning the **C**4 and **R**4 columns with $\boldsymbol{\sigma_{y20}}$**=300** ***MPa***.

L	T (ºC)	***C4***					***R4***				
		$\lambda_{FT.T}$	f_{uT}/σ_{yT}	$f_{uT}/f_{nG.T}$	$f_{uT}/f_{nFT.T}$	$f_{uT}/f_{nF.FT^*}$	$\lambda_{FT.T}$	f_{uT}/σ_{yT}	$f_{uT}/f_{nG.T}$	$f_{uT}/f_{nFT.T}$	$f_{uT}/f_{nF.FT^*}$
L_1	20/100	1.094	0.680	1.122	1.122	1.122	1.601	0.365	1.065	1.025	1.025
	200	1.088	0.665	1.091	1.091	1.155	1.592	0.330	0.954	0.921	0.921
	300	1.080	0.638	1.039	1.039	1.157	1.581	0.361	1.029	0.998	0.998
	400	1.054	0.606	0.965	0.965	1.121	1.543	0.366	0.992	0.976	0.976
	500	1.028	0.627	0.976	0.976	1.163	1.504	0.383	0.988	0.986	0.986
	600	1.076	0.584	0.948	0.948	1.115	1.575	0.350	0.990	0.962	0.962
	700	1.094	0.570	0.941	0.941	1.077	1.601	0.340	0.993	0.955	0.955
	800	0.965	0.664	0.980	0.980	1.097	1.412	0.423	0.974	0.974	1.015
L_2	20/100	1.206	0.595	1.093	1.093	1.093	1.737	0.323	1.110	1.019	1.019
	200	1.199	0.587	1.071	1.071	1.121	1.727	0.293	0.998	0.919	0.919
	300	1.191	0.570	1.032	1.032	1.129	1.715	0.319	1.069	0.988	0.988
	400	1.162	0.552	0.972	0.972	1.104	1.674	0.322	1.029	0.965	0.965
	500	1.133	0.574	0.982	0.982	1.143	1.633	0.337	1.023	0.974	0.974
	600	1.186	0.531	0.956	0.956	1.096	1.709	0.309	1.028	0.953	0.953
	700	1.206	0.517	0.950	0.950	1.062	1.737	0.300	1.031	0.947	0.947
	800	1.063	0.615	0.988	0.988	1.091	1.532	0.374	1.000	0.988	0.988
L_3	20/100	1.312	0.525	1.080	1.080	1.080	1.872	0.290	1.159	1.019	1.019
	200	1.305	0.520	1.060	1.060	1.098	1.861	0.265	1.045	0.921	0.921
	300	1.296	0.509	1.029	1.029	1.103	1.848	0.285	1.110	0.983	0.983
	400	1.264	0.501	0.978	0.978	1.086	1.804	0.287	1.066	0.957	0.957
	500	1.233	0.522	0.986	0.986	1.120	1.759	0.300	1.060	0.966	0.966
	600	1.291	0.481	0.966	0.966	1.078	1.841	0.276	1.067	0.947	0.947
	700	1.312	0.467	0.961	0.961	1.049	1.872	0.268	1.071	0.941	0.941
	800	1.157	0.565	0.990	0.990	1.079	1.651	0.333	1.034	0.978	0.978
L_4	20/100	1.413	0.471	1.087	1.087	1.087	2.005	0.264	1.212	1.023	1.023
	200	1.405	0.467	1.066	1.066	1.091	1.994	0.242	1.097	0.929	0.929
	300	1.395	0.459	1.036	1.036	1.089	1.980	0.259	1.156	0.984	0.984
	400	1.361	0.455	0.989	0.989	1.071	1.932	0.260	1.106	0.955	0.955
	500	1.328	0.475	0.993	0.993	1.099	1.884	0.271	1.099	0.962	0.962
	600	1.390	0.437	0.981	0.981	1.065	1.972	0.250	1.109	0.946	0.946
	700	1.413	0.424	0.978	0.978	1.041	2.005	0.243	1.115	0.942	0.942
	800	1.246	0.519	0.993	0.993	1.066	1.768	0.300	1.069	0.971	0.971
L_5	20/100	1.508	0.429	1.113	1.107	1.107	2.136	0.244	1.268	1.032	1.032
	200	1.499	0.425	1.088	1.088	1.101	2.124	0.224	1.151	0.940	0.940
	300	1.489	0.418	1.057	1.057	1.089	2.109	0.238	1.207	0.990	0.990
	400	1.453	0.416	1.007	1.007	1.065	2.059	0.238	1.151	0.957	0.957
	500	1.417	0.434	1.006	1.006	1.086	2.008	0.248	1.141	0.962	0.962
	600	1.483	0.400	1.004	1.004	1.061	2.102	0.229	1.155	0.949	0.949
	700	1.508	0.384	0.995	0.989	0.989	2.136	0.223	1.162	0.946	0.946
	800	1.329	0.476	0.998	0.998	1.056	1.884	0.273	1.106	0.968	0.968
L_6	20/100	1.597	0.396	1.152	1.087	1.087	2.266	0.226	1.325	1.042	1.042
	200	1.588	0.392	1.126	1.068	1.068	2.253	0.208	1.203	0.949	0.949
	300	1.577	0.385	1.092	1.043	1.043	2.237	0.221	1.259	0.997	0.997
	400	1.539	0.384	1.037	1.013	1.013	2.183	0.220	1.197	0.962	0.962
	500	1.501	0.401	1.029	1.028	1.028	2.130	0.229	1.186	0.967	0.967
	600	1.571	0.370	1.040	0.996	0.996	2.229	0.212	1.202	0.955	0.955
	700	1.597	0.360	1.046	0.987	0.987	2.266	0.207	1.210	0.952	0.952
	800	1.408	0.439	1.007	1.007	1.050	1.998	0.251	1.145	0.968	0.968

Table A4.4: Numerical failure loads and their DSM estimates concerning the **C**$_4$ and **R**$_4$ columns with σ_{y20}=**450** ***MPa***.

L	*T* (ºC)	***C4***					***R4***				
		$\lambda_{FT.T}$	f_{uT}/σ_{yT}	$f_{uT}/f_{nG.T}$	$f_{uT}/f_{nFT.T}$	$f_{uT}/f_{nF.FT*}$	$\lambda_{FT.T}$	f_{uT}/σ_{yT}	$f_{uT}/f_{nG.T}$	$f_{uT}/f_{nFT.T}$	$f_{uT}/f_{nF.FT*}$
L_1	20/100	1.340	0.511	1.082	1.082	1.082	1.961	0.265	1.162	0.994	0.994
	200	1.332	0.507	1.066	1.066	1.100	1.950	0.243	1.053	0.903	0.903
	300	1.323	0.501	1.042	1.042	1.112	1.936	0.262	1.120	0.965	0.965
	400	1.291	0.499	1.003	1.003	1.106	1.889	0.266	1.082	0.946	0.946
	500	1.259	0.520	1.010	1.010	1.139	1.843	0.278	1.076	0.954	0.954
	600	1.318	0.480	0.993	0.993	1.101	1.929	0.256	1.086	0.938	0.938
	700	1.340	0.467	0.990	0.990	1.074	1.961	0.249	1.092	0.934	0.934
	800	1.182	0.566	1.016	1.016	1.102	1.729	0.309	1.054	0.970	0.970
L_2	20/100	1.477	0.443	1.103	1.103	1.103	2.127	0.240	1.238	1.010	1.010
	200	1.469	0.440	1.085	1.085	1.102	2.116	0.220	1.125	0.921	0.921
	300	1.458	0.435	1.059	1.059	1.099	2.101	0.236	1.189	0.977	0.977
	400	1.423	0.436	1.019	1.019	1.086	2.050	0.239	1.144	0.953	0.953
	500	1.388	0.455	1.019	1.019	1.110	1.999	0.248	1.132	0.958	0.958
	600	1.453	0.420	1.016	1.016	1.084	2.093	0.230	1.150	0.947	0.947
	700	1.477	0.409	1.018	1.018	1.066	2.127	0.224	1.158	0.945	0.945
	800	1.302	0.500	1.016	1.016	1.080	1.876	0.274	1.100	0.965	0.965
L_3	20/100	1.607	0.394	1.160	1.088	1.088	2.292	0.220	1.316	1.028	1.028
	200	1.598	0.391	1.138	1.072	1.072	2.280	0.202	1.196	0.937	0.937
	300	1.587	0.386	1.109	1.052	1.052	2.264	0.216	1.260	0.992	0.992
	400	1.549	0.388	1.060	1.029	1.029	2.209	0.217	1.208	0.964	0.964
	500	1.510	0.404	1.050	1.043	1.043	2.155	0.226	1.195	0.968	0.968
	600	1.581	0.374	1.067	1.015	1.015	2.255	0.210	1.216	0.959	0.959
	700	1.607	0.365	1.076	1.009	1.009	2.292	0.205	1.226	0.958	0.958
	800	1.417	0.443	1.028	1.028	1.070	2.022	0.247	1.153	0.969	0.969
L_4	20/100	1.730	0.358	1.223	1.071	1.071	2.456	0.202	1.391	1.044	1.044
	200	1.721	0.355	1.199	1.056	1.056	2.442	0.186	1.264	0.952	0.952
	300	1.708	0.351	1.168	1.035	1.035	2.425	0.198	1.330	1.006	1.006
	400	1.667	0.352	1.116	1.012	1.012	2.366	0.199	1.274	0.977	0.977
	500	1.626	0.365	1.101	1.021	1.021	2.308	0.207	1.258	0.979	0.979
	600	1.702	0.341	1.127	1.002	1.002	2.416	0.193	1.283	0.973	0.973
	700	1.730	0.333	1.138	0.996	0.996	2.456	0.188	1.295	0.972	0.972
	800	1.526	0.399	1.060	1.043	1.043	2.166	0.226	1.210	0.977	0.977
L_5	20/100	1.846	0.331	1.287	1.062	1.062	2.616	0.187	1.461	1.057	1.057
	200	1.836	0.328	1.262	1.046	1.046	2.602	0.172	1.326	0.962	0.962
	300	1.823	0.324	1.229	1.026	1.026	2.584	0.184	1.397	1.018	1.018
	400	1.779	0.325	1.174	1.002	1.002	2.521	0.185	1.338	0.989	0.989
	500	1.735	0.336	1.155	1.009	1.009	2.459	0.191	1.320	0.990	0.990
	600	1.816	0.316	1.188	0.994	0.994	2.574	0.178	1.348	0.985	0.985
	700	1.846	0.309	1.199	0.989	0.989	2.616	0.164	1.277	0.924	0.924
	800	1.628	0.365	1.105	1.023	1.023	2.308	0.209	1.268	0.987	0.987
L_6	20/100	1.955	0.309	1.347	1.053	1.053	2.775	0.155	1.363	0.953	0.953
	200	1.945	0.306	1.320	1.038	1.038	2.760	0.159	1.381	0.969	0.969
	300	1.931	0.303	1.287	1.018	1.018	2.740	0.170	1.459	1.028	1.028
	400	1.884	0.304	1.229	0.995	0.995	2.674	0.172	1.398	0.999	0.999
	500	1.838	0.314	1.208	1.000	1.000	2.608	0.178	1.380	1.001	1.001
	600	1.924	0.295	1.244	0.987	0.987	2.730	0.166	1.409	0.995	0.995
	700	1.955	0.288	1.257	0.983	0.983	2.775	0.162	1.421	0.994	0.994
	800	1.725	0.339	1.150	1.010	1.010	2.447	0.194	1.324	0.996	0.996

Table A4.5: Numerical failure loads and their DSM estimates concerning the **C4** and **R4** columns with σ_{y20}**=600 *MPa***.

L	*T* (°C)	***C4***					***R4***				
		$\lambda_{FT.T}$	f_{uT}/σ_{yT}	$f_{uT}/f_{nG.T}$	$f_{uT}/f_{nFT.T}$	$f_{uT}/f_{nF.FT*}$	$\lambda_{FT.T}$	f_{uT}/σ_{yT}	$f_{uT}/f_{nG.T}$	$f_{uT}/f_{nFT.T}$	$f_{uT}/f_{nF.FT*}$
L_1	20/100	1.547	0.411	1.121	1.089	1.089	2.264	0.216	1.264	0.995	0.995
	200	1.538	0.408	1.102	1.076	1.076	2.251	0.197	1.136	0.897	0.897
	300	1.528	0.406	1.080	1.061	1.061	2.235	0.215	1.225	0.971	0.971
	400	1.491	0.411	1.042	1.042	1.091	2.181	0.218	1.182	0.951	0.951
	500	1.454	0.428	1.038	1.038	1.108	2.128	0.226	1.168	0.953	0.953
	600	1.522	0.396	1.047	1.032	1.032	2.227	0.211	1.192	0.947	0.947
	700	1.547	0.387	1.055	1.024	1.024	2.264	0.206	1.201	0.945	0.945
	800	1.364	0.472	1.028	1.028	1.081	1.996	0.248	1.127	0.954	0.954
L_2	20/100	1.705	0.363	1.204	1.069	1.069	2.456	0.198	1.362	1.022	1.022
	200	1.696	0.361	1.184	1.057	1.057	2.443	0.181	1.229	0.926	0.926
	300	1.684	0.358	1.158	1.040	1.040	2.426	0.196	1.312	0.992	0.992
	400	1.643	0.362	1.114	1.023	1.023	2.367	0.198	1.264	0.970	0.970
	500	1.603	0.375	1.098	1.032	1.032	2.309	0.205	1.248	0.971	0.971
	600	1.678	0.351	1.127	1.015	1.015	2.417	0.192	1.276	0.967	0.967
	700	1.705	0.344	1.140	1.011	1.011	2.456	0.187	1.288	0.967	0.967
	800	1.504	0.410	1.057	1.054	1.054	2.166	0.224	1.200	0.969	0.969
L_3	20/100	1.856	0.329	1.293	1.061	1.061	2.647	0.171	1.366	0.982	0.982
	200	1.845	0.327	1.270	1.048	1.048	2.632	0.166	1.314	0.947	0.947
	300	1.832	0.325	1.243	1.033	1.033	2.614	0.179	1.395	1.010	1.010
	400	1.788	0.328	1.195	1.015	1.015	2.551	0.181	1.345	0.987	0.987
	500	1.744	0.338	1.173	1.020	1.020	2.488	0.188	1.326	0.988	0.988
	600	1.826	0.319	1.211	1.009	1.009	2.604	0.175	1.357	0.984	0.984
	700	1.856	0.312	1.227	1.007	1.007	2.647	0.174	1.390	0.999	0.999
	800	1.637	0.365	1.116	1.029	1.029	2.335	0.205	1.272	0.984	0.984
L_4	20/100	1.998	0.303	1.380	1.058	1.058	2.835	0.155	1.421	0.981	0.981
	200	1.987	0.301	1.356	1.045	1.045	2.820	0.152	1.381	0.957	0.957
	300	1.973	0.299	1.328	1.030	1.030	2.800	0.165	1.471	1.023	1.023
	400	1.925	0.302	1.275	1.011	1.011	2.732	0.167	1.419	1.001	1.001
	500	1.878	0.311	1.250	1.015	1.015	2.665	0.173	1.401	1.003	1.003
	600	1.965	0.294	1.294	1.007	1.007	2.789	0.161	1.431	0.998	0.998
	700	1.998	0.287	1.306	1.001	1.001	2.835	0.157	1.444	0.997	0.997
	800	1.762	0.334	1.184	1.019	1.019	2.501	0.188	1.344	0.998	0.998
L_5	20/100	2.132	0.281	1.458	1.053	1.053	3.021	0.137	1.425	0.949	0.949
	200	2.120	0.280	1.433	1.040	1.040	3.004	0.140	1.440	0.962	0.962
	300	2.105	0.278	1.404	1.026	1.026	2.983	0.152	1.539	1.032	1.032
	400	2.054	0.280	1.348	1.007	1.007	2.911	0.153	1.479	1.006	1.006
	500	2.004	0.289	1.322	1.010	1.010	2.840	0.160	1.469	1.013	1.013
	600	2.097	0.273	1.368	1.002	1.002	2.972	0.149	1.499	1.007	1.007
	700	2.132	0.267	1.385	1.000	1.000	3.021	0.145	1.510	1.005	1.005
	800	1.880	0.310	1.249	1.013	1.013	2.664	0.174	1.411	1.010	1.010
L_6	20/100	2.258	0.262	1.525	1.044	1.044	3.204	0.122	1.423	0.915	0.915
	200	2.245	0.261	1.500	1.032	1.032	3.186	0.129	1.489	0.961	0.961
	300	2.230	0.259	1.470	1.018	1.018	3.164	0.140	1.599	1.036	1.036
	400	2.176	0.262	1.413	1.001	1.001	3.088	0.142	1.547	1.017	1.017
	500	2.122	0.270	1.386	1.005	1.005	3.012	0.148	1.530	1.020	1.020
	600	2.221	0.255	1.432	0.995	0.995	3.152	0.137	1.557	1.011	1.011
	700	2.258	0.249	1.450	0.992	0.992	3.204	0.134	1.568	1.009	1.009
	800	1.991	0.290	1.309	1.007	1.007	2.826	0.162	1.473	1.019	1.019

Table A5.1: Numerical failure loads and their DSM estimates concerning the **C5** and **R5** columns with σ_{y20}=75 ***MPa***.

L	*T* (ºC)	***C5***					***R5***				
		$\lambda_{FT.T}$	f_{uT}/σ_{yT}	$f_{uT}/f_{nG.T}$	$f_{uT}/f_{nFT.T}$	$f_{uT}/f_{nF.FT*}$	$\lambda_{FT.T}$	f_{uT}/σ_{yT}	$f_{uT}/f_{nG.T}$	$f_{uT}/f_{nFT.T}$	$f_{uT}/f_{nF.FT*}$
L_1	20/100	0.508	0.931	1.037	1.037	1.037	0.917	0.728	1.036	1.036	1.036
	200	0.505	0.871	0.969	0.969	1.066	0.912	0.667	0.944	0.944	1.014
	300	0.501	0.806	0.895	0.895	1.067	0.905	0.641	0.903	0.903	1.032
	400	0.489	0.757	0.837	0.837	1.055	0.883	0.581	0.805	0.805	0.965
	500	0.477	0.769	0.846	0.846	1.098	0.862	0.602	0.821	0.821	1.011
	600	0.499	0.743	0.825	0.825	1.065	0.902	0.554	0.779	0.779	0.950
	700	0.508	0.736	0.820	0.820	1.022	0.917	0.541	0.768	0.768	0.908
	800	0.448	0.786	0.854	0.854	1.005	0.809	0.633	0.833	0.833	0.950
L_2	20/100	0.620	0.899	1.056	1.056	1.056	0.987	0.682	1.026	1.026	1.026
	200	0.616	0.840	0.985	0.985	1.078	0.982	0.625	0.936	0.936	0.999
	300	0.612	0.770	0.901	0.901	1.064	0.975	0.608	0.905	0.905	1.024
	400	0.597	0.708	0.821	0.821	1.025	0.951	0.555	0.810	0.810	0.960
	500	0.582	0.724	0.834	0.834	1.071	0.928	0.577	0.827	0.827	1.006
	600	0.609	0.688	0.803	0.803	1.024	0.971	0.529	0.785	0.785	0.944
	700	0.620	0.678	0.796	0.796	0.980	0.987	0.515	0.775	0.775	0.905
	800	0.546	0.746	0.846	0.846	0.988	0.870	0.610	0.837	0.837	0.948
L_3	20/100	0.725	0.857	1.068	1.068	1.068	1.056	0.637	1.016	1.016	1.016
	200	0.721	0.804	1.000	1.000	1.088	1.050	0.581	0.921	0.921	0.978
	300	0.716	0.737	0.913	0.913	1.067	1.043	0.575	0.907	0.907	1.016
	400	0.699	0.669	0.820	0.820	1.011	1.018	0.529	0.816	0.816	0.955
	500	0.681	0.688	0.836	0.836	1.059	0.993	0.550	0.832	0.832	0.998
	600	0.713	0.644	0.797	0.797	1.001	1.039	0.504	0.792	0.792	0.940
	700	0.725	0.633	0.789	0.789	0.959	1.056	0.490	0.782	0.782	0.902
	800	0.639	0.715	0.848	0.848	0.983	0.932	0.585	0.841	0.841	0.946
L_4	20/100	0.823	0.807	1.072	1.072	1.072	1.124	0.593	1.007	1.007	1.007
	200	0.819	0.762	1.008	1.008	1.090	1.118	0.539	0.910	0.910	0.960
	300	0.813	0.701	0.924	0.924	1.069	1.110	0.542	0.907	0.907	1.006
	400	0.793	0.635	0.827	0.827	1.005	1.084	0.503	0.822	0.822	0.950
	500	0.774	0.657	0.843	0.843	1.054	1.057	0.524	0.836	0.836	0.990
	600	0.810	0.610	0.802	0.802	0.993	1.106	0.479	0.800	0.800	0.935
	700	0.823	0.596	0.791	0.791	0.949	1.124	0.466	0.791	0.791	0.900
	800	0.726	0.686	0.855	0.855	0.984	0.992	0.559	0.844	0.844	0.941
L_5	20/100	0.914	0.751	1.066	1.066	1.066	1.192	0.552	1.001	1.001	1.001
	200	0.909	0.715	1.010	1.010	1.085	1.185	0.502	0.904	0.904	0.948
	300	0.902	0.663	0.933	0.933	1.066	1.177	0.510	0.910	0.910	0.997
	400	0.881	0.604	0.836	0.836	1.003	1.148	0.478	0.830	0.830	0.946
	500	0.859	0.626	0.853	0.853	1.050	1.120	0.498	0.842	0.842	0.983
	600	0.899	0.578	0.810	0.810	0.988	1.172	0.455	0.809	0.809	0.930
	700	0.914	0.564	0.800	0.800	0.946	1.192	0.442	0.801	0.801	0.899
	800	0.806	0.659	0.864	0.864	0.986	1.051	0.534	0.848	0.848	0.938
L_6	20/100	0.997	0.695	1.053	1.053	1.053	1.257	0.515	0.998	0.998	0.998
	200	0.992	0.667	1.006	1.006	1.074	1.250	0.468	0.901	0.901	0.938
	300	0.985	0.624	0.937	0.937	1.059	1.242	0.480	0.915	0.915	0.991
	400	0.961	0.574	0.845	0.845	1.000	1.212	0.454	0.838	0.838	0.942
	500	0.937	0.597	0.862	0.862	1.046	1.182	0.473	0.848	0.848	0.976
	600	0.981	0.548	0.820	0.820	0.984	1.237	0.432	0.819	0.819	0.927
	700	0.997	0.534	0.810	0.810	0.944	1.257	0.419	0.813	0.813	0.898
	800	0.879	0.631	0.872	0.872	0.987	1.109	0.509	0.851	0.851	0.934

Table A5.2: Numerical failure loads and their DSM estimates concerning the $\mathbf{C_5}$ and $\mathbf{R_5}$ columns with σ_{y20}=150 *MPa*.

L	T (ºC)	C_5					R_5				
		$\lambda_{FT.T}$	f_{uT}/σ_{yT}	$f_{uT}/f_{nG.T}$	$f_{uT}/f_{nFT.T}$	$f_{uT}/f_{nF.FT^*}$	$\lambda_{FT.T}$	f_{uT}/σ_{yT}	$f_{uT}/f_{nG.T}$	$f_{uT}/f_{nFT.T}$	$f_{uT}/f_{nF.FT^*}$
L_1	20/100	0.718	0.886	1.099	1.099	1.099	1.297	0.511	1.032	1.032	1.032
	200	0.714	0.767	0.950	0.950	1.034	1.289	0.464	0.931	0.931	0.965
	300	0.709	0.768	0.948	0.948	1.109	1.280	0.485	0.963	0.963	1.035
	400	0.692	0.715	0.873	0.873	1.077	1.249	0.466	0.895	0.895	0.997
	500	0.675	0.730	0.883	0.883	1.120	1.219	0.486	0.905	0.905	1.032
	600	0.706	0.697	0.859	0.859	1.081	1.275	0.446	0.880	0.880	0.987
	700	0.718	0.688	0.854	0.854	1.040	1.297	0.433	0.875	0.875	0.959
	800	0.633	0.751	0.889	0.889	1.031	1.143	0.524	0.906	0.906	0.988
L_2	20/100	0.876	0.805	1.110	1.110	1.110	1.396	0.460	1.040	1.040	1.040
	200	0.871	0.734	1.008	1.008	1.086	1.388	0.418	0.936	0.936	0.960
	300	0.865	0.709	0.969	0.969	1.113	1.378	0.440	0.974	0.974	1.028
	400	0.844	0.651	0.878	0.878	1.059	1.345	0.427	0.911	0.911	0.991
	500	0.823	0.671	0.891	0.891	1.104	1.312	0.446	0.916	0.916	1.019
	600	0.862	0.629	0.858	0.858	1.053	1.373	0.408	0.899	0.899	0.981
	700	0.876	0.616	0.850	0.850	1.012	1.396	0.398	0.900	0.900	0.962
	800	0.773	0.699	0.898	0.898	1.028	1.231	0.484	0.912	0.912	0.982
L_3	20/100	1.025	0.701	1.088	1.088	1.088	1.494	0.418	1.063	1.063	1.063
	200	1.020	0.655	1.012	1.012	1.077	1.485	0.380	0.957	0.957	0.970
	300	1.012	0.638	0.980	0.980	1.103	1.475	0.401	0.996	0.996	1.030
	400	0.988	0.593	0.892	0.892	1.050	1.439	0.392	0.932	0.932	0.989
	500	0.964	0.614	0.906	0.906	1.094	1.404	0.409	0.933	0.933	1.012
	600	1.009	0.569	0.871	0.871	1.039	1.470	0.374	0.925	0.925	0.981
	700	1.025	0.555	0.861	0.861	0.999	1.494	0.364	0.925	0.925	0.965
	800	0.904	0.648	0.913	0.913	1.030	1.317	0.446	0.923	0.923	0.979
L_4	20/100	1.164	0.601	1.059	1.059	1.059	1.590	0.383	1.104	1.047	1.047
	200	1.158	0.573	1.004	1.004	1.055	1.581	0.349	0.995	0.948	0.948
	300	1.149	0.563	0.979	0.979	1.078	1.570	0.367	1.033	0.990	0.990
	400	1.122	0.535	0.905	0.905	1.038	1.532	0.361	0.966	0.947	0.947
	500	1.094	0.556	0.918	0.918	1.078	1.495	0.377	0.959	0.959	1.012
	600	1.145	0.511	0.884	0.884	1.024	1.564	0.345	0.963	0.926	0.926
	700	1.164	0.498	0.879	0.879	0.992	1.590	0.335	0.966	0.916	0.916
	800	1.027	0.595	0.924	0.924	1.026	1.402	0.412	0.939	0.939	0.981
L_5	20/100	1.292	0.520	1.046	1.046	1.046	1.685	0.354	1.148	1.032	1.032
	200	1.285	0.501	1.000	1.000	1.037	1.676	0.324	1.038	0.938	0.938
	300	1.276	0.496	0.980	0.980	1.055	1.664	0.340	1.073	0.976	0.976
	400	1.245	0.479	0.917	0.917	1.023	1.624	0.334	1.003	0.933	0.933
	500	1.215	0.500	0.927	0.927	1.057	1.584	0.348	0.997	0.948	0.948
	600	1.271	0.459	0.902	0.902	1.012	1.658	0.319	1.001	0.914	0.914
	700	1.292	0.446	0.897	0.897	0.984	1.685	0.310	1.005	0.904	0.904
	800	1.140	0.540	0.931	0.931	1.017	1.486	0.373	0.941	0.941	0.966
L_6	20/100	1.410	0.457	1.051	1.051	1.051	1.778	0.331	1.194	1.023	1.023
	200	1.402	0.443	1.010	1.010	1.034	1.768	0.304	1.083	0.933	0.933
	300	1.392	0.440	0.991	0.991	1.042	1.756	0.317	1.114	0.965	0.965
	400	1.359	0.431	0.933	0.933	1.012	1.714	0.311	1.041	0.922	0.922
	500	1.325	0.450	0.939	0.939	1.040	1.671	0.324	1.033	0.936	0.936
	600	1.387	0.412	0.922	0.922	1.003	1.749	0.298	1.040	0.904	0.904
	700	1.410	0.400	0.920	0.920	0.981	1.778	0.290	1.045	0.895	0.895
	800	1.244	0.491	0.938	0.938	1.007	1.568	0.355	0.997	0.957	0.957

Table A5.3: Numerical failure loads and their DSM estimates concerning the **C**$_5$ and **R**$_5$ columns with σ_{y20}=**300** ***MPa***.

L	T (ºC)	C_5					R_5				
		$\lambda_{FT.T}$	f_{uT}/σ_{yT}	$f_{uT}/f_{nG.T}$	$f_{uT}/f_{nFT.T}$	$f_{uT}/f_{nF.FT*}$	$\lambda_{FT.T}$	f_{uT}/σ_{yT}	$f_{uT}/f_{nG.T}$	$f_{uT}/f_{nFT.T}$	$f_{uT}/f_{nF.FT*}$
L_1	20/100	1.015	0.732	1.126	1.126	1.126	1.834	0.319	1.224	1.020	1.020
	200	1.010	0.711	1.089	1.089	1.161	1.823	0.295	1.117	0.936	0.936
	300	1.002	0.675	1.028	1.028	1.158	1.810	0.310	1.157	0.975	0.975
	400	0.978	0.635	0.948	0.948	1.118	1.767	0.308	1.095	0.943	0.943
	500	0.954	0.655	0.959	0.959	1.160	1.723	0.320	1.085	0.956	0.956
	600	0.999	0.614	0.931	0.931	1.114	1.804	0.297	1.101	0.931	0.931
	700	1.015	0.601	0.925	0.925	1.075	1.834	0.290	1.112	0.927	0.927
	800	0.895	0.687	0.961	0.961	1.086	1.617	0.351	1.047	0.977	0.977
L_2	20/100	1.239	0.565	1.074	1.074	1.074	1.974	0.294	1.307	1.019	1.019
	200	1.232	0.557	1.052	1.052	1.098	1.963	0.273	1.199	0.939	0.939
	300	1.223	0.544	1.017	1.017	1.106	1.949	0.285	1.233	0.972	0.972
	400	1.194	0.529	0.961	0.961	1.084	1.902	0.282	1.164	0.938	0.938
	500	1.165	0.550	0.970	0.970	1.121	1.855	0.292	1.147	0.945	0.945
	600	1.219	0.508	0.946	0.946	1.076	1.942	0.273	1.175	0.929	0.929
	700	1.239	0.494	0.939	0.939	1.043	1.974	0.268	1.189	0.927	0.927
	800	1.093	0.592	0.976	0.976	1.073	1.741	0.318	1.099	0.960	0.960
L_3	20/100	1.450	0.447	1.077	1.077	1.077	2.113	0.275	1.397	1.024	1.024
	200	1.442	0.443	1.057	1.057	1.077	2.101	0.256	1.289	0.950	0.950
	300	1.432	0.435	1.027	1.027	1.072	2.086	0.265	1.316	0.976	0.976
	400	1.397	0.433	0.980	0.980	1.053	2.036	0.263	1.241	0.941	0.941
	500	1.363	0.452	0.983	0.983	1.078	1.986	0.271	1.219	0.945	0.945
	600	1.426	0.416	0.974	0.974	1.047	2.078	0.255	1.257	0.935	0.935
	700	1.450	0.404	0.974	0.974	1.027	2.113	0.251	1.277	0.936	0.936
	800	1.279	0.494	0.980	0.980	1.047	1.863	0.293	1.158	0.951	0.951
L_4	20/100	1.646	0.371	1.147	1.065	1.065	2.249	0.259	1.492	1.034	1.034
	200	1.637	0.368	1.124	1.048	1.048	2.236	0.242	1.383	0.962	0.962
	300	1.626	0.362	1.092	1.024	1.024	2.221	0.250	1.407	0.986	0.986
	400	1.586	0.362	1.039	0.993	0.993	2.167	0.248	1.326	0.950	0.950
	500	1.547	0.378	1.031	1.005	1.005	2.114	0.255	1.297	0.950	0.950
	600	1.620	0.348	1.040	0.978	0.978	2.212	0.242	1.348	0.948	0.948
	700	1.646	0.339	1.046	0.971	0.971	2.249	0.238	1.371	0.950	0.950
	800	1.452	0.416	1.005	1.005	1.039	1.983	0.273	1.223	0.949	0.949
L_5	20/100	1.828	0.321	1.222	1.045	1.045	2.383	0.246	1.591	1.046	1.046
	200	1.817	0.318	1.197	1.028	1.028	2.370	0.231	1.477	0.976	0.976
	300	1.805	0.313	1.162	1.004	1.004	2.353	0.238	1.502	0.998	0.998
	400	1.761	0.313	1.106	0.973	0.973	2.296	0.236	1.416	0.963	0.963
	500	1.718	0.326	1.095	0.984	0.984	2.240	0.242	1.383	0.961	0.961
	600	1.798	0.301	1.109	0.961	0.961	2.344	0.230	1.442	0.962	0.962
	700	1.828	0.293	1.117	0.956	0.956	2.383	0.227	1.468	0.965	0.965
	800	1.612	0.356	1.053	0.995	0.995	2.102	0.257	1.294	0.953	0.953
L_6	20/100	1.994	0.284	1.288	1.028	1.028	2.515	0.235	1.691	1.059	1.059
	200	1.983	0.281	1.261	1.011	1.011	2.501	0.220	1.570	0.988	0.988
	300	1.969	0.277	1.224	0.987	0.987	2.483	0.227	1.597	1.011	1.011
	400	1.922	0.277	1.165	0.957	0.957	2.423	0.225	1.508	0.976	0.976
	500	1.874	0.288	1.153	0.966	0.966	2.364	0.231	1.470	0.973	0.973
	600	1.962	0.267	1.170	0.946	0.946	2.474	0.220	1.536	0.976	0.976
	700	1.994	0.259	1.176	0.938	0.938	2.515	0.217	1.563	0.978	0.978
	800	1.759	0.315	1.112	0.980	0.980	2.218	0.244	1.370	0.961	0.961

Table A5.4: Numerical failure loads and their DSM estimates concerning the **C_5** and **R_5** columns with $\boldsymbol{\sigma_{y20}}$**=450 *MPa***.

L	T (ºC)	***C_5***					***R_5***				
		$\lambda_{FT.T}$	f_{uT}/σ_{yT}	$f_{uT}/f_{nG.T}$	$f_{uT}/f_{nFT.T}$	$f_{uT}/f_{nF.FT^*}$	$\lambda_{FT.T}$	f_{uT}/σ_{yT}	$f_{uT}/f_{nG.T}$	$f_{uT}/f_{nFT.T}$	$f_{uT}/f_{nF.FT^*}$
L_1	20/100	1.243	0.562	1.074	1.074	1.074	2.246	0.258	1.481	1.027	1.027
	200	1.236	0.559	1.060	1.060	1.105	2.233	0.242	1.376	0.959	0.959
	300	1.228	0.550	1.034	1.034	1.123	2.217	0.253	1.416	0.993	0.993
	400	1.198	0.542	0.989	0.989	1.115	2.164	0.253	1.349	0.968	0.968
	500	1.169	0.564	0.998	0.998	1.152	2.111	0.259	1.317	0.966	0.966
	600	1.223	0.522	0.976	0.976	1.109	2.209	0.247	1.374	0.967	0.967
	700	1.243	0.508	0.971	0.971	1.077	2.246	0.243	1.398	0.969	0.969
	800	1.097	0.608	1.005	1.005	1.105	1.980	0.276	1.236	0.961	0.961
L_2	20/100	1.518	0.417	1.094	1.084	1.084	2.418	0.241	1.609	1.044	1.044
	200	1.509	0.415	1.076	1.071	1.071	2.404	0.227	1.497	0.976	0.976
	300	1.498	0.411	1.051	1.051	1.081	2.387	0.237	1.540	1.010	1.010
	400	1.462	0.413	1.012	1.012	1.067	2.330	0.237	1.467	0.984	0.984
	500	1.426	0.431	1.011	1.011	1.088	2.272	0.243	1.430	0.981	0.981
	600	1.493	0.397	1.010	1.010	1.064	2.378	0.232	1.496	0.985	0.985
	700	1.518	0.386	1.014	1.004	1.004	2.418	0.228	1.523	0.988	0.988
	800	1.338	0.475	1.004	1.004	1.061	2.132	0.257	1.334	0.969	0.969
L_3	20/100	1.776	0.334	1.202	1.051	1.051	2.587	0.228	1.740	1.061	1.061
	200	1.766	0.332	1.180	1.037	1.037	2.573	0.215	1.621	0.994	0.994
	300	1.754	0.329	1.152	1.018	1.018	2.555	0.224	1.665	1.028	1.028
	400	1.711	0.331	1.104	0.994	0.994	2.493	0.224	1.588	1.002	1.002
	500	1.669	0.344	1.093	1.004	1.004	2.432	0.229	1.547	0.998	0.998
	600	1.747	0.319	1.111	0.984	0.984	2.545	0.219	1.619	1.003	1.003
	700	1.776	0.310	1.116	0.976	0.976	2.587	0.216	1.648	1.005	1.005
	800	1.566	0.378	1.057	1.021	1.021	2.282	0.242	1.439	0.984	0.984
L_4	20/100	2.016	0.283	1.314	1.040	1.040	2.754	0.216	1.867	1.076	1.076
	200	2.005	0.281	1.290	1.025	1.025	2.739	0.203	1.735	1.005	1.005
	300	1.991	0.278	1.257	1.005	1.005	2.720	0.212	1.789	1.043	1.043
	400	1.943	0.280	1.204	0.981	0.981	2.654	0.212	1.707	1.017	1.017
	500	1.895	0.290	1.188	0.987	0.987	2.589	0.218	1.663	1.014	1.014
	600	1.984	0.271	1.214	0.973	0.973	2.710	0.208	1.739	1.018	1.018
	700	2.016	0.263	1.219	0.965	0.965	2.754	0.204	1.769	1.020	1.020
	800	1.778	0.317	1.142	0.998	0.998	2.429	0.230	1.547	0.999	0.999
L_5	20/100	2.238	0.246	1.407	1.025	1.025	2.919	0.205	1.991	1.089	1.089
	200	2.226	0.245	1.382	1.011	1.011	2.902	0.192	1.845	1.014	1.014
	300	2.210	0.242	1.348	0.992	0.992	2.882	0.201	1.907	1.055	1.055
	400	2.157	0.244	1.292	0.969	0.969	2.812	0.202	1.821	1.030	1.030
	500	2.104	0.253	1.275	0.975	0.975	2.743	0.207	1.776	1.028	1.028
	600	2.202	0.236	1.302	0.961	0.961	2.871	0.197	1.854	1.029	1.029
	700	2.238	0.230	1.313	0.957	0.957	2.919	0.194	1.884	1.031	1.031
	800	1.974	0.275	1.222	0.983	0.983	2.574	0.219	1.654	1.014	1.014
L_6	20/100	2.442	0.215	1.465	0.996	0.996	3.080	0.195	2.106	1.097	1.097
	200	2.429	0.214	1.442	0.985	0.985	3.063	0.182	1.948	1.020	1.020
	300	2.412	0.212	1.409	0.968	0.968	3.041	0.191	2.018	1.064	1.064
	400	2.354	0.214	1.354	0.948	0.948	2.968	0.192	1.928	1.039	1.039
	500	2.296	0.223	1.338	0.956	0.956	2.895	0.197	1.883	1.038	1.038
	600	2.403	0.207	1.362	0.938	0.938	3.030	0.187	1.962	1.037	1.037
	700	2.442	0.201	1.370	0.931	0.931	3.080	0.184	1.991	1.037	1.037
	800	2.154	0.243	1.286	0.966	0.966	2.716	0.209	1.758	1.026	1.026

Table A5.5: Numerical failure loads and their DSM estimates concerning the **C**$_5$ and **R**$_5$ columns with σ_{y20}=**600** ***MPa***.

L	*T* (ºC)	***C***$_5$					***R***$_5$				
		$\lambda_{FT.T}$	f_{uT}/σ_{yT}	$f_{uT}/f_{nG.T}$	$f_{uT}/f_{nFT.T}$	$f_{uT}/f_{nF.FT*}$	$\lambda_{FT.T}$	f_{uT}/σ_{yT}	$f_{uT}/f_{nG.T}$	$f_{uT}/f_{nFT.T}$	$f_{uT}/f_{nF.FT*}$
L_1	20/100	1.436	0.444	1.053	1.053	1.053	2.593	0.226	1.731	1.054	1.054
	200	1.428	0.446	1.046	1.046	1.067	2.579	0.212	1.611	0.986	0.986
	300	1.418	0.444	1.031	1.031	1.079	2.560	0.223	1.667	1.027	1.027
	400	1.384	0.451	1.005	1.005	1.083	2.499	0.224	1.597	1.005	1.005
	500	1.349	0.471	1.009	1.009	1.111	2.437	0.230	1.560	1.004	1.004
	600	1.412	0.434	0.999	0.999	1.079	2.551	0.220	1.632	1.008	1.008
	700	1.436	0.421	0.998	0.998	1.057	2.593	0.216	1.659	1.010	1.010
	800	1.266	0.519	1.015	1.015	1.085	2.287	0.244	1.453	0.991	0.991
L_2	20/100	1.752	0.337	1.179	1.042	1.042	2.792	0.212	1.882	1.071	1.071
	200	1.743	0.335	1.161	1.031	1.031	2.776	0.199	1.748	1.000	1.000
	300	1.730	0.333	1.137	1.015	1.015	2.757	0.209	1.813	1.044	1.044
	400	1.689	0.338	1.097	0.999	0.999	2.690	0.211	1.741	1.025	1.025
	500	1.647	0.351	1.086	1.009	1.009	2.624	0.216	1.698	1.023	1.023
	600	1.724	0.326	1.105	0.989	0.989	2.746	0.206	1.774	1.026	1.026
	700	1.752	0.318	1.113	0.984	0.984	2.792	0.203	1.803	1.027	1.027
	800	1.545	0.387	1.055	1.029	1.029	2.462	0.229	1.582	1.009	1.009
L_3	20/100	2.051	0.276	1.325	1.035	1.035	2.988	0.199	2.027	1.085	1.085
	200	2.039	0.275	1.305	1.023	1.023	2.971	0.186	1.876	1.010	1.010
	300	2.025	0.273	1.278	1.007	1.007	2.950	0.197	1.954	1.059	1.059
	400	1.976	0.276	1.231	0.990	0.990	2.879	0.198	1.875	1.039	1.039
	500	1.927	0.286	1.213	0.994	0.994	2.808	0.204	1.833	1.038	1.038
	600	2.017	0.268	1.244	0.984	0.984	2.939	0.194	1.912	1.039	1.039
	700	2.051	0.262	1.256	0.981	0.981	2.988	0.191	1.941	1.040	1.040
	800	1.808	0.312	1.163	1.003	1.003	2.635	0.216	1.711	1.027	1.027
L_4	20/100	2.328	0.235	1.454	1.027	1.027	3.181	0.188	2.163	1.095	1.095
	200	2.315	0.234	1.432	1.016	1.016	3.163	0.175	1.997	1.015	1.015
	300	2.299	0.233	1.402	1.000	1.000	3.141	0.186	2.086	1.068	1.068
	400	2.244	0.235	1.351	0.982	0.982	3.065	0.187	2.004	1.049	1.049
	500	2.188	0.244	1.331	0.987	0.987	2.989	0.193	1.961	1.050	1.050
	600	2.290	0.228	1.365	0.977	0.977	3.129	0.183	2.040	1.048	1.048
	700	2.328	0.223	1.375	0.971	0.971	3.181	0.179	2.069	1.047	1.047
	800	2.053	0.265	1.273	0.993	0.993	2.805	0.205	1.836	1.041	1.041
L_5	20/100	2.585	0.202	1.538	1.000	1.000	3.370	0.176	2.279	1.094	1.094
	200	2.570	0.201	1.517	0.991	0.991	3.351	0.164	2.105	1.016	1.016
	300	2.552	0.200	1.487	0.977	0.977	3.328	0.175	2.208	1.073	1.073
	400	2.491	0.203	1.437	0.963	0.963	3.248	0.177	2.126	1.056	1.056
	500	2.429	0.211	1.420	0.969	0.969	3.167	0.182	2.081	1.057	1.057
	600	2.543	0.196	1.448	0.954	0.954	3.315	0.172	2.159	1.052	1.052
	700	2.585	0.192	1.459	0.949	0.949	3.370	0.169	2.187	1.050	1.050
	800	2.279	0.230	1.363	0.979	0.979	2.972	0.194	1.954	1.052	1.052
L_6	20/100	2.820	0.173	1.571	0.953	0.953	3.556	0.157	2.271	1.038	1.038
	200	2.805	0.173	1.552	0.946	0.946	3.537	0.154	2.200	1.011	1.011
	300	2.785	0.173	1.526	0.936	0.936	3.512	0.165	2.318	1.072	1.072
	400	2.718	0.176	1.481	0.926	0.926	3.427	0.167	2.234	1.057	1.057
	500	2.651	0.183	1.467	0.935	0.935	3.343	0.172	2.191	1.060	1.060
	600	2.774	0.170	1.488	0.915	0.915	3.499	0.162	2.266	1.052	1.052
	700	2.820	0.165	1.496	0.908	0.908	3.556	0.159	2.293	1.049	1.049
	800	2.487	0.201	1.420	0.952	0.952	3.137	0.184	2.065	1.058	1.058